Classification of base geometries in F-theory

by

Yinan Wang

B. S., Peking University (2013)

Submitted to the Department of Physics
in partial fulfillment of the requirements for the degree of

Doctor of Philosophy in Physics

at the

MASSACHUSETTS INSTITUTE OF TECHNOLOGY

June 2018

Author ..... Signature redacted

Department of Physics
May 3, 2018

Certified by ..... Signature redacted

Washington Taylor
Professor
Thesis Supervisor

Accepted by ..... Signature redacted

Scott A. Hughes
Interim Associate Department Head

Classification of base geometries in F-theory

by

Yinan Wang

Submitted to the Department of Physics
on May 3, 2018, in partial fulfillment of the
requirements for the degree of
Doctor of Philosophy in Physics

Abstract

F-theory is a powerful geometric framework to describe strongly coupled type IIB superstring theory. After we compactify F-theory on elliptically fibered Calabi-Yau manifolds of various dimensions, we produce a large number of minimal supergravity models in six or four spacetime dimensions. In this thesis, I will describe a current classification program of these elliptic Calabi-Yau manifolds. Specifically, I will be focusing on the part of classifying complex base manifolds of these elliptic fibrations. Besides the usual algebraic geometric description of these base manifolds, F-theory provides a physical language to characterize them as well. One of the most important physical feature of the bases is called the "non-Higgsable gauge groups", which is the minimal gauge group in the low energy supergravity model for any elliptic fibration on a specific base. I will present the general classification program of complex base surfaces and threefolds using algebraic geometry machinery and the language of non-Higgsable gauge groups. While the complex base surfaces can be completely classified in principle, the zoo of generic complex threefolds is not well understood. However, I will present an exploration of the subset of toric threefold bases. I will also describe examples of base manifolds with non-Higgsable U(1)s, which lead to supergravity models in four and six dimensions with a U(1) gauge group but no massless charged matter.

Thesis Supervisor: Washington Taylor
Title: Professor

Acknowledgments

First, I would like to thank my research advisor Prof. Wati Taylor for his continuous support, guidance and inspiration. I feel extremely lucky that my computer programming skills match his enthusiasm in computational mathematics. This is crucial for our string geometric classification projects to succeed. I was also influenced by his persistence in one subfield that is considered too complicated to work out by many people.

I have benefited a lot from the group meetings organized by Wati. The discussions with my fellow students Samuel Johnson, Nikhil Raghuram, Yu-Chien Huang and Andrew Turner are very helpful and I want to thank them as well.

I would also like to thank Prof. Barton Zwiebach and my collaborator Olaf Hohm for their early research guidance in the field of double/exceptional field theory, which is an indispensable starting point for my graduate level research. I would like to thank them for the recommendations for various purposes as well.

I have also benefited from other faculty members at CTP, from their teaching and guidance on the oral exam. They include Prof. Hong Liu, Tracy Slatyer, William Detmold, Jesse Thaler and Robert Jaffe. I would also like to thank other graduate students for valuable discussions, including Usman Naseer, Nick Rodd, Srivatsan Rajagopal and Yifan Wang. I would like to thank the CTP staff members Scott Morley, Charles Suggs and Joyce Berggren for their support as well. I have really enjoyed my life at CTP and I will cherish this part of memory forever.

Of course, I would like to thank Prof. Hong Liu again and Prof. Xiao-Gang Wen for their parts on my thesis committee.

Besides the people at MIT, I would like to thank my colleagues at Northeastern University: Prof. James Halverson, Dr. Cody Long, Jiahua Tian and Ben Sung. Our shared interest always pushes us further. I would also like to thank Harvard people including Prof. Xi Yin, Prof. Cumrun Vafa, Dr. Dan Xie and Shuheng Shao for teaching and discussions.

Finally, I would like to thank my family for their love and support and my friends

for regular dining activities.

Contents

List of Figures

List of Tables

Chapter 1

Introduction and summary

The development of modern high energy physics was dominated by the quantum field theory paradigm[113, 134]. In this picture, spacetime is filled by fluctuating "quantum fields" which vary over space and time. Certain fluctuations or "asymptotic states" of these quantum fields can be interpreted as particles. Quantum field theory provides powerful tools to calculate the outcome of colliding particles via the summation of loop diagrams, see Figure 1-1. The predictions of such calculations can be verified at collider experiments, such as the LHC (Large Hadron Collider). One significant victory of quantum field theory is the establishment of the standard model of particle physics, which includes the electroweak interaction and strong interaction. The Higgs particle, responsible for electroweak $SU(2)\times U(1)$ gauge symmetry breaking and the generation of fermion particle masses, was predicted in the standard model and then discovered in 2012. The toolkits and ideas of quantum field theory have been broadly applied to condensed matter physics as well.

Despite the power of quantum field theory, it has a number of fundamental problems. First, the theory itself is only mathematically well defined for a few special

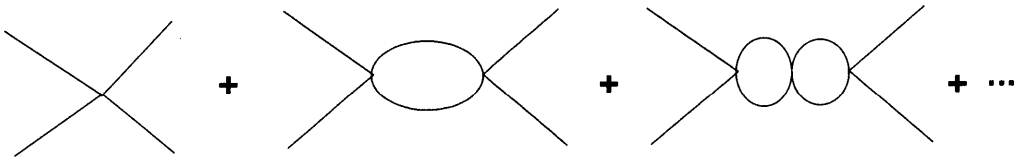

Figure 1-1: A graphic representation of the summation of loop diagrams in quantum field theory

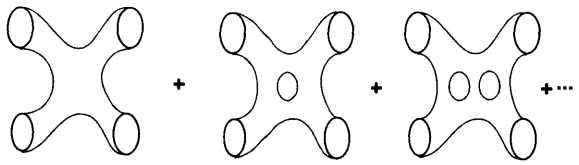

Figure 1-2: A graphic representation of the summation of loop diagrams in string theory

cases, such as topological field theories or conformal field theories which are scale invariant. One reason is that many quantum field theories suffer from "UV (Ultra Violet) divergence," which means that the computed scaling amplitudes for the loop diagrams in Figure 1-1 will diverge to infinity. To overcome this problem, one needs to add a counter term with divergent coefficient into the Lagrangian of the quantum field theory to cancel the divergence. The whole process is iterative, and it is called "renormalization" of quantum field theory.

Another more fundamental problem appears when one includes gravity into the theory. Even if we use the linearized version of the Einstein Hilbert term:

$$\int \sqrt{-g} R d^4x, \tag{1.0.1}$$

where R is the Ricci scalar, the Lagrangian will appear "non-renormalizable" in the sense that there will be infinitely many types of counter terms in the renormalization process.

These observations indicate that our current quantum field theories of the standard model and gravity are "effective theories" that only approximately hold at a low energy scale $\Lambda \ll \Lambda_{pl}$ that is much lower than the Planck scale $\Lambda_{pl} \sim 10^{19}$GeV. To obtain the whole picture of fundamental physics, we need to construct a theory that is UV complete at the Planck scale and higher.

Up to now, the most well established framework to unify quantum field theory and gravity is string theory[114, 64, 17]. It is analogous to the quantum field theory paradigm, with the particles replaced by higher dimensional objects such as strings. Now the summation of scattering amplitudes in Figure 1-1 is replaced by Figure 1-2.

With the "worldline" of point particles replaced by the "worldsheet" of strings, the

loop amplitude becomes UV finite[1], which fundamentally solves the UV divergence problem in quantum field theory. The worldsheet theory of strings in a D-dimensional background is described by 1+1 dimensional conformal field theory (CFT), where the quantum fields $X^\mu(\mu = 0, \ldots, D-1)$ correspond to the spacetime coordinates. Certain excited states on the strings correspond to a rank-2 traceless tensor in spacetime, which is the graviton. The scattering amplitudes of gravitons can be computed for an arbitrarily high energy scale. In this sense, string theory is really a theory of quantum gravity.

A self-consistency condition is that the worldsheet CFT should be free of Weyl anomalies (of conformal symmetry) when the D-dimensional background is flat Minkowski space. This constraint fixes the spacetime dimension $D = 26$ for the bosonic string theory, where the worldsheet quantum fields are all bosonic (X^μ). The bosonic string theory suffers from the existence of a tachyon with mass $m^2 < 0$, which indicates the instability of the theory. To overcome this problem, people introduced supersymmetry into string theory.

Supersymmetry originally was constructed as an extension of the Poincaré algebra in 4D. It is a counter example to the original Coleman-Mandula theorem [32] which says that the symmetry of quantum field theory can only be a direct product of the Poincaré group and an internal symmetry group, by including a set of Fermionic generators into the Poincaré algebra to form the Super-Poincaré algebra[70]. In particle physics, supersymmetry was introduced to solve the "hierarchy problem" of the Higgs boson, which comes from the fact that the 1-loop diagram of Higgs scalar will lead to a Λ^2 divergence. To get the real world Higgs mass $m_h \approx 126GeV$, the bare mass $m_0 \approx \sqrt{m_h^2 + \Lambda^2}$ will be extremely fine tuned. In the supersymmetric extensions of the standard model such as MSSM (minimal supersymmetric standard model), every particle has a new superpartner particle. After they are included in the loop diagrams, the Λ^2 divergence will be cancelled and the divergence will be proportional to $\log \Lambda$ (see for example Vol. 3 of [134]). Up to now, no low energy supersymmetric

[1]Although the summation of all the loop diagrams is still divergent, which means that the series of loop diagrams is an asymptotic series in the string coupling constant g_s. This is a generic feature of perturbative quantum field/string theory.

partner has yet been found at the LHC. Nonetheless, supersymmetry is still a very useful theoretical physics tool to regulate divergence and make the theory simpler.

After including fermionic quantum fields into the string worldsheet theory, they become "superstring theories" and generally have $D = 10$ spacetime dimensions to cancel the Weyl anomaly. In the 1980s, five different versions of superstring theories were discovered, which are the type I, type IIA, type IIB, heterotic $E_8 \times E_8$ and heterotic SO(32) theory. Type I, heterotic $E_8 \times E_8$ and SO(32) theories all have $\mathcal{N} = 1$ supersymmetry in 10D with 16 supercharges, while IIA and IIB theories have $\mathcal{N} = (1,1)$ and $\mathcal{N} = (0,2)$ respectively with 32 supercharges (for the notion of supersymmetry see Appendix A).

One crucial ingredient of string theory is the existence of non-perturbative extended objects along with the fundamental strings we were talking about. An important class of these objects is called D-branes, which are originally created as the Dirichlet boundary condition of strings. From the worldsheet perspective, open strings can attach to these D-branes and the vector modes of the open string A_μ emerge as gauge bosons. From the spacetime supergravity point of view, the D-branes have actions and dynamics by themselves as well. In type IIA and IIB superstring theory, the set of stable D-branes is different. IIA superstring theory has D-branes with even space dimensions, such as the D0, D2, D4, D6 branes. In contrast, IIB theory has odd space dimensional D-branes: D1, D3, D5, D7 branes. A Dp-brane couples to a $(p+1)$-form "RR" field in a natural way:

$$L = \int C_{p+1} d^{p+1}x \tag{1.0.2}$$

where the integration is over the D-brane world volume. It also couples to a $(7-p)$-form gauge field magnetically, since the field strength of $(7-p)$-form is Hodge dual to the field strength of $(p+1)$-form field in 10D.

In 1990s, it was speculated that different versions of superstring theory can be identified with each other in certain limits. This idea, called "duality", has a central status in the contemporary string theory framework as well. For example, if one puts the IIA string theory on a circle with radius R, then it is dual to the IIB string theory

on a circle with radius $1/R$ (in string units). This is called "T-duality," which only exists in the string theory paradigm but not in quantum field theory. D-branes in the IIA picture will be mapped to branes in the IIB theory with different dimensions. Similarly, heterotic $E_8 \times E_8$ and SO(32) theories can be related with T-duality as well.

Another type of string duality is called "S-duality", which relates the weakly coupled version of one theory to the strongly coupled version of another one. For example, type I superstring theory is S-dual to heterotic SO(32) theory, and as will be discussed more thoroughly in the next section, type IIB superstring theory has a self S-duality.

The last piece of this string duality web comes from 11D $\mathcal{N} = 1$ supergravity with 32 supercharges, which is the highest dimension a supergravity theory can live in. In 1995, Edward Witten proposed the existence of a more unified "M-theory" in 11D as well that can unify all the different pieces of superstring theory. In M-theory, the fundamental objects are M2 and M5 membranes rather than the one-dimensional fundamental string. The 11D supergravity hence can be thought of a classical limit of M-theory in the same spacetime background. IIA superstring theory comes from M-theory compactified on a torus, where the string coupling constant is proportional to the radius of the torus in the string unit. Type I superstring theory and type $E_8 \times E_8$ heterotic string theory follow from M-theory on an "orbifold" $S^1/\mathbb{Z}_2$[81]. We draw the picture of string duality web in Figure 1-3.

What we have discussed before is mostly about string theories in high dimensions. Since the birth of superstring theory, people have been trying to construct the known 4D physics in the string theory framework. To reduce the spacetime dimension from 10/11D to four, a simple practice is to set the spacetime background $M_{10} = R^{3,1} \times M_6$ or $M_{11} = R^{3,1} \times M_7$ where M_6 and M_7 are some real six or seven dimensional compact manifold with a certain topology.

For certain classes of these compact manifolds, the 4D physics has different amount of supersymmetry. If they are simply flat tori, then the number of supercharges is not reduced and the 4D theory is $\mathcal{N} = 8$ or $\mathcal{N} = 4$ supergravity. To reproduce real

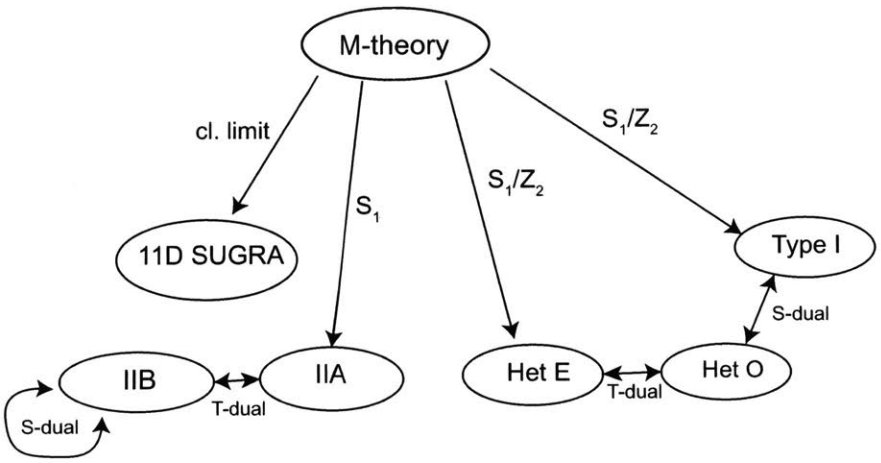

Figure 1-3: String duality web known in mid-1990s, with M-theory, type I, IIA, IIB, heterotic $E_8 \times E_8$ (Het E) and SO(32) (Het O) and 11D supergravity.

world physics, the 4D supersymmetry can only be maximally $\mathcal{N} = 1$, otherwise there is no chiral matter in the theory, which contradicts the basic feature of the standard model. From the 10D superstring theories, a common class of compact manifolds is the "Calabi-Yau" manifolds which are complex manifolds with vanishing Ricci tensor:

$$R_{\mu\nu} = 0. \tag{1.0.3}$$

Real $2n$-dimensional Calabi-Yau manifolds are usually called "Calabi-Yau n-folds" in terms of the number of complex dimensions. The holonomy group is SU(n) and only a $1/2^{n-1}$ proportion of supersymmetry is preserved after the compactification. There are two ways to get 4D $\mathcal{N} = 1$ supergravity from 10D superstring theory:

(1) Compactify heterotic string theory on a Calabi-Yau threefold.

(2) Compactify type IIA/IIB superstring theory on a Calabi-Yau orientifold, which breaks down half of the supersymmetry further.

Many models have been constructed using these two methods, for example[3, 25, 29, 35].

Another way to get 4D $\mathcal{N} = 1$ models is to compactify 11D M-theory on a real seven dimensional "G_2 manifold" with G_2 holonomy group. However, it is not clear how to realize standard model in it up to now.

One may ask if there is a way to directly reproduce non-supersymmetric models

from compactification. Since the solution of the vacuum Einstein equation in the compact dimensions will lead to the Ricci-flat condition: $R_{\mu\nu} = 0$, the compact manifold is generally Calabi-Yau or a manifold with special holomony, such as G_2. If one starts from superstring theory with spacetime supersymmetry, then usually a part of the supersymmetry will be preserved at least at the compactification scale. There exists string theory in 10D without spacetime supersymmetry, such as the SO(16)× SO(16) heterotic string theory[21, 45, 60] (although it is not clear if they are actually self-consistent). We will not consider the possibility of such non-supersymmetric model in this thesis. There is always assumed to be supersymmetry at the high compactification energy scale, with a possibly spontaneous supersymmetry breaking at a lower energy scale.

The specific value of these energy scales are related with the geometric sizes of the compact space, which are dynamical variables in string theory that are not predetermined when we choose their topology in the beginning. The set of such dynamical variables are usually called "moduli". If there is a moduli potential in the Lagrangian, then vacuum expectation value of moduli can be in principle determined by the "moduli stablization" process.

One simple way to introduce this moduli potential is using quantized RR form fields in superstring theory. The outcome is a vast set of vacuum solutions from a single geometry, which are called the "flux vacua". A famous number in the literature is 10^{500}, which is the number of flux vacua on a single geometry in a IIB orientifold construction[40].

The existence of such huge number of vacuum solutions in string theory leads to philosophical questions. On one hand, with such an almost infinite number of models, it is easier to find a model with the specific parameters in our standard model. On the other hand, one can argue that string theory has no predictability if there are so many possible universes that are not our universe. Here I will present the physical reasons that the grand set of string solutions including all the possible geometries, which is called the "landscape", has the value of being studied.

(1) There has been a misconception that any (anomaly free) physical model can

be realized in string theory. However, this is not true as we know that there cannot be infinitely many gauge fields in any string compactification model. If we can classify the string theory vacuum solutions, then we can make a list of the constraints on low energy physics from string theory. Furthermore, there is a "string universality conjecture"[1, 93, 120], which says that any UV complete (supersymmetric) gravity theories in $D \geq 4$ can be constructed with a superstring setup. This comes from the belief that superstring theory is the only way to unify gravity and quantum field theory using the paradigm of QFT. If this conjecture is true, then we can classify all the possible $D \geq 4$ supergravity theories at the level of low energy effective action and see what is allowed. The theories that satisfy the known low energy constraints such as anomaly cancellations but do not have a superstring construction are put into the "swampland"[27, 128]. They may either have some secret inconsistency or can be realized in string theory in a more exotic setup. The results are very interesting in either of these possibilities. If we can make a complete survey of the swampland, we may be able to discover new constraints on quantum gravity along with the existing quantum gravity conjectures such as the weak gravity conjecture[7].

(2) By more carefully studying the physical mechanics of moduli stabilization and the transition between geometries, we can have a feeling of what is the most common or prefered supergravity model from string theory constructions. This will provide hints of the most natural way to realize the standard model and even beyond standard model physics, such as the nature of dark matter.

Following this logic, it is natural to ask what is the largest or most dominant class of string vacuum solutions. Up to now, this biggest set is the "F-theory" constructions, which is a geometric description of strongly coupled type IIB superstring theory with 7-branes[127, 109, 108]. In the early days of F-theory, it was speculated that the theory lives in a 12-dimensional spacetime with two additional real dimensions than superstring theory. After we compactify the 12D theory on a special class of Calabi-Yau manifolds: elliptic fibered Calabi-Yau manifold, we will get supergravity in even dimensions. For example, if we compactify F-theory on an elliptic Calabi-Yau threefold (CY3), then we get 6D $\mathcal{N} = (1, 0)$ supergravity. If we use an elliptic

Calabi-Yau fourfold (CY4), then we will get a 4D $\mathcal{N} = 1$ supergravity. For the case of Calabi-Yau twofold, they are generally called "K3 surfaces" and we will get 8D $\mathcal{N} = 1$ supergravity if we compactify F-theory on it. However, from today's perspective, the two additional dimensions are completely auxillary and they are not needed to be considered as actual spacetime dimensions[2].

The "F" in F-theory hence means fibration, which is a generalization of fiber bundle in the sense that the fiber can be singular (or degenerate). The singular fiber will encode the essential physical information of the low dimensional supergravity. For example, singular fibers over a real codimension-2 submanifold of the base correspond to 7-branes, and open string modes attached to them will give rise to gauge fields. Unlike the weakly coupled IIB theory, in F-theory there exist strongly coupled 7-brane configurations giving rise to exceptional gauge groups: G_2, F_4, E_6, E_7 and E_8. As will be seen in detail later, these exceptional gauge groups will frequently appear in the F-theory landscape. Singular fibers over a real codimension-4 submanifold of the base correspond to the intersection of 7-branes. The open string modes stretched between intersecting 7-branes will then give rise to charged matter under the gauge groups. Furthermore, a singular fiber over a real codimension-6 submanifold encodes the information of the interaction of three quantum fields, which is the Yukawa coupling in 4D or lower dimensions.

The topological classification of F-theory geometric models hence consists of two parts: the classification of topologically distinct bases and the classification of different fibrations on a single base, which give rise to different elliptic Calabi-Yau manifolds. The bases are general complex manifolds that are not necessarily Calabi-Yau. For each base, there exists a "generic fibration" where the gauge group is minimal. Due to this feature, this is physically called the "non-Higgsable phase" and the minimal gauge groups are called non-Higgsable gauge groups. As will be briefly explained in Chapter 2, the generic fibration contains more flux vacua than the non-generic ones and they are the central object of this thesis.

[2]In a reformulation of maximally supersymmetric supergravity called "exceptional field theory" in 9D, the 12 dimensions are considered as physical dimensions[129, 18].

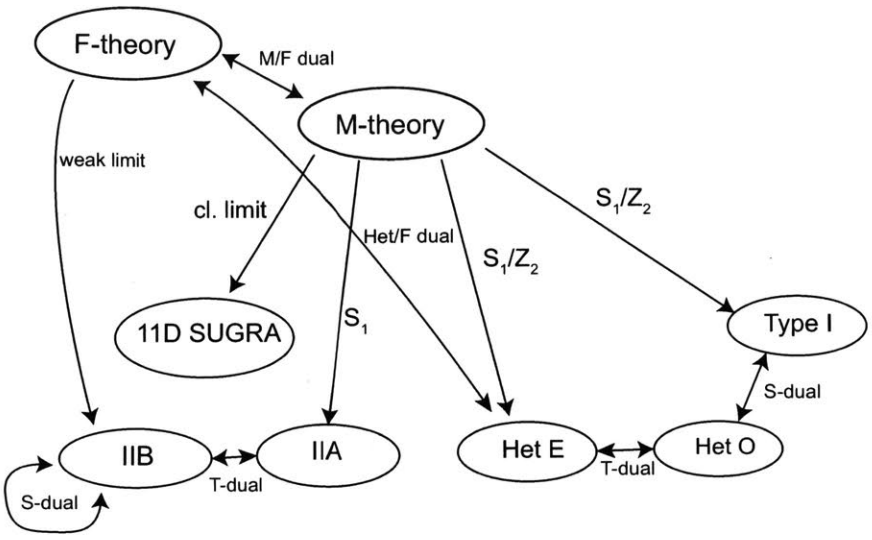

Figure 1-4: String duality web including F-theory.

In fact, if the bases are Calabi-Yau then the fibration can only be a trivial direct product of the base manifold and the 2-torus, and it will be reduced to a weakly coupled type IIB model. In this sense, F-theory provides a way to describe supersymmetric superstring compactification on manifolds with non-vanishing curvature. It is much more general than the weakly couple type IIB constructions.

From the perspective of the string duality web, F-theory touches many corners in Figure 1-3. As will be described in detail in Chapter 2, the definition of F-theory relies on the "F/M-theory duality". Another elegant story is the "heterotic/F-theory" duality, where F-theory on a K3 surface is dual to heterotic $E_8 \times E_8$ string theory on a two torus T^2. This duality will not be covered in this thesis. Finally, with the trivial weak limit reduction to type IIB, we can complete our duality web in Figure 1-4.

From the phenomonology model building perspective, there has been a vast literature of realizing the supersymmetric standard model with the SU(5) GUT (Grand Unified Theory) type construction, for example [15, 16, 46]. GUT is an old idea from 1970s, which comes from the observation that the standard model gauge group SU(3)$\times$ SU(2)$\times$ U(1) (before electroweak gauge symmetry breaking) and matter representations can be simply embedded in the group SU(5) and its smallest representations. The gauge coupling of the three fundamental interactions: the strong, weak and electric interaction could be unified at the "GUT scale"$\sim 10^{16}$GeV where the

gauge group appears to be SU(5). However, the types of fibration used in these kind of constructions is always non-generic and they are not a central object of this thesis.

In the recent a few years, there has been a lot of activity on constructing superconformal field theories (SCFTs) with a top-down approach from F-theory, for example [39, 76, 77]. The $\mathcal{N} = (2,0)$ and $(1,0)$ SCFTs in 6D are generally strongly coupled without a Lagrangian description, and their constructions are only possible under the string theory framework. It was claimed that all the 6D $\mathcal{N} = (1,0)$ SCFTs can be constructed with F-theory, following the string universality philosophy. In contrast to the supergravity case, they are using non-compact Calabi-Yau threefolds with non-compact bases to decouple gravity from the theory. They will be mentioned in the later parts of the thesis but they are not our central focus.

As a brief summary, F-theory has the following nice features:

(1) F-theory provides a vast playground allowing a larger number of geometries and flux vacua than perturbative superstring theory.

(2) F-theory describes compactification on a manifold with non-vanishing Ricci curvature and still preserves a part of supersymmetry.

(3) F-theory allows the construction of exceptional gauge groups that cannot be described in a simple D-brane stack description.

(4) Geometric engineering from F-theory helps us to classify and understand strongly coupled superconformal field theories.

Apart from the physical interests, F-theory is related to many fields of modern mathematics. The most crucial mathematical tool is complex algebraic geometry[66, 74], which studies algebraic equations in complex number field. The underlying reason for this is the "GAGA principle", which roughly states that the algebraic objects also have analytic structures that can be studied with complex differential geometry. We will be only focusing on the geometries with algebraic descriptions in this thesis.

Since the compact manifolds in F-theory are elliptically fibered Calabi-Yau manifold, the beautiful mathematical theory of elliptic curves is closely involved. A well known achievement of the elliptic curve theory is the proof of Fermat's last theorem by Andrew Wiles. In F-theory, the U(1) gauge groups are deeply connected with

a mathematical structure of elliptic curves called "Mordell-Weil group", as will be explained in Chapter 2.

As we have mentioned before, an important piece of F-theory (mainly for 4D F-theory) is the flux that give rise to flux vacua. In 4D F-theory, the relevant flux is the G_4 4-form field. To study the property of flux and its interaction with the geometry, one need to use Hodge theory and mirror symmetry techniques. They will not be covered in this thesis, but one should keep in mind that they are crucial to compute the actual energy scales, mass spectrum and the cosmological constant in an F-theory model.

In this thesis, I will provide a broad review of our current knowledge about the set of compact base manifolds used in F-theory, which is the foundation stone of the geometric classification program of F-theory. This thesis has the following structure: in Chapter 2, I will provide essential physical and mathematical background to establish the setups we are going to use. In section 2.1, I will briefly review type IIB superstring theory and define F-theory, in more detail than the broad introduction in this Chapter. In section 2.2, I will provide the basic tools of complex algebraic geometry that will be used through out the thesis. In section 2.3, I will talk about elliptic curves and elliptic fibrations. In section 2.4, I will cover a special subset of complex algebraic geometry: toric geometry.

Chapter 3 will focus on 6D F-theory and the classification of base surfaces. I will briefly review the general structures and the classification of toric surface bases at first. Then I will present the machinery for classifying general non-toric base surfaces in our paper[125].

Chapter 4 is about 4D F-theory and the exploration of the vast zoo of base threefolds. First, I will define the set of bases we are studying. Then I will present two different Monte Carlo methods to probe this big set in our papers[124, 126] and discuss the results. Apart from this, I will also present a geometry with the largest number of flux vacua up to now[123]. Finally, a grand picture of the set of base threefolds will be established and the physical implications will be discussed.

Chapter 5 is about bases with non-Higgsable Abelian gauge groups, which are

qualitatively different from the non-Abelian gauge groups. Generic fibration over these bases will lead to models with U(1) gauge group but no massless charged matter under it. The discussion follows my paper[130].

Finally, I will briefly summarize the important things we have learned and the open questions in Chapter 6.

Chapter 2

Physics and Mathematics background

2.1 Type IIB superstring theory and F-theory

In this section, we provide a brief overview of the physical origin of F-theory, partly following [133].

2.1.1 IIB superstring theory and 7-branes

In the worldsheet construction of superstring theory, a closed string has two types of oscillation modes: left-moving modes and right-moving modes. For the fermionic quantum field on the string, they could be either periodic or anti-periodic. The periodic and anti-periodic boundary conditions are called Ramond (R) or Neveu-Schwarz (NS) boundary conditions respectively.

In type IIB superstring theory, the massless fields from a closed string are given by a product of representations of the SO(8) little group of the 10D spacetime. The massless bosonic fields include the NS-NS fields and R-R fields, where both the left-moving and right-moving modes obey NS or R type boundary condition.

For the NS-NS fields, they are a product of vector representations 8_v of SO(8):

$$\mathbf{8}_v \times \mathbf{8}_v = \mathbf{1} + \mathbf{28} + \mathbf{35}. \tag{2.1.1}$$

The singlet **1** is the "dilaton" ϕ, which is a scalar that indicates the string coupling strength $g_s = e^{\phi}$. The representation **28** is a rank-2 antisymmetric tensor field B_2 that couples to the fundamental string, and the representation **35** is a traceless rank-2 symmetric tensor field, which is the metric $g_{\mu\nu}$.

For the R-R fields, they are a product of spinor representations 8_s of SO(8):

$$\mathbf{8}_s \times \mathbf{8}_s = \mathbf{1} + \mathbf{28} + \mathbf{35}_+. \tag{2.1.2}$$

The singlet **1** is the R-R 0-form field C_0, which is different from the dilaton ϕ, while the rank-2 antisymmetric tensor **28** gives the R-R 2-form field C_2. $\mathbf{35}_+$ is a self-dual rank-4 antisymmetric tensor that gives the R-R 4-form field C_4.

The classical effective action of 10D IIB supergravity is given as follows[114]:

$$S = S_{NS} + S_R + S_{CS} \tag{2.1.3}$$

$$S_{NS} = -\frac{1}{2G_{10}^2}\int d^{10}x\sqrt{-g}e^{-2\phi}(R + 4\partial_\mu\phi\partial^\mu\phi - \frac{1}{2}|H_3|^2) \tag{2.1.4}$$

$$S_R = -\frac{1}{4G_{10}^2}\int d^{10}x\sqrt{-g}(|F_1|^2 + |\tilde{F}_3|^2 + \frac{1}{2}|\tilde{F}_5|^2) \tag{2.1.5}$$

$$S_{CS} = -\frac{1}{4G_{10}^2}\int C_4 \wedge H_3 \wedge \tilde{F}_3, \tag{2.1.6}$$

where $F_1 = dC_0$, $H_3 = dB_2$, $\tilde{F}_3 = F_3 - C_0 \wedge H_3$, $\tilde{F}_5 = F_5 - \frac{1}{2}C_2 \wedge H_3 + \frac{1}{2}B_2 \wedge dC_2$. G_{10} is the Newton's constant in 10D. As one can see, the NS-NS part action S_{NS} contains the Einstein-Hilbert term and the kinetic term for NS-NS fields B_2 and ϕ. The R-R part S_R contains the kinetic term for R-R fields C_0, C_2 and C_4. The final part S_{CS} is a 10D Chern-Simons term and there is no metric in the integration.

Apart from the action, a self-duality constraint

$$\star\tilde{F}_5 = \tilde{F}_5 \tag{2.1.7}$$

has to be imposed by hand. In this sense the IIB supergravity action is actually a "pseudo action".

An interesting feature of this action is the presence of an $\mathrm{SL}(2,\mathbb{R})$ symmetry. If we define the Einstein frame metric

$$g_{E,\mu\nu} = e^{-\phi/2} g_{\mu\nu} \tag{2.1.8}$$

and the axiodilaton

$$\tau = C_0 + ie^{-\phi}. \tag{2.1.9}$$

Then the action (2.1.3) is invariant under the following $\mathrm{SL}(2,\mathbb{R})$ group action:

$$\tau \to \frac{a\tau + b}{c\tau + d}\ ,\ \begin{pmatrix} B_2 \\ C_2 \end{pmatrix} \to \begin{pmatrix} d & c \\ b & a \end{pmatrix}\ ,\ g_{E,\mu\nu} \to g_{E,\mu\nu}\ ,\ \tilde{F}_5 \to \tilde{F}_5\ (ad - bc = 1). \tag{2.1.10}$$

We can see that under this $\mathrm{SL}(2,\mathbb{R})$ group action, the C_0 and $e^{-\phi}$ field are actually mixed up, and the same for the B_2 and C_2 fields. As we have mentioned in Chapter 1, R-R fields can couple to D-branes with various dimensions. A p-form field with $(p+1)$-form field strength can couple electrically to a D$(p-1)$-brane and magnetically to a D$(7-p)$-brane. Hence the C_4 can couple to a D3-brane both electrically and magnetically, C_2 can couple to a D1-brane electrically and D5-brane magnetically. C_0 can couple to a D7-brane magnetically and the "D(-1)-brane" electrically. The D(-1)-brane in string theory is an instanton object.

Hence logically we will expect mixed objects in IIB string theory that are transformed by the group action as well. Since C_2 and B_2 couple to the D1 string and fundamental F1 string respectively, there should exist a bound state with p copies of F1 strings and q copies of D1 string, which is called a "(p,q)"-string. Since $p, q \in \mathbb{Z}$, the symmetry group $\mathrm{SL}(2,\mathbb{R})$ is actually broken to the $\mathrm{SL}(2,\mathbb{Z})$ subgroup. Similarly,

the axiodilaton τ should magnetically couple to "(p,q) 7-branes", which are $SL(2,\mathbb{Z})$ transformations of the D7-brane.

Notice that the 7-brane in 10D has similar properties to a cosmological string in 4D. A loop around it cannot be continuously deformed to a trivial one. The axiodilaton field τ around that loop will be transformed under a monodromy action. A heuristic argument is that the Dp-brane acts as a source term in the normal $(9-p)$ spatial dimensions, and the field Φ it sources will obey the Laplace's equation:

$$\Delta\Phi \approx \delta(r), \tag{2.1.11}$$

which leads to $\Phi \approx 1/r^{7-p}$ for $p < 7$ and $\Phi \approx \ln r$ for $p = 7$. In a more careful analysis[24], if we put the D7-brane in the $0, 1, \ldots, 7$ spacetime dimensions and use the complex variable $z = x_8 + ix_9$ to describe the two normal dimensions, the equation of motion from the D7-brane action will give:

$$\partial_{\bar{z}}\tau(z,\bar{z}) = 0 \tag{2.1.12}$$

which means that $\tau(z)$ is a holomorphic function in z. Furthermore, if the D7-brane is located at $z = 0$: we have

$$j(\tau) \propto 1/z \tag{2.1.13}$$

where $j(\tau)$ is the modular j-function with the expansion

$$j(\tau) = e^{-2\pi i\tau} + 744 + 196884e^{2\pi i\tau} + \ldots. \tag{2.1.14}$$

The form of $\tau(z)$ close to the D7-brane ($z = 0$) is then

$$\tau(z) \approx \frac{1}{2\pi i}\ln z. \tag{2.1.15}$$

From this equation, we can see that the axiodilaton τ indeeds transform as $\tau \to \tau + 1$ if we go around the D7-brane. Similarly, τ can undergo a more general $SL(2,\mathbb{Z})$ transformation around a (p,q)-brane. Notice that since the string coupling $g_s = e^{\phi}$,

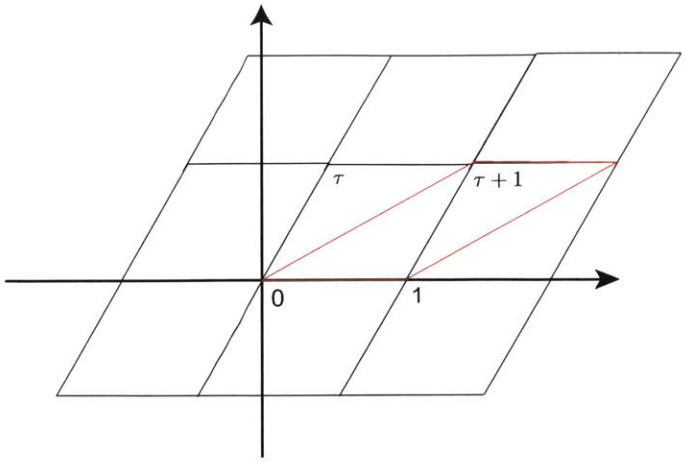

Figure 2-1: A 2-torus defined as a quotient of the complex plane, which stays the same if we replace τ by $\tau + 1$.

actually

$$\tau = C_0 + \frac{i}{g_s}. \tag{2.1.16}$$

Hence if we set $C_0 = 0$ for simplicity, then an $\mathrm{SL}(2,\mathbb{Z})$ transformation $\tau \to -1/\tau$ will transform g_s to $1/g_s$. This means that in the presence of general (p,q) 7-branes, weakly coupled IIB string theory can actually be transformed to a strongly coupled theory if one go around these 7-branes. In the presence of mutiple separated (p,q) 7-brane configurations, there does not exist a single $\mathrm{SL}(2,\mathbb{Z})$ frame where all of them can be transformed to D7-branes, and it is not clear which kinds of separate (p,q)-brane configurations are self-consistent.

This problem gives birth to F-theory, which provides an elegant geometric solution.

2.1.2 F-theory and M/F-duality

The hint of a geometric structure behind $\mathrm{SL}(2,\mathbb{Z})$ monodromy comes from the fact that $\mathrm{SL}(2,\mathbb{Z})$ is the modular group of a 2-torus. A 2-torus can be described as a quotient of the complex plane if we identify z with $z+1$ and $z+\tau$ for any $z \in \mathbb{C}$; see Figure 2-1. Now if we replace τ by $\tau + 1$, the 2-torus is actually unchanged. If we replace τ by $-1/\tau$, then the 2-torus can be mapped to the original one after a rotation and rescaling.

This suggests that we can put a 2-torus over each point on the compact manifold

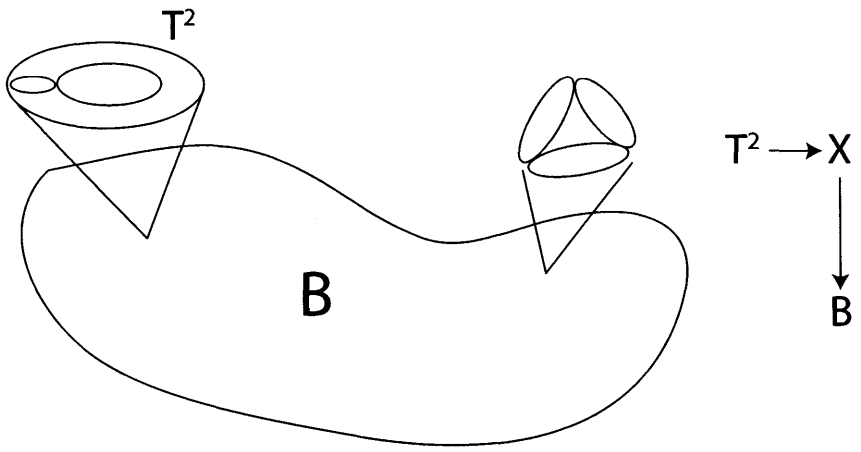

Figure 2-2: A elliptic fibered manifold X over the base B. A generic fiber will have the topology of T^2 but the fiber may be singular over some subsets of B.

B in the IIB compactification, which gives a T^2 fibration over B, see Figure 2-2. The value of the axiodilaton τ is identified with the parameter τ (known as the complex structure) of T^2. For a fiber bundle, the fiber over any point $p \in B$ should be homeomorphic. This is not required for a fibration, as the fiber could be singular over some subsets of B. These singular fibers exactly correspond to the point where τ cannot be defined uniquely, i. e. the location of 7-branes.

In order for the low dimensional theory to preserve a part of supersymmetry, the total space X is required to be Calabi-Yau. To understand this statement, we present a common definition of F-theory starting from M-theory.

First, we consider M-theory on a complex d-dimensional manifold X, which give rise to a supergravity theory in $(11-2d)$-dimensions. We take X to be a direct product $X = B \times T^2$, and denote the two S^1 cycles of the T^2 by S_{1A} and S_{1B}, and their radius R_A and R_B. Then we take the radii $R_A \to 0$. Since the string coupling $g_s \propto R_A$, this leads to weakly coupling IIA superstring theory compactified on $B \times S_{1B}$. Now we perform a T-duality in the S_{1B} direction, which maps the IIA theory to a weakly coupled IIB superstring theory on $B \times S'_{1B}$, where S'_{1B} has radius $R'_B = 1/R_B$. Hence if we shrink the radius $R_B \to 0$, then the size of S'_{1B} will grow to infinity and we will get a supergravity in $(10 - 2d)$ dimensions. Effectively, this is equivalent to a IIB theory on compactified on B.

Now, if we take X to be a T^2 fibration, this T-duality story still holds fiber by fiber despite the fact that τ varies over the base B. We have the following M/F-theory duality that generally holds:

If the elliptic fibers of X are shrunk to be zero size, which leads to a usually singular Calabi-Yau space X_{sing}, then M-theory on X_{sing} is dual to F-theory on X_{sing}.

Because of the existence of singular fibers in X that correspond to multiple (p, q) 7-brane configurations, there usually does not exist a single $\mathrm{SL}(2, \mathbb{Z})$ transformation that transform all the (p, q) 7-branes to D7 or O7-branes (Orientifold branes). Hence we will often find that the resulting theory is not weakly coupled IIB even in the limit $vol(T^2) \to 0$.

Now with the direct correspondence between M-theory and F-theory, we see that the Calabi-Yau condition of X should be satisfied since the supersymmetry property is directly transfered between theories that are dual to each other.

2.1.3 Gauge group and matter in F-theory

In the F-theory construction, the compact space is the singular one X_{sing}. To write down the physical fields in the low energy effective theory, we should first analyze the M-theory dual description on X where the fibers are not shrunk.

In M-theory, the fundamental object is the M2-brane that couples to a 3-form field C_3 electrically. As we have mentioned before, the complex codimension-one locus of 7-branes on B has singular fiber in X. These singular fiber is a union of multiple $\mathbb{P}^1$ (topologically 2-sphere) that are connected as an affine Dynkin diagram, as we will explain in the next section. If we call these 2-sphere components $\Gamma_1, \ldots, \Gamma_n$ (excluding the affine node), then the 1-form field

$$A_i = \int_{\Gamma_i} C_3 \ (i = 1, \ldots, n) \tag{2.1.17}$$

will correspond to U(1) gauge fields on the individual 7-branes.

Besides that, M2-brane wrapping different connected combinations of $\Gamma_1, \ldots, \Gamma_n$ will give rise to massive states in the M-theory description, with their mass pro-

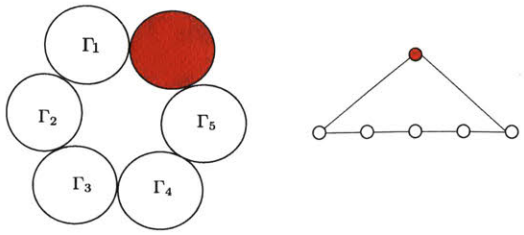

Figure 2-3: A singular fiber with the topology of $\hat{A}_5$ affine Dynkin diagram.

portional to the area of the wrapped 2-cycle. In the F-theory limit where Γ_is are shrunk to zero size, these states become massless as well. The claim is that A_is and the M2-brane wrapping states exactly correspond to the Cartan subalgebra and W-bosons of a non-Abelian gauge group[1]. For example, if the affine dynkin diagram is $\hat{A}_n$ (see Figure 2-3), there are n Cartan generators and $n(n+1)/2$ connected 2-cycles $\Gamma_i \bigcup \Gamma_{i+1} \ldots \Gamma_j$. Taking account of two orientations, these will produce $n(n+1)$ W-bosons. Then we have exactly $n^2 + 2n$ gauge bosons for SU$(n+1)$.

As we will see in the next section, all the simple Lie groups can be realized in this way, including the exceptional ones.

Matter fields charged under these non-Abelian gauge groups are physically given by open string modes between two stacks of 7-branes. Geometrically, this happens at the complex codimension-two locus where additional 2-cycles appear in the fiber.

Unlike the non-Abelian gauge groups, the Abelian gauge groups have a completely different origin in F-theory. In the perturbative string theory, you will usually expect that the gauge group from a stack of N D-branes is U(N). However, in the case of D7-branes, this U(1) is broken by a world volume coupling term of the D7-brane[48].

In fact, the Abelian groups in F-theory come from global data of the elliptic fibration: additional "rational sections" of the fibration. A section of a fibration is constructed by picking a point in the fiber for each point on the base, and it is topologically homeomorphic to the base. A rational section is a collection of "rational points" of elliptic curves, as we will discuss in the next section. Since these sections S_I are a real codimension-two subset of X, the Poincaré dual of them are 2-forms ω_I.

[1]The affine node does not contribute to the gauge group. The reason is M2-brane wrapping the affine node is identical to wrapping a generic smooth fiber T^2. The state from wrapping generic fiber corresponds to a KK (Kaluza-Klein) mode in the compactified theory.

Now the U(1) gauge fields are given by the decomposition of the M-theory 3-form field:

$$C_3 = \sum_I A_I \wedge \omega_I + \dots . \tag{2.1.18}$$

The matter charged under Abelian gauge groups comes from M2-brane wrapping additional 2-cycles over complex codimension-two locus on B as well, similar to the non-Abelian case.

2.2 Basics of complex algebraic geometry

2.2.1 Divisor and line bundles

In this section, we will define the terminology from complex algebraic geometry that will be used later, mostly using differential geometry language following [66].

The classical goal of algebraic geometry is to study the properties of algebraic equations in different number fields, using geometric intuition and terminology.

An *algebraic variety* is the set of points that solve a number of algebraic equations $f_i(x_1, \dots, x_n) = 0$ in an ambient space parametrized by the variables $x_1, \dots, x_n$. In this thesis, we always assume that the ambient space is complex projective space. The reason for using the complex field is the properties of algebraic completeness and the validity of fundamental theorem of algebra. For example, the algebraic equation $x^2 + 1 = 0$ does not have a solution if $x \in \mathbb{R}$, but it has two solutions if $x \in \mathbb{C}$.

The *projective space* $\mathbb{P}^n$ is a quotient of $\mathbb{C}^{n+1}$ by the identification $(x_1, x_2, \dots, x_{n+1}) \sim (\lambda x_1, \lambda x_2, \dots, \lambda x_{n+1})$ for $\lambda \neq 0$. The point $(x_1, x_2, \dots, x_{n+1}) = (0, 0, \dots, 0)$ is not included in $\mathbb{P}^n$. Similarly, a *weighted projective space* $\mathbb{P}^{k_1,k_2,\dots,k_n}$ is a quotient of $\mathbb{C}^{n+1}$ by the identification $(x_1, x_2, \dots, x_{n+1}) \sim (\lambda^{k_1} x_1, \lambda^{k_2} x_2, \dots, \lambda^{k_{n+1}} x_{n+1})$ for $\lambda \neq 0$.

$\mathbb{P}^n$ can be considered as the "compactification" of $\mathbb{C}^n$ where the points at infinity are included. The advantage is that for example considering two linear equations $ax + by = c$ and $ax + by = d (c \neq d)$ in $\mathbb{C}^2$. These two complex lines do not intersect each other since there is no common solution to them. However in $\mathbb{P}^2$, the well-defined algebraic equations invariant under the rescaling $(x, y, z) \sim (\lambda x, \lambda y, \lambda z)$ are

the homogeneous linear equations $ax+by=cz$ and $ax+by=dz$. Then they intersect at a point $(x,y,z)=(-b,a,0)$.

These homogeneous algebraic equations in $\mathbb{P}^n$ are called the *projective varieties*. In general, a degree d hypersurface of $\mathbb{P}^n$ is the solution to the following algebraic equation:

$$\sum_{a_1+\cdots+a_{n+1}=d} C_{a_1,a_2,\ldots,a_{n+1}} \prod_{i=1}^{n+1} x_i^{a_i} = 0 \tag{2.2.19}$$

In projective space $\mathbb{P}^n$, the *Bezóut's theorem* says that n hypersurfaces of degree $d_1, d_2, \ldots, d_n$ always intersect at $N = \prod_i d_i$ points, counting multiplicity. This fact shows that it makes sense to put all the hypersurfaces in $\mathbb{P}^n$ with the same degree into one class, since they have similar properties. In general, they are called a *divisor class*, which we will define as follows.

A *Weyl divisor* is a formal sum of hypersurfaces D_i in M:

$$D = \sum a_i D_i, \tag{2.2.20}$$

where $a_i \in \mathbb{Z}$. If $a_i \geq 0$ for all i, then it is called an *effective divisor*.

For a meromorphic function f on the complex manifold M, we can define a divisor with f as the defining function as follows.

Suppose F is the local defining equation of hypersurface D_i, then we define $\mathrm{ord}_{D_i}(G)$ of a holomorphic function G to be the maximal value of a such that we can write $G = F^a H$ in locally near a point $p \in D_i$. For a holomorphic function, this definition is independent of the point p. Now suppose that f can be written locally as $f = g/h$ where g and h are holomorphic functions that are relatively prime, then we define

$$\mathrm{ord}_{D_i}(f) = \mathrm{ord}_{D_i}(g) - \mathrm{ord}_{D_i}(h), \tag{2.2.21}$$

and the associated divisor

$$D = \sum \mathrm{ord}_{D_i}(f) D_i. \tag{2.2.22}$$

We can see that the negative coefficient of D_i actually means that the defining function

f has poles on D_i.

A very important fact about divisors is that they have a correspondence with *holomorphic line bundles* on M, which are vector bundles of rank 1 where the fibers are the vector space of holomorphic functions.

More precisely, for a holomorphic line bundle $\pi : L \to M$ on M, we can find a trivialization

$$\varphi_a : L_{U_\alpha} \to U_\alpha \times \mathbb{C} \tag{2.2.23}$$

on each coordinate patch U_α which together covers M. $L_{U_\alpha} = \pi^{-1}U_\alpha$, which is a subset of L. Now the line bundle is parametrized by the transition function $g_{\alpha\beta} : U_\alpha \bigcap U_\beta \to \mathbb{C}^*$ between different coordinate patches:

$$g_{\alpha\beta}(z) = (\varphi_\alpha \circ \varphi_\beta^{-1})|_{L_z}. \tag{2.2.24}$$

Since the line bundle is holomorphic, $g_{\alpha\beta}$ is non-vanishing and statisfies

$$g_{\alpha\beta}g_{\beta\alpha} = 1 \ , \ g_{\alpha\beta}g_{\beta\gamma}g_{\gamma\alpha} = 1. \tag{2.2.25}$$

The set of line bundles on M has a group structure called the *Picard group* $\mathrm{Pic}(M)$. Suppose that the line bundles L and L' have transition functions $\{g_{\alpha\beta}\}$ and $\{g'_{\alpha\beta}\}$ respectively, then the group multiplication is given by the tensor product, $L \otimes L'$ with transition function $\{g_{\alpha\beta}g'_{\alpha\beta}\}$. The inverse is given by the *dual bundle*: L^* with transition function $\{g_{\alpha\beta}^{-1}\}$.

Now the map from divisors to line bundles is easy to define. Suppose that the divisor D has non-zero meromorphic local defining equations $\{f_\alpha\}$ in the local coordinate patches $\{U_\alpha\}$. Then $g_{\alpha\beta} = f_\alpha/f_\beta$ gives the transition function of the *associated line bundle* $[D]$ that satisfies (2.2.25). Note that for two divisors D and D' with local defining functions $\{f_\alpha\}$ and $\{f_{\alpha'}\}$, the divisor $D+D'$ defined by $\{f_\alpha f_{\alpha'}\}$ exactly equals to the line bundle $[D]\otimes[D']$. Hence the map from the set of divisors to $\mathrm{Pic}(M)$ is a homomorphism.

Moreover, if $D = (f)$ is defined by a global meromorphic function f on M, then

f_α can be taken to be in the same form for any coordinate patch U_α, and $f_\alpha/f_\beta \equiv 1$, which means that the associated line bundle $[D] = [(f)]$ is trivial. We can thus define an equivalence relation $D \sim D'$ if $D = D' + (f)$, which is called *linear equivalence.* After taking the quotient of the set of divisors by linear equivalence, we get the set of *divisor classes*, which is completely isomorphic to the Picard group of line bundles. In the later part of the discussion, we often do not distinguish between line bundle and divisor class. For example, we also use the notation $L + L'$ and $-L$ to denote the Picard group operation instead of $L \otimes L'$ and L^*. In this decription of Picard group as a linear space, its rank $\mathrm{rk}(\mathrm{Pic}(M))$ is called *Picard rank.*

The divisor classes are also isomorphic to the set of real homology class $H^{2n-2}(M, \mathbb{Z})$ for M with complex dimension n, and we can define intersection numbers of n divisors $D_1 \cdot D_2 \cdot \cdots \cdot D_n \in \mathbb{Z}$.

The condition that a divisor is effective is equivalent to the existence of a global holomorphic section of its associated line bundle. The set of holomorphic sections of a line bundle L is denoted as $\mathcal{O}(L)$, which is a linear space usually refered to as the *linear system* $|L|$. Its dimension is $H^0(M, \mathcal{O}(L))$, or simply written as $H^0(L)$ in the later parts of the thesis.

Since the sum of two effective divisors is another effective divisor, the set of effective divisor classes form an integral cone in $\mathbb{Z}^{\mathrm{rk}(\mathrm{Pic}(M))}$, which is called the *effective cone.* Similarly, the set of complex curves in $H^2(M, \mathbb{Z})$ forms the *Mori cone* of curves. For complex surfaces,the effective cone is equivalent to the Mori cone.

Now we are going to introduce two of the most important line bundles that we will always encounter later.

The first one is the *canonical bundle* K_M, which is defined by

$$K_M = \bigwedge^{\dim(M)} T_M^*, \tag{2.2.26}$$

where T_M is the holomorphic tangent bundle of M in usual (complex) differential geometry and T_M^* is its dual (cotangent bundle). Its dual bundle $-K_M$ is called *anticanonical bundle.* The canonical bundle encodes the curvature information of the

manifold. If the manifold is Calabi-Yau, then its canonical bundle is trivial $K_M \sim 0$.

The second one is the *normal bundle* N_D of a hypersurface D in M, defined by

$$N_D = \frac{T_M|_D}{T_D}. \tag{2.2.27}$$

It is usually computed by the adjunction formula

$$N_D = D|_D. \tag{2.2.28}$$

Another adjunction formula helps to compute the canonical bundle of the hypersurface D embedded in the manifold M:

$$K_D = K_M|_D + N_D = (K_M + D)|_D. \tag{2.2.29}$$

As an example, for the complex projective space $\mathbb{P}^n$, the canonical bundle is

$$K(\mathbb{P}^n) = -(n+1)H, \tag{2.2.30}$$

where H is corresponds to the hyperplane divisor class (hypersurface of degree 1). The intersection number of n copies of H is

$$H^n = 1, \tag{2.2.31}$$

and the intersection numbers among n divisors a_1H, $a_2H, \ldots, a_nH$ is then

$$\prod_{i=1}^{n} a_i H = \prod_{i=1}^{n} a_i, \tag{2.2.32}$$

which gives an example of the Bezóut's theorem that we introduced earlier.

We can use the adjunction formula to compute the normal bundle of divisors in $\mathbb{P}^n$. For example, for the degree-$(n+1)$ hypersurface $D = (n+1)H$, we have $K_D \sim 0$, which means that D is Calabi-Yau. We have thus found a way to construct a series of Calabi-Yau manifolds.

Another example is the computation of the genus of curves on $\mathbb{P}^2$. Since $K(\mathbb{P}^2) = -3H$, the canonical class of the curve $C = aH$ is given by

$$K_C = a(a-3)H \cdot H = a^2 - 3a. \tag{2.2.33}$$

Since for a curve C, $K_C = 2g - 2$, we can compute its genus

$$g = \frac{a^2 - 3a}{2} + 1. \tag{2.2.34}$$

For example, the degree 1 line and degree 2 conic on $\mathcal{P}^2$ has genus $g = 0$, which are called *rational curves.* The degree 3 cubic has genus $g = 1$, which is an elliptic curve.

2.2.2 Birational geometry

A fundamental problem in algebraic geometry is the classification of topologically distinct manifolds. Since there are infinitely many of them, a more tractable approach is to classify these manifolds up to a weaker equivalence called *birational equivalence.*

A rational map $f : X \to Y$ is a locally polynomial map from an open subset $U \subset X$ to Y. X and Y are birationally equivalent if there exist rational maps $f : X \to Y$ and $f^{-1} : Y \to X$. For example,

$$x = \frac{2t}{1+t^2}\ ,\ y = \frac{1-t^2}{1+t^2} \tag{2.2.35}$$

maps the line to the a circle $x^2 + y^2 = 1$, despite that they have different topology.

A complex manifold of dimension n is called *rational* if it is birational equivalent to $\mathbb{P}^n$.

A very important class of birational maps is the *blow up* map. Suppose that we want to blow up a complex codimension-k subset U in a n-dimensional manifold X, which is defined by local equations

$$x_1 = x_2 = \cdots = x_k = 0 \tag{2.2.36}$$

in the local coordinate patch $\Delta \supset U$, then we define the submanifold $\tilde{\Delta} \in \Delta \times \mathbb{P}^{k-1}$ as

$$\tilde{\Delta} = \{x_i y_j = x_j y_i, \forall i, j\}. \tag{2.2.37}$$

Here $(y_1, \ldots, y_k)$ are homogeneous projective coordinates of $\mathbb{P}^{k-1}$. We can define the projection map $\pi : \tilde{\Delta} \to \Delta$ by restricting to the x_i components of (x_i, y_i). Then we define the *exceptional divisor* E to be the locus $\pi^{-1}(U)$. Note that E always have the topology of a $\mathbb{P}^{k-1}$ bundle over U from this definition. It is also easy to check that the projection map

$$\pi : \tilde{\Delta} - E \to \Delta - U \tag{2.2.38}$$

is an isomorphism. Hence we can define the blow up of X to be

$$Y = (X - U) \bigcup \tilde{\Delta}. \tag{2.2.39}$$

Since E is a new generator in the Picard group of Y, we have

$$\mathrm{rk}(\mathrm{Pic}(Y)) = \mathrm{rk}(\mathrm{Pic}(X)) + 1. \tag{2.2.40}$$

The canonical line bundle of Y is related to K_X by

$$K_Y = \pi_* K_X + kE \tag{2.2.41}$$

where π_* is the pullback map from $\mathrm{Pic}(X)$ to $\mathrm{Pic}(Y)$. In the later discussions, we often omit this π_*.

If U is contained in a divisor $D \subset X$ with multiplicity $m = mult_D(X)$, then after the blow up, D will be transformed to

$$D' = D - mE, \tag{2.2.42}$$

via a *proper transformation.*

The reversal operation of blow up is called blow down or contract the exceptional

divisor E. For a complex surface, the exceptional divisor is always a $\mathbb{P}^1$ and has self-intersection (-1). Hence the only curves that can be contracted on a surface are rational (-1)-curves.

The proper transformation of a divisor () has self-intersection number

$$D'^2 = (D - mE)^2 = D^2 + m^2E^2 = D^2 - m^2. \tag{2.2.43}$$

As an application, the birational classification of complex surfaces can be achieved by blowing down the complex surface recursively until it cannot be blown down anymore. This is called "minimal model program" of surfaces that is well established. On the other hand, the similar program: "Mori program" of complex threefold is highly complicated involving singularities[98]. We will use necessary results from them in Chapter 3 and 4.

2.3 Mathematics of elliptic fibration

An elliptic curve is a complex one-dimensional manifold with the topology of T^2. There are two ways to describe it: the quotient of complex plane in Figure 2-1 and the following hypersurface equation in an ambient space Y known as the Weierstrass equation:

$$y^2 = x^3 + fxz^4 + gz^6. \tag{2.3.44}$$

Here (x, y, z) are coordinates of the complex weighted projective space $\mathbb{P}^{2,3,1}$.

For a single elliptic curve, f and g are complex numbers. While for an elliptic fibration $\pi : X \to B$, f and g are polynomials in terms of local coordinates on B, and they are called *Weierstrass polynomials.*

Apparently, the point $(x, y, z) = (1, 1, 0)$ is always a solution to (2.3.44), which is called the zero point of the elliptic curve. In the case of an elliptic fibration, we can pick this zero point for every $p \in B$, which forms the "zero section" Z. In this sense, if there is a Weierstrass equation then the elliptic fibration always has a global section.

Outside of the zero section, we can set $z = 1$ by rescaling, and simplify (2.3.44) to

$$y^2 = x^3 + fx + g, \tag{2.3.45}$$

which is more commonly used in the later discussions.

Equation (2.3.45) is singular whenever $\Delta = 4f^3 + 27g^2 = 0$ on B. We define this quantity Δ as the *Discriminant* of the elliptic fibration and the subset $\Gamma \in B$ where $\Delta = 0$ the discriminant locus. For a general elliptic fibration, it is known that the canonical class of X is given by

$$K_X \sim K_B + \sum_i \frac{\delta_i}{12}[\Gamma_i], \tag{2.3.46}$$

where Γ_is are the irreducible components of the discriminant locus and $\delta_i = \mathrm{ord}_{\Gamma_i}(\Delta)$[87]. Hence in order to have $K_X \sim 0$, we have

$$\sum_i \delta_i[\Gamma_i] = -12K_B \tag{2.3.47}$$

or

$$\Delta \in \mathcal{O}(-12K_B). \tag{2.3.48}$$

Since $\Delta = 4f^3 + 27g^2$, it is required that f and g are holomorphic sections of line bundles:

$$f \in \mathcal{O}(-4K_B)\ ,\ g \in \mathcal{O}(-6K_B). \tag{2.3.49}$$

The Weierstrass model defined in this way is usually singular. For example, if $f \sim u^2$, $g \sim u^2$, then the equation

$$y^2 = x^3 + f_2u^2x + g_2u^2 \tag{2.3.50}$$

is clearly singular at $x = y = u = 0$. To get a valid M-theory description, we need to resolve this singularity by blowing up the codimension-two locus $x = y = u = 0$. The resolution process of such singular Weierstrass models have been extensively

ord(f)	ord(g)	ord(Δ)	Kodaira's fiber type	Topology
≥ 0	≥ 0	0	I_0	a smooth elliptic curve
0	0	1	I_1	a nodal curve with a double point
0	0	$n \geq 2$	I_n	affine $\hat{A}_{n-1}$
≥ 1	1	2	II	a cusp curve
1	≥ 2	3	III	affine $\hat{A}_1$, two $\mathbb{P}^1$s intersect at a double point
≥ 2	2	4	IV	affine $\hat{A}_2$, three $\mathbb{P}^1$s intersect at a triple point
2	3	$6+n$	I_n^*	affine $\hat{D}_{n+4}$
≥ 3	4	8	IV^*	affine $\hat{E}_6$
3	≥ 5	9	III^*	affine $\hat{E}_7$
≥ 4	5	10	II^*	affine $\hat{E}_8$

Table 2.1: Kodaira's classification of elliptic fiber for the case of elliptic surfaces.

studied[53, 94, 51, 52]. A common description of the blow up process is by the replacement

$$x = \xi x_1 \ , \ y = \xi y_1 \ , \ u = \xi u_1, \tag{2.3.51}$$

where (x_1, y_1, u_1) are projective coordinates of a $\mathcal{P}^2$ and $\xi = 0$ is the exceptional divisor. The equation (2.3.50) is transformed to

$$y_1^2\xi^2 = x_1^3\xi^3 + f_2u^2x\xi^3 + g_2u^2\xi^2. \tag{2.3.52}$$

After the factor ξ^2 is removed from this hypersurface equation, the equation

$$y_1^2 = x_1^3\xi + f_2u_1^2x_1\xi + g_2u_1^2 \tag{2.3.53}$$

is smooth because the locus $x_1 = y_1 = u_1 = 0$ was removed. This resolution is called a *crepant resolution* since the canonical divisor of the hypersurface is unchanged. This is because although we have blown up a codimension-two locus on X and modified K_X by $2E$ following (2.2.41), this $2E$ term is removed from (2.3.52) to (2.3.53).

After this resolution, the elliptic fiber over $u = 0$ becomes a union of $\mathbb{P}^1$s in the form of affine Dynkin diagram, as we have mentioned before. All the possible topological types of these singular fibers for elliptic surfaces have been classified by Kodaira[87]. They can be computed systematically by "Tate's algorithm"[119] according the order of vanishing of f, g and Δ. We list them in Table 2.1.

From the topology of the singular fibers, we can see that the gauge groups in 8D F-theory from elliptic K3 are ADE ones, i. e. SU(N), SO($2N$), E_6, E_7 and E_8. For elliptic threefolds and fourfolds, the Kodaira's classification still roughly holds for singular fibers over codimension-one locus on the base. However, for some of the Kodaira fiber types, the actual topology and gauge group in F-theory is determined by additional information called "monodromy"[63].

For example, in the case of type IV singular fiber, as we described in (2.3.50). After the resolution, if we look at the exceptional divisor $\xi = 0$, the equation (2.3.53) becomes

$$y_1^2 - g_2 u_1^2 = 0, \tag{2.3.54}$$

now if g_2 is a complete square, then this exceptional divisor is reducible and the topology of the singular fiber is $\hat{A}_2$, giving SU(3) gauge group. Otherwise, the topology is $\hat{A}_1$ and the gauge group is SU(2).

Similar thing happens for type I_0^* fiber, suppose that f and g have the following series expansion near a divisor $u = 0$:

$$f = \sum_{i=2}^{m} f_i u^i \ , \ g = \sum_{i=3}^{n} g_i u^i, \tag{2.3.55}$$

then the criterion is about the cubic polynomial

$$M(\psi) = \psi^3 + f_2 \psi + g_3. \tag{2.3.56}$$

If $M(\psi)$ is completely irreducible, has two components or three components, then the gauge group is G_2, SO(7) or SO(8) respectively.

For the case of type IV^*, it is similar to type IV. If g_4 is a complete square, then the gauge group is E_6, otherwise it is F_4. We write a complete list of the criteria for gauge groups in Table 4.1.

In this thesis, we never allow the cases where $\text{ord}(f) \geq 4$ and $\text{ord}(g) > 6$. This is called "codimension-one (4,6) singularity" and the singular Weierstrass model cannot be resolved while preserving the Calabi-Yau property. Hence the F-theory

ord(f)	ord(g)	ord(Δ)		$M(\psi)$	Gauge group
0	0	2	I_2	-	SU(2)
0	0	$n \geq 3$	I_n	$\psi^2 + (9g/2f)\|_{u=0}$	Sp$\lfloor \frac{n}{2} \rfloor$ or SU(n)
1	≥ 2	3	III	-	SU(2)
≥ 2	2	4	IV	$\psi^2 - g_2$	SU(2) or SU(3)
≥ 2	≥ 3	6	I_0^*	$\psi^3 + f_2\psi + g_3$	G_2 or SO(7) or SO(8)
2	3	$2n+1 (n \geq 3)$	I_{2n-5}^*	$\psi^2 + \frac{1}{4}\Delta_{2n+1}(2uf/9g)^3\|_{u=0}$	SO($4n-3$) or SO($4n-2$)
2	3	$2n+2 (n \geq 3)$	I_{2n-4}^*	$\psi^2 + \Delta_{2n+2}(2uf/9g)^2\|_{u=0}$	SO($4n-1$) or SO($4n$)
≥ 3	4	8	IV^*	$\psi^2 - g_2$	F_4 or E_6
3	≥ 5	9	III^*	-	E_7
≥ 4	5	10	II^*	-	E_8

Table 2.2: The list of the criteria for all the gauge groups in F-theory on a divisor $u = 0$. $M(\psi)$ is the "monodromy cover polynomial". When $M(\psi)$ is completely irreducible, the gauge group is given by the leftmost one. When $M(\psi)$ is completely reducible, the gauge group is given by the rightmost one.

low energy description does not have supersymmetry even at the compactification scale. Although it is not proven, it is also possible that none of the geometries with codimension-one (4,6) singularity can give a valid supergravity solution to the Einstein equations.

Apart from the non-Abelian gauge groups, Abelian gauge group may appear if the Weierstrass equation (2.3.44) has additional rational sections other than the zero section $(x, y, z) = (1, 1, 0)$. That is, if there exists global holomorphic functions λ, α and b that satisfies

$$\alpha^2 = \lambda^3 + f\lambda b^4 + gb^6. \tag{2.3.57}$$

These rational sections form the *Mordell-Weil group* $MW(X)$ of the elliptic fibration, which is highly non-trivial to compute. It is an additive group following the addition of points on an elliptic curves. For two points (x_1, y_1) and (x_2, y_2) on an elliptic curve $y^2 = x^3 + fx + g$, their addition (x_3, y_3) is computed as

$$\lambda = \frac{y_2 - y_1}{x_2 - x_1} \ , \ x_3 = \lambda^2 - x_1 - x_2 \ , \ y_3 = \lambda(x_1 - x_3) - y_1. \tag{2.3.58}$$

The doubling of (x_1, y_1) is given by the same formula with $\lambda = (3x_1^2 + a)/(2y_1)$, and the inverse of a point is simply $(x_1, -y_1)$. It is then obvious that the addition of two rational sections is another rational section of the elliptic fibration.

The rank of this additive group is called *Mordell-Weil rank* $\mathrm{rk}(MW(X))$, which quantify the number of U(1) gauge groups in the low energy effective theory.

For a "generic elliptic fibration", we mean that f and g are generic holomorphic sections of line bundles $-4K_B$ and $-6K_B$, such that Δ vanishes to the lowest order on any divisor on B. In this case, the gauge groups are minimal for any possible fibration over B, and they are called "non-Higgsable gauge groups" that characterize the base geometry[101].

For example, any gauge group from I_n fiber in Table 4.1 is not non-Higgsable. Since if $\mathrm{ord}(f,g)=0$ and $\mathrm{ord}(\Delta)>1$, f and g have to be non-generic polynomials for $\Delta=4f^3+27g^2$ vanishes to higher order at $u=0$. The only possible Kodaira singular fibers on a generic fibration are I_0, I_1, II, III, IV, I_0^*, IV^*, III^* and II^*, and the only possible non-Higgsable gauge groups are SU(2), SU(3), G_2, SO(7), SO(8), F_4, E_6, E_7 and E_8.

2.4 Toric geometry

We have seen that the computation of holomorphic section of line bundles is crucial in the F-theory applications. However, they are usually hard to write out for a general complex manifold. Nonetheless, there exists a class of algebraic varieties called *toric variety*, which is relatively simple[59, 36, 34]. They have been applied to a lot of string geometry constructions, for example[95, 2, 56, 57], and we are also going to use them in the later chapters.

The formal definition of toric variety is a complex algebraic variety X with a complex torus $T=(\mathbb{C}^*)^r$ dense in X, such that there exists an action of T on X whose restriction to $T\subset X$ is the complex multiplication.

For example, $\mathbb{P}^r$ is toric since we can take

$$T=\{x:x_i\neq 0\ (i=1,\ldots,r+1)\}\subset\mathbb{P}^r \tag{2.4.59}$$

and the action of T on X is just the complex multiplication by x.

For more general toric varieties, they are constructed according to discrete combinatoric data called *toric fan*. A toric fan Σ is a collection of strongly convex polyhedral cones $\sigma \in N = \mathbb{Z}^r$. A k-dimensional strongly convex polyhedral cone generated by vectors $v_1, v_2, \ldots, v_k$ is the set

$$\sigma = \{\sum_{i=1}^{k} a_i v_i | a_i \geq 0\}, \tag{2.4.60}$$

which satisfies $\sigma \bigcap (-\sigma) = 0$.

A toric fan Σ always satisfies the following two conditions:

(1) each face of a cone $\sigma \in \Sigma$ is also a cone in Σ

(2) $\forall \sigma_1, \sigma_2 \in \Sigma$, $\sigma_1 \bigcap \sigma_2 \in \Sigma$.

We denote the set of k-dimensional cones in Σ by $\Sigma(k)$. The set of 1-dimensional rays $\Sigma(1)$ are $v_1, \ldots, v_n$, where $n = |\Sigma(1)|$. We use $v_{i,j}$ to denote the j-th component of the vector v_i, $(j = 1, \ldots, r)$.

Now we can explicitly define the geometry of the toric variety X_Σ associated to Σ as a quotient space of $\mathbb{C}^n$.

For each $v_i \in \Sigma(1)$, we assign a local coordinate x_i. Then for any subset $S \subset \Sigma(1)$ that does not span a cone of Σ, we define a linear space $V(S) \subset \mathbb{C}^n$ to be the subspace with $x_i = 0$ for all $v_i \in S$. Now we define $Z(\Sigma)$ to be the union of all the $V(S)$ and the toric variety X_Σ will be defined as

$$X_\Sigma = (\mathbb{C}^n - Z(\Sigma))/G \tag{2.4.61}$$

The group G is defined by the kernel of $\phi : (\mathbb{C}^*)^n \to (\mathbb{C}^*)^r$:

$$\phi : (x_1, \ldots, x_n) \to (\prod_{i=1}^{n} x_i^{v_{i,1}}, \ldots, \prod_{i=1}^{n} x_i^{v_{i,r}}). \tag{2.4.62}$$

Since the group G reduces a n-dimensional vector space to a r-dimensional one, we see that X_Σ is indeed a r-dimensional toric variety.

Another way to think about toric variety is that each r-dimensional cone $\sigma \in \Sigma(r)$

generated by $v_1, \ldots, v_r$ corresponds to a coordinate patch where $x_1 = x_2 = \cdots = x_r = 0$ can happen, but the other $x_i \neq 0$. Then the whole X_Σ is glued together by these coordinate patches.

A toric variety is smooth if and only if all the r-dimensional cones $\sigma \in \Sigma(r)$ have unit volume, or equivalently the matrix $v_{i,j}$ has determinant ± 1. Hence for a smooth toric variety, the 1D ray v_i always satisfy

$$\gcd(v_{i,1}, v_{i,2}, \ldots, v_{i,r}) = 1. \tag{2.4.63}$$

Another nice property of the toric fan of a smooth toric variety is that for any $\sigma \in \Sigma(r)$, we can find a $\mathrm{SL}(r, \mathbb{Z})$ transformation to transform the generator of σ to $v_1 = (1, 0, 0, \ldots, 0)$, $v_2 = (0, 1, 0, \ldots, 0), \ldots, v_r = (0, 0, \ldots, 1)$.

A toric variety is compact if and only if $\bigcup \sigma = \mathbb{Z}^r$, or equivalently the 1D rays $v_1, \ldots, v_n$ span $\mathbb{Z}^r$.

The subset of a toric varieties $x_1 = x_2 = \cdots = x_k = 0$ corresponds to the cone $\sigma \in \Sigma(k)$ generated by rays $v_1, \ldots, v_k$. A *toric divisor* $D_i \in X_\Sigma$ corresponds to the 1D ray v_i whose local equation is $x_i = 0$. A codimension-two locus $D_i \bigcap D_j \in X_\Sigma$ corresponds to the 2D cone $v_i v_j$ with local equation $x_i = x_j = 0$, etc. All these subsets are G-invariant.

In fact, the Picard group and the effective cone of divisors of X_Σ is generated by these toric divisors (classes) D_i. The Picard rank $\mathrm{rk}(\mathrm{Pic}(X_\Sigma)) = n - r$, because of the following r linear equivalence relations between D_is:

$$\sum_{i=1}^{n} v_{i,j} D_i = 0 \ , \ (j = 1, \ldots, r). \tag{2.4.64}$$

Similarly, the Mori cone of curves is generated by the toric curves given by cones $\sigma \in \Sigma(k-1)$.

The canonical divisor of a toric variety is given by

$$K_{X_\Sigma} = -\sum_{i=1}^{n} D_i. \tag{2.4.65}$$

For a compact toric variety, we can never have $K_{X_\sigma} = 0$ or X_σ is Calabi-Yau.

The intersection numbers between r toric divisors are computed as follows. For smooth toric varieties, the intersection number between r distinct $D_1, \ldots, D_r$ is 1 if $v_1, \ldots, v_r$ are generators of the same r-dimensional cone, but 0 if otherwise. Actually, if v_i and v_j are not contained in any cone $\sigma \in \Sigma(2)$ simultaneously, then any intersection number involving D_i and D_j vanishes, since from the definition x_i and x_j cannot vanish simultaneously. The other intersection numbers involving self-intersections can all be computed recursively using (2.4.64).

The blow up of toric variety along a $(r-k)$-dimensional toric subvariety $D_1 D_2 \ldots D_k$ can be easily discribed by adding a new ray $v_E = \sum_{i=1}^{k} v_i$ to the toric fan. The original k-dimensional cone $v_1 v_2 \ldots v_k$ is subdivided into $v_1 v_2 \ldots v_{k-1} v_E$, $v_1 v_2 \ldots v_{k-2} v_k v_E$, $\ldots$, $v_2 v_3 \ldots v_k v_E$. Any higher dimensional cone including $v_1 v_2 \ldots v_k$ as a subcone is also subdivided in this way.

One of the most important feature of toric varieties is that the holomorphic section of line bundles on X_Σ is generated by monomials that correspond to points in the dual lattice $M = N^* = \mathbb{Z}^r$. For a line bundle

$$L = \sum_{i=1}^{n} a_i D_i \tag{2.4.66}$$

in terms of the toric divisors, we define the polytope

$$\mathcal{L} = \{u \in M = \mathbb{Z}^r | \forall v_i \ , \ \langle u, v_i \rangle \geq -a_i\}, \tag{2.4.67}$$

where $\langle u, v \rangle$ is the Euclidean inner product on $\mathbb{Z}^r$. Now a general holomorphic section of L is written as

$$s_L = \sum_{u \in \mathcal{L}} c_u \prod_{i=1}^{n} x_i^{\langle u, v_i \rangle + a_i}, \tag{2.4.68}$$

where c_u are complex coefficients. From the definition of $\mathcal{L}$, one can easily see that s_L indeed has no pole anywhere.

For the most important line bundles $-4K_B$ and $-6K_B$ in F-theory, they are

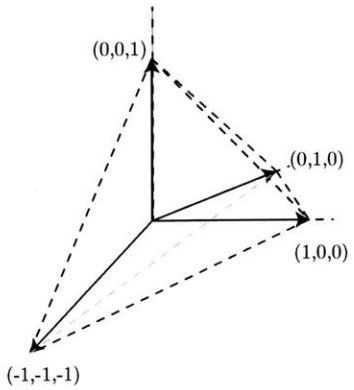

Figure 2-4: The toric fan of $\mathbb{P}^3$.

generated by monomials that correspond to points in the following two polytopes:

$$\mathcal{F} = \{u \in M = \mathbb{Z}^r | \forall v_i \ , \ \langle u, v_i \rangle - 4\}, \tag{2.4.69}$$

$$\mathcal{G} = \{u \in M = \mathbb{Z}^r | \forall v_i \ , \ \langle u, v_i \rangle - 6\}. \tag{2.4.70}$$

The order of vanishing of $f \in \mathcal{O}(-4K_B)$ and $g \in \mathcal{O}(-6K_B)$ on a divisor D_i is then given by

$$\text{ord}_{D_i}(f) = \min_{u \in \mathcal{F}} \langle u, v_i \rangle + 4 \ , \ \text{ord}_{D_i}(g) = \min_{u \in \mathcal{G}} \langle u, v_i \rangle + 6, \tag{2.4.71}$$

for the case of a generic fibration over $B = X_\Sigma$. They are crucial for the identification of non-Higgsable gauge groups on D_i.

To determine the actual gauge group, we also need the monodromy cover information, see Table 4.1. For the case of type IV fiber, the gauge group is SU(3) if and only if the g_2 coefficient only has one monomial that is a complete square. For the case of type IV^* fiber, the gauge group is E_6 if and only if the g_4 coefficient only has one monomial that is a complete square.

As an simple example of toric variety, $\mathbb{P}^n$ is given by a fan $\Sigma \subset \mathbb{Z}^n$ with 1D rays $v_1 = (1, 0, \ldots, 0)$, $v_2 = (0, 1, \ldots, 0)$, $v_n = (0, 0, \ldots, 1)$ and $v_{n+1} = (-1, -1, \ldots, -1)$, see Figure 2-4 for the case of $\mathbb{P}^3$. The set of n-dimensional cones are $\{v_1 v_2 \ldots v_n$, $v_1 v_3 \ldots v_{n+1}$,$v_2 v_3 \ldots v_{n+1}\}$.

Because of the linear equivalence (2.4.64), all the divisors $D_1, D_2, \ldots, D_{n+1}$ are linearly equivalent to the degree 1 hypersurface H. The canonical divisor is then

$$K(\mathbb{P}^n) = -(n+1)H. \tag{2.4.72}$$

The Picard group of $\mathbb{P}^n$ is one dimensional and generated by the toric divisor H. Using (2.4.67) and (2.4.68), we can see that the holomorphic section of the line bundle dH is given by the points in the polytope

$$p(dH) = \{u = (u_1, \ldots, u_n) | \forall i, u_i \geq 0 \ , \ \sum_{i=1}^{n} u_i \leq d\}, \tag{2.4.73}$$

where each of the point u gives the monomial

$$m_u = x_{n+1}^{d-\sum_{i=1}^{n} u_i} \prod_{i=1}^{n} x_i^{u_i}. \tag{2.4.74}$$

They are exactly the components of a homogeneous polynomial of degree d.

The line bundle $-4K_{\mathbb{P}^n}$ and $-6K_{\mathbb{P}^n}$ are $4(n+1)H$ and $6(n+1)H$ respectively. For generic sections of these line bundles, f and g does not vanish on any codimension-1 locus and there is no non-Higgsable gauge group.

Chapter 3

Classification of complex base surfaces

3.1 6D F-theory and non-Higgsable clusters

F-theory compactified on an elliptic Calabi-Yau threefold has a low energy description of 6D $(1,0)$ supergravity. The massless particle spectrum includes supergravity multiplet, tensor multiplet, vector multiplet and hypermultiplet. The particle spectrum of these supermultiplets can be found in Appendix A.

We usually denote the number of tensor multiplets, vector multiplets and hypermultiplets by T, V and H respectively.

In six-dimensions, there exists pure gravitational anomaly since $d \equiv 2(\text{mod } 4)$[4]. The anomaly comes from 1-loop rectangle diagram, and it can be cancelled by "generalized Green-Schwarz mechanism"[65, 117, 50, 54] including the tree level diagram with a 2-form tensor field, see Figure 3-1.

Suppose that the gauge group of the 6D supergravity is a product of non-Abelian groups $G = \prod_\kappa G_\kappa$, and the field strength of G_κ is F_κ. For a gauge group G_κ, there are charged hypermultiplets under representations R_κ^I labeled by I.

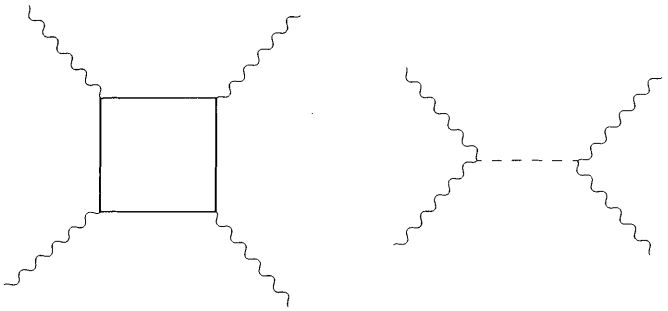

Figure 3-1: A picture of Green-Schwarz mechanism in 6D. The wavy lines are graviton, solid lines are fermions and the dased line is the 2-form tensor field.

The anomaly cancellation criterion is that the 8-form anomaly polynomial

$$\begin{aligned} I_8(R,F) = &-\frac{1}{5760}(H-V+29T-273)\left[\mathrm{tr}R^4+\frac{5}{4}(\mathrm{tr}R^2)^2\right]-\frac{1}{128}(9-T)(\mathrm{tr}R^2)^2 \\ &-\frac{1}{96}\left[\sum_\kappa \mathrm{Tr}F_\kappa^2-\sum_{I,\kappa}x_I^\kappa \mathrm{tr}_{R_\kappa^I}F_\kappa^2\right] \\ &+\frac{1}{24}\left[\sum_\kappa \mathrm{Tr}F_\kappa^4-\sum_{I,\kappa}x_I^\kappa \mathrm{tr}_{R_\kappa^I}F_\kappa^4-6\sum_{I,\kappa,\lambda}x_I^{\kappa\lambda}(\mathrm{tr}_{R_\kappa^I}F_\kappa^2)(\mathrm{tr}_{R_\lambda^I}F_\lambda^2)\right] \end{aligned} \tag{3.1.1}$$

can be factorized into

$$I_8 = -\frac{1}{32}\Omega_{\alpha\beta}X_4^\alpha X_4^\beta. \tag{3.1.2}$$

In I_8, x_I^κ and $x_I^{\kappa\lambda}$ are the multiplicity of representations under R_I^κ and $(R_I^\kappa, R_I^\lambda)$. tr and Tr denotes the trace under fundamental and adjoint representation respectively.

The matrix $\Omega_{\alpha\beta}$ is the symmetric metric of group $\mathrm{SO}(1,T)$, and X_4 is a four form field in the vector representationof $\mathrm{SO}(1,T)$, which has the component

$$X_4^\alpha = \frac{1}{2}a^\alpha \mathrm{tr}R^2+\sum_\kappa\left(\frac{2b_\kappa^\alpha}{\lambda_\kappa}\right)\mathrm{tr}F_\kappa^2. \tag{3.1.3}$$

The coefficients in X_4^α is chosen as a normalization convention, the factors λ_κ are given in Table 3.1.

From (3.1.1), (3.1.2) and (3.1.3), we can write down the following six anomaly

group	SU(N)/SO(N)/Sp(N)	G_2	F_4/E_6	E_7	E_8
λ_κ	1	2	6	12	60

Table 3.1: The group theory numbers λ for each simple Lie group.

cancellation equations:

$$273 = H - V + 29T \tag{3.1.4}$$

$$a \cdot a = 9 - T \tag{3.1.5}$$

$$a \cdot b_\kappa = \frac{1}{6}\lambda_\kappa(A^\kappa_{adj} - \sum_I x^\kappa_I A^\kappa_I) \tag{3.1.6}$$

$$b_\kappa \cdot b_\kappa = -\frac{1}{3}\lambda^2_\kappa(C^\kappa_{adj} - \sum_I x^\kappa_I C^\kappa_I) \tag{3.1.7}$$

$$b_\kappa \cdot b_\lambda = \lambda_\kappa\lambda_\lambda \sum_I x^{\kappa\lambda}_I A^\kappa_I A^\lambda_I (i \neq j) \tag{3.1.8}$$

$$0 = B^\kappa_{adj} - \sum_I x^\kappa_I B^\kappa_I. \tag{3.1.9}$$

where A_I, B_I and C_I are group theory coefficients for a representation R_I defined as follows:

$$\mathrm{tr}_{R_I} F^2 = A_I \mathrm{tr} F^2 \ , \ \mathrm{tr}_{R_I} F^4 = B_R(\mathrm{tr}F^2)^2 + C_R \mathrm{tr}F^4. \tag{3.1.10}$$

These coefficients can be found in the Appendix B of [83].

One can also include a number of Abelian group factors $U(1)_i (i = 1, \ldots, n)$ into the game. Then I_8 is modified and X^α_4 has an additional term $\sum_{ij} 2b^\alpha_{ij} F_i F_j$[112]. The anomaly cancellation equations (3.1.4-3.1.9) will still hold, but there are four additional anomaly cancellation equations:

$$a \cdot b_{ij} = -\frac{1}{6}\sum_I x_I q_{I,i} q_{I,j} \tag{3.1.11}$$

$$0 = \sum_I x^\kappa_I E^\kappa_I q_{I,i} \tag{3.1.12}$$

$$b_\kappa \cdot b_{ij} = \sum_I x^\kappa_I A^\kappa_I q_{I,i} q_{I,j} \tag{3.1.13}$$

$$b_{ij} \cdot b_{kl} + b_{ik} \cdot b_{jl} + b_{il} \cdot b_{jk} = \sum_I x_I q_{I,i} q_{I,j} q_{I,l} q_{I,l}, \tag{3.1.14}$$

where $q_{I,i}$ is U(1) charge under the group $U(1)_i$, x_I is the multiplicity of such U(1) presentation and E_I is the group theory coefficient defined as

$$\mathrm{tr}_{R_I} F^3 = E_I \mathrm{tr} F^3. \tag{3.1.15}$$

In the geometric description of F-theory, the vectors a and b_κ are directly mapped to divisor classes on the base surface S, and the dot product is exactly the intersection number between divisors[92, 91].

For a given surface S generated by blowing up $\mathbb{P}^2$ consecutively r times, a convenient basis of $\mathrm{Pic}(S)$ consists of the divisor class of the hyperplane H on the original $\mathbb{P}^2$ and the exceptional divisors $E_1, E_2, \ldots, E_r$. The intersection matrix on this basis is given by the $\mathrm{SO}(1,T)$ metric

$$H \cdot H = 1 \ , \ H \cdot E_i = 0 \ , \ E_i \cdot E_j = -\delta_{ij}. \tag{3.1.16}$$

Hence the Picard rank is $\mathrm{rk}(\mathrm{Pic}(S)) = r + 1$.

More generally, the Hodge index theorem states that for any surface with $\mathrm{rk}(\mathrm{Pic}(S)) = r+1$, the signature of the intersection matrix is $(1, r)$. When $r > 1$, there is always a basis in which the intersection product takes the form (3.1.16); for $r = 1$, there are surfaces where the intersection form has the structure of the matrix

$$U = \begin{pmatrix} 0 & 1 \\ 1 & 0 \end{pmatrix} \tag{3.1.17}$$

The canonical divisor class of $\mathbb{P}^2$ is $K_{\mathbb{P}^2} = -3H$, and after r blow-ups it is in the form of

$$K_S = -3H + \sum_{i=1}^{r} E_i. \tag{3.1.18}$$

Hence if we identify $r = T$ and $a = -K_S$ the anticanonical divisor of S, then we directly verify the anomaly cancellation equation (3.1.5) from the expression of K_S and (3.1.16), since $K_S \cdot K_S = 9 - r$.

We then identify b_κ with the curve C_κ where the gauge group G_κ lives on. Then

the equations (3.1.5-3.1.9) are rewritten into equations of the intersection numbers of divisors on S.

The order of vanishing of (f, g) on a curve C and the gauge group can be computed using *Zariski decomposition* techniques[136]. The *Zariski decomposition theorem* states that any effective divisor D on a rational surface S can be decomposed into $D = N + P$. $N = \sum n_i N_i$ is the "negative part", which is a non-negative linear combination of negative rational curves (genus-0 curve with negative self-intersection) N_i, and the intersection matrix $(N_i \cdot N_j)$ is negative definite. P is a "nef" divisor which means that for any curve $C \subset S$, $P \cdot C \geq 0$.

The order of vanishing of f is then computed by the minimal integral value of a in the Zariski decomposition

$$-4K = aC + X \tag{3.1.19}$$

such that $X \cdot C \geq 0$.

Similarly, the order of vanishing of g is given by the minimal integral value of b in

$$-6K = bC + X \tag{3.1.20}$$

such that $X \cdot C \geq 0$.

The lowest order term in f or g on C is a single monomial if and only if $C \cdot X = 0$ in (3.1.19) or (3.1.20) respectively, which helps to identify the monodromy cover polynomials in Table 4.1.

For example, if C is a rational curve with self-intersection (-3) (refered to as (-3)-curve) that does not intersect with any curve with self-intersection (-2) or lower, then from the adjunction formula of curve on a surface

$$K \cdot C + C \cdot C = 2g - 2, \tag{3.1.21}$$

we see that $-K \cdot C = -1$. Then take the dot product of equation (3.1.19,3.1.20) with C, we see that the minimal values of a and b are 2 in both of the cases. Moreover, since $C \cdot X = 0$ in (3.1.20), we see that the g_2 coefficient in g is indeed a complete

square of complex number. Hence the gauge group is SU(3) according to Table 4.1.

For other cases and configurations of intersecting curves, the analysis can be done similarly. In general, we require that (f, g) does not vanish to order $(4, 6)$ or higher on curves and points on S. As we have said before, codimension-1 (4,6) locus indicates the break down of a supersymmetric solution. The appearance of codimension-2 (4,6) signify the existence of a (1,0) superconformal field theory at that point[39]. If we blow up this point, mathematically we add an exceptional divisor into the Picard group. Physically, this exceptional divisor gives a new tensor multiplet where the vacuum expectation value of the scalar field in it is proportional to the volume of the exceptional divisor. This corresponds to moving into the tensor branch of this (1,0) SCFT and it no longer has conformal symmetry. In our purpose of classification of supergravity theory, we exclude the existence of such (1,0) SCFT and always blow up these codimension-2 (4,6) points.

With these constraints, the only possible local configurations of curves with (-2) or lower curves are listed in Table 3.2, which are called non-Higgsable clusters[101]. The matter representations are computed by the anomaly cancellation equations (3.1.6,3.1.7,3.1.8). The representation $\frac{1}{2}\mathbf{56}$ means that the matter fields in the fundamental representations $\mathbf{56}$ of E_7 are half-hypermultiplets, which is pseudo-real[118].

Other configurations, such as two (-3)-curves intersecting each other, suffer from the issue of codimension-two (4,6) singularity at the intersection point. If we blow up this intersection point, each of the (-3)-curve C is properly transformed to a (-4)-curve, see (2.2.43), and the configuration is now (-4,-1,-4) with two non-Higgsable SO(8) gauge groups, which is completely fine. On the other hand, the configuration (-4,-1,-5) is not allowed and still needs to be blown up to get rid of codimension-two (4,6) singularity. A complete list of allowed non-Higgsable clusters connected by (-1)-curves can be found in [101]. Another simple analytic rule is the E_8 ruleheckman2015atomic, which states that the curve configuration $(-m, -1, -n)$ has no codimension-two (4,6) singularity if and only if the non-Higgsable gauge group G_L and G_R on the (-m) and (-n)-curve satisfies

$$G_L \times G_R \subset E_8. \tag{3.1.22}$$

Cluster	G	rk(G)	matter rep.	V	H_{charged}
(-12)	E_8	8	-	248	0
(-8)	E_7	7	$\frac{1}{2}\mathbf{56}$	133	0
(-7)	E_7	7	-	133	28
(-6)	E_6	6	-	78	0
(-5)	F_4	4	-	52	0
(-4)	SO(8)	4	-	28	0
(-3, -2, -2)	$G_2\times$ SU(2)	3	$(\mathbf{7}+\mathbf{1}, \frac{1}{2}\cdot\mathbf{2})$	17	8
(-3, -2)	$G_2\times$ SU(2)	3	$(\mathbf{7}+\mathbf{1}, \frac{1}{2}\cdot\mathbf{2})$	17	8
(-3)	SU(3)	2	-	8	0
(-2, -3, -2)	SU(2)×SO(7)×SU(2)	5	$(\mathbf{1},\mathbf{8},\frac{1}{2}\cdot\mathbf{2})+(\frac{1}{2}\cdot\mathbf{2},\mathbf{8},\mathbf{1})$	27	16
(-2, -2, ..., -2)	no gauge group	0	-	0	0

Table 3.2: List of "non-Higgsable clusters" of irreducible effective divisors with self-intersection (-2) or below, and corresponding contributions to the gauge algebra and matter content of the 6D theory associated with F-theory compactifications on a generic elliptic fibration (with section) over a base containing each cluster. The quantities V and H_{charged} denote the number of vector and charged hypermultiplets. Non-Higgsable gauge group cannot appear on (-1) or higher curves.

If there exists a curve of (-13) or lower on S, then (f, g) will vanish to order $(4, 6)$ or higher on that curve, which is strictly forbidden.

The total number of vector multiplets equals to the sum of the contributions from local non-Higgsable clusters in Table3.2 and the number of non-Higgsable U(1)s, which will be discussed in detail in Chapter 5. Actually, we can compute the Hodge numbers of the elliptic Calabi-Yau manifold X over S after the resolution using the physical spectrum of the 6D (1,0) supergravity. $h^{1,1}(X)$ is calculated by the Shioda-Tate-Wazir formula[132]

$$h^{1,1}(X) = h^{1,1}(S) + \text{rk}(G) + 1, \tag{3.1.23}$$

where G includes both the non-Abelian and Abelian factors. The Hodge number $h^{1,1}(S)$ counts the dimension of the space of harmonic (1,1) form on S. From the Poincaré duality, this space of harmonic (1,1) form is isomorphic to the Picard group of divisor classes, hence $h^{1,1}(S)$ =rk(Pic(S)).

$h^{2,1}(X)$ characterizes the number of complex structure moduli of X, and it is

related to the number of neutral hypermultiplets[54]

$$h^{2,1}(X) = H_{neutral} - 1 \tag{3.1.24}$$

Since $H = H_{neutral} + H_{charged}$, we can compute from (3.1.4):

$$H_{neutral} = 273 - 29T + V - H_{charged}, \tag{3.1.25}$$

hence

$$h^{2,1}(X) = 272 - 29T + V - H_{charged}, \tag{3.1.26}$$

where $H_{charged}$ is the number of hypermultiplets charged under non-Abelian or Abelian groups.

3.2 Classification of toric and semi-toric base surfaces

A general classification theorem of base surfaces of elliptic Calabi-Yau threefold was proven by Grassi[61], which states that S is either a rational surface or an Enriques surface. An Enriques surface is a complex algebraic surface with $h^{1,1}(S) = 10$. There is no curve with self-intersection (-3) or lower on an Enriques surface[13], so there is no non-Higgsable gauge group. Along with the reason that Enriques surfaces are not connected to the set of rational surfaces by birational equivalence, we do not consider this class of bases in this thesis.

Then the only class is the rational surfaces, and it is known from the minimal model program that all the smooth rational surfaces can be constructed by a series of blow ups from $\mathbb{P}^2$ or Hirzebruch surfaces $\mathbb{F}_n (n \geq 0)$. The Hirzebruch surface is a $\mathbb{P}^1$-bundle over $\mathbb{P}^1$ with a rational $(-n)$-curve. We show the curves on $\mathbb{F}^n$ in Figure 3-2. F and F' are the $\mathbb{P}^1$ fibers, which are in the same divisor class. S_0 and S_∞ are two different sections of the $\mathbb{P}^1$-bundle, with different self-intersection.

In the toric geometry language, the curves in Figure 3-2 are all toric divisors of

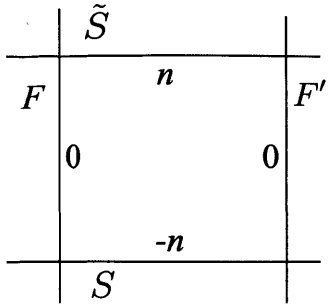

Figure 3-2: Loop of irreducible effective curves on the Hirzebruch surface $\mathbb{F}_n$, corresponding to irreducible toric divisors associated with rays in the toric fan. $F = F'$ correspond to the same divisor class, and $\tilde{S} = S + nF$. The self-intersections of each curve are labeled beside it.

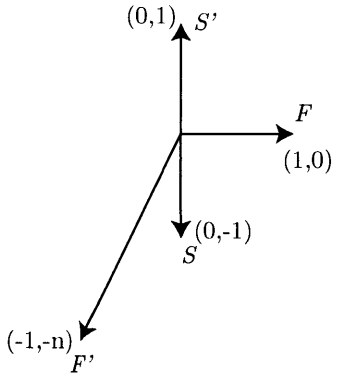

Figure 3-3: The toric fan of Hirzebruch surface $\mathbb{F}_n$

$\mathbb{F}_n$. The toric fan Σ of $\mathbb{F}_n$ is shown in Figure 3-3. The self-intersections of the divisors in Figure 3-3 can be simply read off by the following formula: if the toric divisor D_i has two neighbors D_{i-1} and D_{i+1}, with toric ray v_{i-1} and v_{i+1}, then D_i^2 is computed by

$$v_{i-1} + v_{i+1} = -D_i^2 v_i. \tag{3.2.27}$$

This can be simply proven by the linear equivalence of divisors on a toric variety (2.4.64). Since all the 2D cone in the toric fan of a smooth toric variety has unit volume, we can always find a $\mathrm{SL}(2,\mathbb{Z})$ transformation that maps v_{i-1}, v_i and v_{i+1} to $(-1,-n)$, $(0,1)$ and $(1,0)$ respectively. Then we have linear equivalence relation

$$-nD_{i-1} + D_i + X = 0, \tag{3.2.28}$$

where X is a linear combination of divisors that do not intersect D_i. Then we take the dot product of D_i with the above equations, and get $D_i^2 = n$.

From (2.4.65), we can compute

$$-K_{\mathbb{F}_n} = 2S + (n+2)F. \tag{3.2.29}$$

To describe the Picard group of $\mathbb{F}_n$, we can choose the following set of generators for $n = 2k+1$:

$$H \cdot H = 1 \ , \ H \cdot E = 0 \ , \ E \cdot E = -1, \tag{3.2.30}$$

and we have

$$S = -kH + (k+1)E \ , \ \tilde{S} = (k+1)H - kE \ , \ F = F' = H - E, \tag{3.2.31}$$

which gives the correct intersection numbers.

For $n = 2k$, we can use the following generators (3.1.17):

$$P^2 = Q^2 = 0 \ , \ P \cdot Q = 1, \tag{3.2.32}$$

and

$$S = Q - kP \ , \ \tilde{S} = Q + kP \ , \ F = F' = P. \tag{3.2.33}$$

Since a curve with self-intersection (-13) or lower is not allowed, the only good starting points to blow up are $\mathbb{F}_n (0 \leq n \leq 12)$, as the bases from blowing up $\mathbb{F}_n (n \geq 13)$ will always contain a (-13) or lower curve.

Hence we can explicitly classify all the compact toric bases in 6D F-theory by blowing up $\mathbb{F}_n (0 \leq n \leq 12)$ recursively, which is done by Morrison and Taylor in [105]. In the process, only blow up of toric points (intersection of two toric curves) is allowed. This can be efficiently described by a "cyclic representation", which is a series of numbers $((m_1, m_2, \ldots, m_n))$ denoting the self-intersection of the toric curves

$D_1, \ldots, D_n$ that are connected to each other in a cyclic way:

$$D_i \cdot D_j (i \neq j) = \begin{cases} 1 & (|i-j| = 1 \text{ or } n-1) \\ 0 & \text{otherwise} \end{cases} \tag{3.2.34}$$

For example, the cyclic representation of $\mathbb{F}_n$ is $((n, 0, -n, 0))$, as one can see in Figure 3-2 or Figure 3-3.

The cyclic representations $((m_2, m_3, \ldots, m_n, m_1))$ and $((m_n, m_{n-1}, \ldots, m_1))$ denote the same toric variety as $((m_1, m_2, \ldots, m_n))$. The blow up of toric point $D_k \bigcap D_{k+1}$ on a toric variety $((m_1, \ldots, m_k, m_{k+1}, \ldots, m_n))$ results in $((m_1, m_2, \ldots, m_k - 1, -1, m_{k+1} - 1, \ldots, m_n))$, as the self-intersection numbers of the proper transformation of D_k and D_{k+1} are decreased by one (2.2.43), and there is an exceptional (-1)-curve between them after the blow up.

For example, we start from $\mathbb{P}^2$ with the cyclic representation $((1, 1, 1))$. If we blow up any toric point on it, we always get $((1, 0, -1, 0))$ up to cyclic permutation, which is the cyclic representation of $\mathbb{F}_1$. If we blow up $\mathbb{F}_1$, we can either get $((1, -1, -1, -2, 0))$ or $((0, -1, -1, -1, 0))$. If we continue this procedure, we will encounter codimension-two (4,6) point such as two (-3)-curves intersect each other. Whenever this happen, we allow the blow up procedure to continue despite that these bases with codimension-two (4,6) point are not counted in the final set of 6D F-theory bases, since this codimension-two (4,6) point may be resolved by blowing it up. Finally, if we hit a base with (-13)-curve, the recursion will not continue from here. The order of vanishing of f and g on curves and points can be simply computed using the toric polytope techniques: with the $\mathcal{F}$ and $\mathcal{G}$ polytopes (2.4.69, 2.4.70),

$$\text{ord}_{D_i}(f) = \min_{u \in \mathcal{F}} \langle u, v_i \rangle + 4 \ , \ \text{ord}_{D_i}(g) = \min_{u \in \mathcal{G}} \langle u, v_i \rangle + 6, \tag{3.2.35}$$

$$\text{ord}_{D_i \bigcap D_j}(f) = \min_{u \in \mathcal{F}} \langle u, v_i + v_j \rangle + 8 \ , \ \text{ord}_{D_i \bigcap D_j}(g) = \min_{u \in \mathcal{G}} \langle u, v_i + v_j \rangle + 12. \tag{3.2.36}$$

In [105], they also includes the bases with -9/-10/-11 curves on it. Near such a curve $u = 0$ with self-intersection $p - 12 (p = 1, 2, 3)$, f vanishes to order 4 and g has the

following local expansion

$$g = g_5(v)u^5 + \mathcal{O}(g^6), \tag{3.2.37}$$

where $g_5(v)$ is a degree-p polynomial in v. Hence for a -9/-10/-11 curve, there exists 3/2/1 points on it where (f, g) vanishes to order $(4, 6)$. This problem can be simply resolved by blowing up these points, which lead to p (-1)-curves intersecting a (-12)-curve. Hence strictly speaking, the good bases without these $(4, 6)$ points are non-toric, but they are still counted in [105].

We can make a program that blows up from $\mathbb{P}^2$ and $\mathbb{F}_n (0 \leq n \leq 12)$ recursively and visit all the possible blow up branches. A branch is thrown away if it reaches a base with codimension-1 (4,6) singularity or a good base that has been recorded before. In total, there are 61,539 distinct toric bases including the ones with -9/-10/-11 curves. The maximal number of tensor multiplets is $T = 193$ corresponding to $h^{1,1}(S) = 194$.

An interesting common feature for bases with large $h^{1,1}(S)$ is the appearance of curve chain $(-12, -1, -2, -2, -3, -1, -5, -1, -3, -2, -2, -1, -12)$, which is commonly denoted as $(-12$
$-\ 12)$. In fact, this curve chain exactly comes from the resolution of two E_8 surface singularities intersecting each other at $u = v = 0$:

$$y^2 = x^3 + u^4v^4x + u^5v^5, \tag{3.2.38}$$

which is an important type of "conformal matter" in [39].

To compute the Hodge numbers of the generic elliptic Calabi-Yau threefold X over these bases, we use the Shioda-Tate-Wazir formula (3.1.23) to compute $h^{1,1}(X)$ assuming there is no non-Higgsable U(1) gauge groups. We will generally prove that there is no non-Higgsable U(1)s on any toric bases in Chapter 5. To compute $h^{2,1}(X)$, there are two different methods. First, we can use the anomaly cancellation formula (h21anomaly) with the non-Higgsable clusters on S, assuming there is no U(1) gauge group. Secondly, we can directly count the number of complex structures in the

following way[105]:

$$h^{2,1}(X) = W - w_{aut} + N_{-2} - 1. \tag{3.2.39}$$

W is the total number of Weierstrass moduli computed by the number of lattice points in the polytopes (2.4.69,2.4.70):

$$W = |\mathcal{F}| + |\mathcal{G}|. \tag{3.2.40}$$

It is substracted by the dimension w_{aut} of the automorphism group of S[33]. Denote the polytope with vertices $v_i (i = 1, \ldots, n)$ by Δ^* and its dual polytope by Δ:

$$\Delta = \{u \in \mathbb{Z}^r | \forall i \ , \ \langle u, v_i \rangle \geq -1\}, \tag{3.2.41}$$

then

$$w_{aut} = 2 + \sum_{\text{1D edge } \Theta \in \Delta} l^*(\Theta). \tag{3.2.42}$$

The sum is over 1D edges in Δ, and $l^*(\Theta)$ counts the number of interior lattice points on Θ (not including the two end points).

N_{-2} in (3.2.39) counts the additional complex structure moduli from (-2)-curves that are not in any non-Higgsable cluster.

After checking all the 61,539 cases, the formula (3.2.39) and (3.1.26) exactly matches each other, hence we have verified the assumption that there is no non-Higgsable U(1).

The Hodge number pairs $(h^{1,1}, h^{2,1})$ constructed in this way can all be found in the Kreuzer-Skarke database[90]. The Kreuzer-Skarke database is a systematic classification of general Calabi-Yau threefolds as hypersurface in toric fourfold ambient spaces. The toric ambient spaces are constructed by "reflexive polytopes" (Δ, Δ^*), which means that

$$(\Delta^*)^* = \Delta \tag{3.2.43}$$

using the definition of dual polytope (3.2.41). The two Calabi-Yau threefolds embedded in Δ and Δ^* form a *mirror symmetry* pair where their $h^{1,1}$ and $h^{2,1}$ interchanges[14].

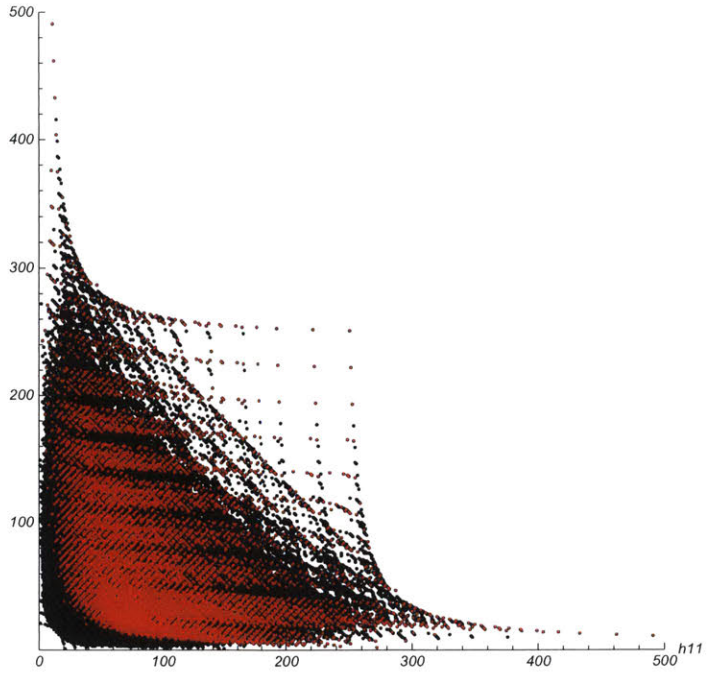

Figure 3-4: The Hodge numbers from Kreuzer-Skarke database (black) and generic elliptic threefolds over toric bases (red).

In total, there are 473,800,776 disctinct reflexive polytopes giving rise to 30,108 distinct Hodge pairs $(h^{1,1}, h^{2,1})$. We plot the Hodge numbers of the generic elliptic threefolds over toric bases versus the Kreuzer-Skarke database in Figure 3-4.

As we can see, the datapoints with large $h^{2,1}(X)$ or $h^{1,1}(X)$ typically matches, which means that most of the Calabi-Yau threefolds with large $h^{2,1}(X)$ or $h^{1,1}(X)$ are elliptically fibered. Especially, the Calabi-Yau threefold with the largest known $h^{1,1}(X)$: $(h^{1,1}, h^{2,1}) = (491, 11)$ is elliptically fibered with the largest $T = 193$. The mirror of this Calabi-Yau threefold is the one with the largest known $h^{2,1}(X)$: $(h^{1,1}, h^{2,1}) = (11, 491)$, which is just the generic elliptic Calabi-Yau threefold over Hirzebruch surface $\mathbb{F}_{12}$.

Apart from the toric bases, another class of 2D "semi-toric" bases have also been classified [97]. Unlike the toric surfaces with an $(\mathbb{C}^*)^2$ action, a semi-toric surface only has a single $\mathbb{C}^*$ action on it. The typical geometric structure of a semi-toric surface has two curves D_0 and D_∞ and a number of chains of rational curves between them, see Figure 3-5. If there are less or equal than two chains between them, then the

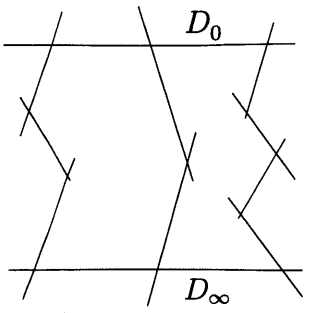

Figure 3-5: A picture of semi-toric surface.

geometry is reduced to a toric surface with a circle of curves.

The allowed blow up operations on this set of semi-toric surfaces are:
(1) blow up of points between two rational curves;
(2) blow up of a generic point on D_0 or D_∞, which adds a new chain of two (-1)-curves between D_0 or D_∞.

There are in total 162,404 distinct semi-toric surfaces including the toric surfaces and the ones with -9/-10/-11 curves. We can also compare the Hodge number $h^{2,1}(X)$ from the anomaly formula (3.1.26) and a Weierstrass model calculation[97], which we will not present the detail. Mismatch was found in some cases, indicating the existence of non-Higgsable U(1)s. We will discuss this issue in more detail in Chapter 5.

3.3 Classification of general non-toric bases

3.3.1 General strategy

Since the complete sets of toric and semi-toric base surfaces in 6D F-theory have been completely classified, a natural idea is to classify the most general non-toric surfaces from blowing up $\mathbb{P}^2$ and $\mathbb{F}_n$. In the mathematical literature, the set of *generalized del Pezzo surfaces* has been classified by Derenthal[43, 42]. A *generalized del Pezzo surface* S is a generated by blowing up $\mathbb{P}^2$ at r points. It is required to be *weak Fano*, which means that $-K \cdot C \geq 0$ for any curve $C \subset S$. Equivalently, this means that there is no (-3) or lower curve on S. The only negative rational curves are then (-2) and (-1) curves, with no non-Abelian non-Higgsable gauge group. In constrast, the

usual del Pezzo surface dP_r is constructed by blow up $\mathbb{P}^2$ at r generic points. As a result, del Pezzo surface only contains (-1)-curves and it is *Fano* which means that $-K \cdot C > 0$ for any curve $C \subset S$.

On generalized del Pezzo surfaces, the configuration of (-2)-curves form a disjoint sum of ADE type Dynkin diagrams with certain constraints[43]. The (-1)-curves are all the rational curves that one can write down, which do not intersect any (-2)-curves negatively. On del Pezzo surfaces, there is no (-2)-curve, and the set of (-1)-curves is everything that one can write down.

From this observation, we should identify the rational curves with self-intersection (-2) or lower after a blow up, and then compute the effective cone $\mathrm{Eff}(S)$ from it.

The set of bases we are studying is the set of rational surfaces with $\mathrm{rk}(\mathrm{Pic}(S)) = h^{1,1}(S) \geq 3$ and an effective anticanonical divisor $-K_S$. The first condition allows the following lemma to be held [10]:

Lemma 1. *For surfaces generated by blowing up $\mathbb{F}_n$ ($n \leq 12$), which have Picard rank greater than 2, when the effective cone is polyhedral (i.e. generated by a finite set of vectors), then the effective cone is generated by rational divisor classes with negative self-intersection.*

For $\mathbb{P}^2$, the effective cone is generated by the hyperplane divisor H with self-intersection 1. For the Hirzebruch surfaces $\mathbb{F}_n$ with Picard rank 2, the effective cone is simply generated by S and F with

$$S \cdot S = -n \ , \ F \cdot S = 1 \ , \ F \cdot F = 0. \tag{3.3.44}$$

Note that curves of negative self-intersection on a base surface that supports an elliptic Calabi-Yau must always be rational. From (2.2.29), an irreducible curve of negative self-intersection with $g \geq 1$ satisfies $-K \cdot C \leq C \cdot C < 0$. From this it follows that $-nK$ contains C at least n times. This means that (f, g) must vanish to at least orders $(4, 6)$ over C which is not allowed.

The effectiveness condition of $-K_S$ ensures that $-4K_S$ and $-6K_S$ has holomorphic section, otherwise f and g will vanish identically on S. This class of surfaces is called

anticanonical rational surfaces[96, 73].

With Lemma 1 to be held, we define Neg(S) as the set of irreducible negative rational curves that generate Eff(S). Clearly for $C, D \in \text{Neg}(S)$, if $C \neq D$, then $C \cdot D \geq 0$. The subset of Neg(S) with (-2) or lower curve is called Sing(S), which corresponds to the non-Higgsable clusters in Table 3.2 as well as ADE type configurations of (-2)-curves.

The dual cone of the effective cone is the nef cone Nef(S), defined as:

$$\text{Nef}(S) = \{D \in \text{Pic}(S) | \forall C \in \text{Eff}(S) \ , \ D \cdot C \geq 0\}. \tag{3.3.45}$$

The nef cone is a subcone of the effective cone, see Corollary II.3 in [73] for example.

We always use the Picard group generators H, $E_1, \ldots, E_r$ (3.1.16), and a divisor class $D = a_0 H + \sum_{i=1}^{r} a_r E_r$ is denoted as a vector $(a_0, a_1, \ldots, a_r)$.

We define the set of genus g, self-intersection $k \geq 0$ divisors C that intersect non-negatively with every curve $D \in \text{Neg}(S)$ by $\mathfrak{C}_{g,k\geq 0}(S) \subset \text{Nef}(S)$. They are all effective curves, as we mentioned before.

We also define $\mathfrak{C}_k(S) = \bigcup_g \mathfrak{C}_{g,k}(S)$, and we always call the one-time blow up of S to be S'.

With this set of notations, when we blow up a point that lies with multiplicity m on a representative of an effective divisor class C and self-intersection k, there is a new effective divisor class $C' = (C, -m)$. Using the adjunction formula (2.2.29), the following lemma holds:

Lemma 2. *If one blows up a curve $C \in \mathfrak{C}_{g,k}(S)$ at an m-point on S, the resulting new effective curve on S' is: $C' = (C, -m) \in \mathfrak{C}_{g-(m^2-m)/2, k-m^2}(S')$.*

This implies that blowing up a single point on a curve will not change its genus, but blowing up an m-point on a curve will decrease the genus of the curve by $(m^2 - m)/2$. Hence we cannot blow up a rational curve at a double point, otherwise the genus will become negative.

On a given base S, the different ways of blowing it up can be classified as follows:

(1) One can blow up a generic point p on S. Then all the elements $C \in \mathrm{Neg}(S)$ are transformed to $C' = (C, 0)$, because they are fixed and they will not pass through a generic point p. The exceptional curve $E' = (0, \ldots, 0, 1)$ is an element in $\mathrm{Neg}(S')$ that is a generator of the new effective cone. The full $\mathrm{Neg}(S')$ that generates $\mathrm{Eff}(S')$ contains other (-1)-curves as well, which will be computed later.

(2) One can choose to blow up a non-generic point, so that a set of curves $C_{0,i} \in \mathfrak{C}_{0,k<0}$ are blown up at a single point. The index i here just labels different curves with the same genus. In the simplest cases, the point blown up lies only on a single rational curve C of negative self-intersection, in which case the transformed curve is $C' = (C, -1)$. The point blown up may also lie at an intersection point between a pair of negative curves C, D, in which case both curves are transformed and $C' \cdot D' = 0$.

(3) There are also situations where a set of curves $C_{1,i} \in \mathfrak{C}_{1,k<3}$ are blown up at a double point, $C_{2,i} \in \mathfrak{C}_{3,k<8}$ are blown at a triple point, and so on. This will produce new negative rational curves of self-intersection < -1 that must be included in $\mathrm{Sing}(S')$ We define the blow-up process to be a "special blow-up" when one or more (-2) or lower curves are generated by blowing up positive curves at points with multiplicity higher than 1.

(4) In some cases it may be possible to choose a non-generic point as in (2) that lies at the intersection of more than two negative curves.

Cases (1) and (2) can be handled in a systematic fashion using the combinatorial data of the effective cone. Case (3) and (4) are subtle and they may or may not give us new bases. In the specific regimes that we completely in Section3.3.3, they never occur.

For the (-1)-curves in $\mathrm{Neg}(S')$, we have the following proposition:

Proposition 1. *The set $\mathfrak{C}_{0,-1}(S')$ of rational (-1)-curves $C = (a, b_1, b_2, \ldots, b_r) \in \mathrm{Neg}(S')$ generated by the blow up method is the solution set to the following Diophan-*

tine equations:

$$\begin{aligned} a^2 - \sum_{i=1}^{r} b_i^2 &= -1 \\ 3a + \sum_{i=1}^{r} b_i &= 1 \end{aligned} \tag{3.3.46}$$

with the additional requirement that the curve intersects non-negatively with all the elements in Sing(S').

The two equations fix the self-intersection and the genus of C by adjunction formula (2.2.29)

To introduce the proof, we think about a divisor class D as a linear system $|D|$ with dimension:

$$\dim(|D|) = h^0(S, \mathcal{O}(D)) - 1 \tag{3.3.47}$$

For general (arbitrary genus) curves, we have[66]

$$h^0(S, \mathcal{O}(D)) \geq (D^2 - K_S \cdot D)/2 + 1, \tag{3.3.48}$$

hence we have the following lemma:

Lemma 3. *A negative divisor class on S is always rigid. For a non-negative effective divisor class D on S, there exists a representative $D \in |D|$ that passes through any $(D^2 - K_S \cdot D)/2$ points in S.*

A point with multiplicity m is counted as m^2 points in this lemma.

For rational curves D, we have a stronger result [88]

$$\dim(|D|) = \max(D^2 + 1, 0). \tag{3.3.49}$$

Hence if the rational curve has negative self-intersection, then $\dim(|D|) = 0$ and the curve is cannot be deformed. If D is irreducible, then it is really a single "fixed" curve.

For example, consider the curves of self-intersection (-1) on a surface formed by blowing up $\mathbb{P}^2$ r times at $p_1, \ldots, p_r$. The divisor classes of degree 1 rational curves with self-intersection (-1) can be written as $H - E_i - E_j$, corresponding to the set of lines that pass through the pairs of points p_i and p_j on the original $\mathbb{P}^2$. There is a unique line that passes through two fixed points in the plane, hence the resulting (-1)-curve is fixed. Similarly, the divisor class of degree 2 rational curves with self-intersection (-1) can be written as $2H - E_i - E_j - E_k - E_l - E_m$, corresponding to the set of conics that pass through five fixed points. We know this divisor is also rigid, since there is a unique conic passing through five fixed points. However, the divisor class of degree 1 rational curves with self-intersection 0, $H - E_i$, corresponds to the set of lines that pass through a particular point p_i, and are free to rotate around p_i. In fact, such lines can pass through every point on $\mathbb{P}^2$.

Now we present the formal proof of Proposition 1:

Proof. We prove this by induction. First one can check the correctness of this statement for $\mathbb{P}^2$ and $\mathbb{F}_n$. Then suppose this is true for a base S; we want to show this is also true for any surface S' that is generated by blowing up S once.

(i) All the curves $C' \in \mathfrak{C}_{0,-1}(S')$ satisfy the requirements in the proposition.

Obviously they satisfy the Diophantine equations. If C' negatively intersects with $D' \in \mathrm{Sing}(S')$, this means $C' = D' + F'$ where F' is some other effective divisor, hence C' is reducible and is not in $\mathrm{Neg}(S')$.

(ii) All the irreducible rational (-1)-curves C' that satisfy the non-negative intersection requirement in the proposition are elements of $\mathfrak{C}_{0,-1}(S')$, and can be generated by the blow-up process. We analyze the different types of solution to (3.3.46) separately.

(a) This is obviously true for the solution $(0, \ldots, 0, 1)$ since it is the exceptional curve $E' \in \mathfrak{C}_{0,-1}(S')$ associated with the blowup $S \to S'$, and none of the other curves has a positive last entry.

(b) For all the solutions of the form $C' = (C, 0)$, where we know that C intersects non-negatively with all the elements in $\mathrm{Sing}(S)$, it follows by induction that $C \in \mathfrak{C}_{0,-1}(S)$. From the general characterization of the blow-up process described earlier,

$C' = (C, 0)$ is still in Eff(S), but it may be represented as a positive linear combination of a lower self-intersection effective curve and the exceptional curve: $C' = (C, -m) + m(0, 1)$. When this happens, however, it means that C' intersects negatively with $(C, -m) \in \text{Sing}(S')$, which contradicts the requirement in the proposition. Hence $C' = (C, 0)$ is irreducible when it satisfies the requirement in proposition, and it is in $\mathfrak{C}_{0,-1}(S')$.

(c) For all the solutions of the form $C' = (C, -m)$, $m > 0$, C is a genus $(m^2 - m)/2$, self intersection $m^2 - 1$ divisor. In fact the solution to the equations (3.3.46) automatically intersects non-negatively with any other solutions (see Theorem 2a in [110]). Together with the assumption that C' intersects non-negatively with all the elements in Sing(S'), we can conclude that C' intersects non-negatively with any other curve in Neg(S'). From this we can also know that C is nef hence is effective on S. Then according to Lemma 3, $C \in \mathfrak{C}_{(m^2-m)/2, m^2-1}(S)$ can be blown up at a generic point with multiplicity m. These statements together guarantee that C' is an irreducible curve on S'. Hence any solution of the form $C' = (C, -m)$, $m > 0$ that satisfies the requirement in the proposition is in Neg(S'). □

Now we need to generate the solutions to the Diophantine equations (3.3.46) using a finite algorithm. In fact, all the solutions can be generated by a series of "q-operations" acting on curves, which are defined as follows [110]:

For a curve in the form $(a, b_1, b_2, \ldots, b_r)$, one picks three numbers i_1, i_2, i_3 out of $\{1, \ldots, r\}$, then performs the following transformation:

$$a \to a+d\ ,\ b_{i_1} \to b_{i_1} - d\ ,\ b_{i_2} \to b_{i_2} - d\ ,\ b_{i_3} \to b_{i_3} - d\ ,\ d = a + b_{i_1} + b_{i_2} + b_{i_3}. \quad (3.3.50)$$

It can be explicitly checked that the two quantities $a^2 - \sum_{i=1}^{r} b_i^2$ and $3a + \sum_{i=1}^{r} b_i$ do not change under this transformation.

In practice, one starts from some low-degree curves, such as all the degree 0 and degree 1 rational (-1)-curves. Then one tries to perform all the q-operations on one curve so that the degree is increased ($d > 0$ in (3.3.50)). If the curve intersects negatively with some element in Sing(S), then we cut this branch. This recursive

algorithm is finite if Eff(S) is finitely generated. We discuss more about the finiteness of curves in section 6.

However, the set of (-1)-curves generated in this way may not be complete. For a consistency check, we compute the dual cone of Neg(S) generated by the method above, and check whether the generators (extremal rays) of this dual cone are non-negative. If a generator is negative, we know it is a (-1)-curve in Neg(S) that was not generated by the q-process. After adding all the (-1)-curves of this kind, we can get a complete set of curves in Neg(S), with a dual cone that contains no negative curves.

3.3.2 The algorithm

Now we are ready to construct a finite recursive algorithm for generating general bases, with specific prescriptions for dealing with the various potential complications discussed in preceding sections.

(1) We start from a base S, with Picard rank $r+1$ and a vector representation of negative curves Neg(S), Sing(S) $\in$ Neg(S). This data should always be finite.

(2) We construct all blowups of S in three possible ways: blow up the intersection point of two curves $C_i, C_j \in$ Neg(S), blow up a generic point on a curve $C_i \in$ Neg(S), or blow up a generic point on the plane. We do not consider blowups at points at which three or more negative curves intersect. The special blow-ups are also excluded in the current algorithm.

After this step we have the new Sing(S').

(3) With this new Sing(S'), we use the q-process to generate the (-1)-curves on S'. In practice, we just start from all the curves of degree 0 and degree 1. If the number of curves in this step reaches a certain large value, then the number of generators is considered to be infinite and the base is discarded.

(4) Then we need to check if the degrees of vanishing of $f \in O(-4K), g \in O(-6K), \Delta \in O(-12K)$ are greater or equal than $(4, 6, 12)$ on any of the divisors.

Practically, we use the method of Zariski decomposition, as in [101]. We decom-

pose $-nK$ as

$$-nK = \sum_{i=1}^{k} a_i C_i + Y \tag{3.3.51}$$

for $n = 4, 6, 12$.

The integral coefficients a_i indicate the orders of vanishing of $-nK$ on the divisors C_i. And $C_i (1 \leq i \leq k)$ are all the elements in $\mathrm{Neg}(S')$. The residual part Y should be an effective $\mathbb{Q}$-divisor, which intersects non-negatively with all curves C_i. We start from $a_1 = a_2 = \cdots = a_k = 0$, and examine $Y \cdot C_i$ for every C_i. If this quantity is negative for C_i, then we add a minimal value to a_i that will make this quantity non-negative and do the check again, until $Y \cdot C_i \geq 0$ for every C_i. If in the process any a_i reaches a certain value (11 for $n = 12$), then the singularity is too bad to be resolved. When this happens the process stops and the base is discarded.

If there is set of coefficients a_i that pass the check, then we examine all the intersection points of pairs of negative curves a_i and a_j. If the sum of coefficients $a_i + a_j > 10$ for $n = 12$, then this intersection point needs to be blown up.

Furthermore, bases containing (-9),(-10),(-11)-curves are not good, since there are always $(4, 6)$ points on these curves. Such points need to be blown up until the curve of large negative self-intersection becomes a (-12)-curve. (Note that the points blown up in this process could be generic points on these curves or points where they intersect with other negative curves).

(5) If no additional points need to be blown up, then we compute the generators of the dual cone of $\mathrm{Neg}(S')$. This is known to be a hard problem, the exact algorithm is described in p.11 of [59]. If the vectors in $\mathrm{Neg}(S')$ are $d = r + 1$ dimensional, then one computes the normal vector u to each of the $(d-1)$-dimensional facets. Then if u or $-u$ intersects non-negatively with all $C \in \mathrm{Neg}(S')$, then u or $-u$ is a generator of $\mathrm{Nef}(S')$. Hence if $n = |\mathrm{Neg}(S')|$, then the computational complexity is at least $\binom{n}{d-1} = \binom{n}{r}$. This turns out to be the major computational difficulty in this program.

After all the generators of the dual cone of $\mathrm{Neg}(S')$ are found, we check if all the generators are non-negative. If not, we add the negative ones into $\mathrm{Neg}(S')$. We repeat the step (4)(5), and finally the dual cone of $\mathrm{Neg}(S')$ will be free of negative

generators, which means that the set Neg(S') contains the complete set of (-1)-curves.

We then further check if $-K = (3, -1, -1, \ldots, -1)$ intersects non-negatively with all the generators. If not, then $-K$ is not in the effective cone hence the base is not allowed.

(6) If the previous test is passed, then this base S' is good. The next step is checking if the intersection structure is isomorphic to one of the bases generated before. The graph isomorphism problem is also known to be hard; it is not clear if there exists a polynomial algorithm. In practice we used the "VFlib" library developed by Pasquale Foggia[55].

(7) If all the tests are passed, add this base to solution set and restart step (1) using S'.

The overall starting points are the bases with $r = 2$ that come from blowing up $\mathbb{F}_n$, and which have no (-9),(-10),(-11) curves. We list their Neg(S) below (the l.h.s. is the cyclic toric diagram for these bases S):

$$\begin{aligned}
((0,0,-1,-1,-1)) &:\{(0,1,0),(0,0,1),(1,-1,-1)\} \\
((1,-1,-1,-2,0)) &:\{(0,1,-1),(0,0,1),(1,-1,-1)\} \\
((2,-1,-1,-3,0)) &:\{(-1,2,0),(0,0,1),(1,-1,-1)\} \\
((3,-1,-1,-4,0)) &:\{(-1,2,-1),(0,0,1),(1,-1,-1)\} \\
((4,-1,-1,-5,0)) &:\{(-2,3,0),(0,0,1),(1,-1,-1)\} \\
((5,-1,-1,-6,0)) &:\{(-2,3,-1),(0,0,1),(1,-1,-1)\} \\
((6,-1,-1,-7,0)) &:\{(-3,4,0),(0,0,1),(1,-1,-1)\} \\
((7,-1,-1,-8,0)) &:\{(-3,4,-1),(0,0,1),(1,-1,-1)\} \\
((11,-1,-1,-12,0)) &:\{(-5,6,-1),(0,0,1),(1,-1,-1)\}
\end{aligned} \tag{3.3.52}$$

So $\mathbb{P}^2$ and $\mathbb{F}_n$ are not counted in the solution set and they have to added in by hand.

Using this algorithm, we can produce a finite list of possible bases in a specific desired range. There are three possible sources of incompleteness or inaccuracy in

such a list:

(i) Bases where the effective cone has an infinite number of generators, or a very large number that exceeds the arbitrary cutoff in the code, will be missed.

For example, we consider a an $r = 9$ base S with

$$\begin{aligned} \text{Sing}(S) &= \{(1,-1,-1,-1,0,0,0,0,0,0),(1,0,0,0,-1,-1,-1,0,0,0), \\ &\quad (1,0,0,0,0,0,0,-1,-1,-1)\} \ . \end{aligned} \tag{3.3.53}$$

This is a generalized del Pezzo surface with three (-2) curves. This surface clearly satisfies the condition that $-K$ is in the effective cone, since $-K$ is the sum of the three (-2) curves. We can prove that there are infinitely many (-1)-curves in the effective cone: suppose that we pick an exceptional curve $C_0 = (0,1,0,0,0,0,0,0,0,0)$. Then at step 1 we perform the q-operation with entries b_1, b_4, b_7. At step 2 we perform the q-operation with entries b_2, b_5, b_8. At step 3 we perform q-operation with entries b_3, b_6, b_9, and we infinitely repeat these three steps. The intersection product with the three curves in Sing(S) is invariant during this process. The degree of the curve at step $2n-1$ equals to n^2. This means that the process will give arbitrarily high degree curves, hence the number of (-1)-curves is infinite.

(ii) Bases that are produced by "special blowups" giving curves of self-intersection -2 or below, or by blowing up points at the intersection of more than two negative curves, will be missed by this algorithm.

(iii) On some bases, there are certain combinations of more than two negative self-intersection curves that are forced to intersect at a common point. This is a part of geometric information about S that is not encoded in the effective cone data. For example, the two cases in Figure 3-6 will lead to different blow up results.

One particular situation of this type involves the 1,700 years old *Pappus's theorem.* For example, consider the configuration of Sing(S) with $r = 9$ in Table 3.3; the corresponding geometrical picture is drawn in Figure 3-7. Note that in the last blow-up at point i, lines gh, cf and bd are guaranteed to intersect at a single point, by Pappus's theorem.

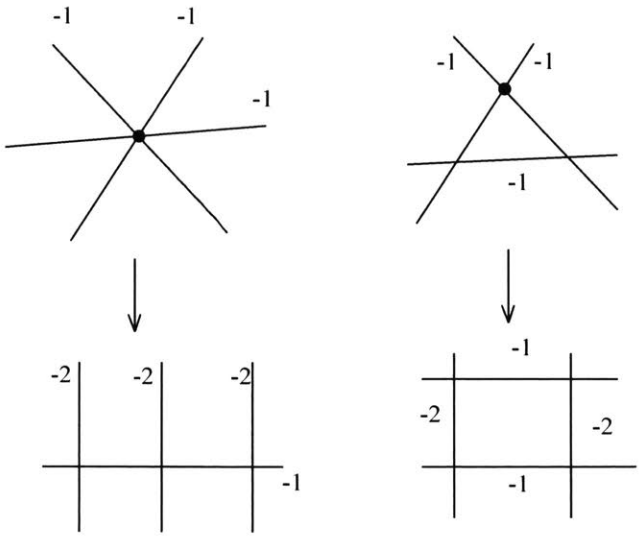

Figure 3-6: Two geometric configurations with the same intersection structure and vector representations of curves, but which can be blown up to give surfaces with distinct intersection structure

curve	point	a	b	c	d	e	f	g	h	i
A	1	-1	-1	-1	0	0	0	0	0	0
B	1	0	0	0	-1	-1	-1	0	0	0
C	1	0	0	0	0	0	0	-1	-1	-1
D	1	-1	0	0	-1	0	0	-1	0	0
E	1	0	-1	0	0	-1	0	0	-1	0
F	1	0	0	-1	0	0	-1	0	0	-1
G	1	-1	0	0	0	0	-1	0	-1	0
H	1	0	-1	0	-1	0	0	0	0	-1
I	1	0	0	-1	0	-1	0	-1	0	0

Table 3.3: A configuration of Sing(S), with 9 (-2)-curves that forms 3 groups of 3 curves that intersect each other

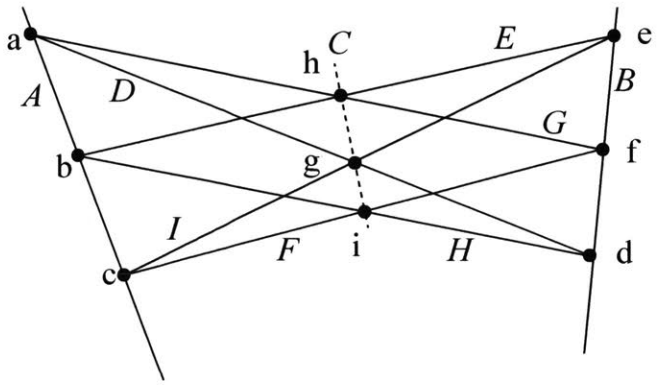

Figure 3-7: The geometry of the blow-up points a,b,c,d,e,f,g,h,i, of the configuration in Table 3.3. This is an example of Pappus's theorem.

There does not exist a complete framework to resolve this issue in every case, and we want to avoid this problem as we can.

3.3.3 Results

Now we are going to present the results in two different regimes where the three subtleties above does not bother us.

Classification of all bases with $h^{1,1}(S) < 8$

If $h^{1,1}(S) < 8$ or $r \leq 6$, we can explicitly determine the set of all combinatorially distinct effective cones. The smallest value of r where the issue arises that three negative curves may intersect each other is 6, where we can have $A = (1, -1, -1, 0, 0, 0, 0)$, $B = (1, 0, 0, -1, -1, 0, 0)$, $C = (1, 0, 0, 0, 0, -1, -1)$. Hence this subtlety will not affect the classification of bases with $r < 7$ if we do not distinguish betweent the two cases in Figure 3-6.

The problem of special blow-ups will neither appear, since the shortest vector representation of a curve that comes from a special blow-up is (3,-1,-1,-1,-1,-1,-1,-2). Moreover, the number of generators of the effective cone is finite for all surfaces in this range. Hence the list of all bases with $h^{1,1}(S) < 8$ generated by our algorithm is indeed complete.

In total there are 468 bases with $8 > h^{1,1}(S) > 0$. This includes the surfaces $\mathbb{P}^2$ and $\mathbb{F}_n$ with $n = 0 \sim 8$ or 12. Among these, 245 are non-toric and 177 are not included in the semi-toric list in [97]. All previously identified toric and semi-toric bases appear in the set generated by our algorithm, which gives a check on the correctness and completeness of the result. It also generates all the generalized del Pezzo surfaces in [43] within this range.

In the counting, we do not include the ones with -9/-10/-11 curves and they are explicitly blown up to get (-12) curves.

We can compute $h^{1,1}(X)$ and $h^{2,1}(X)$ of generic elliptic Calabi-Yau threefolds over these bases using (3.1.23) and (3.1.26), assuming that there is no non-Higgsable U(1).

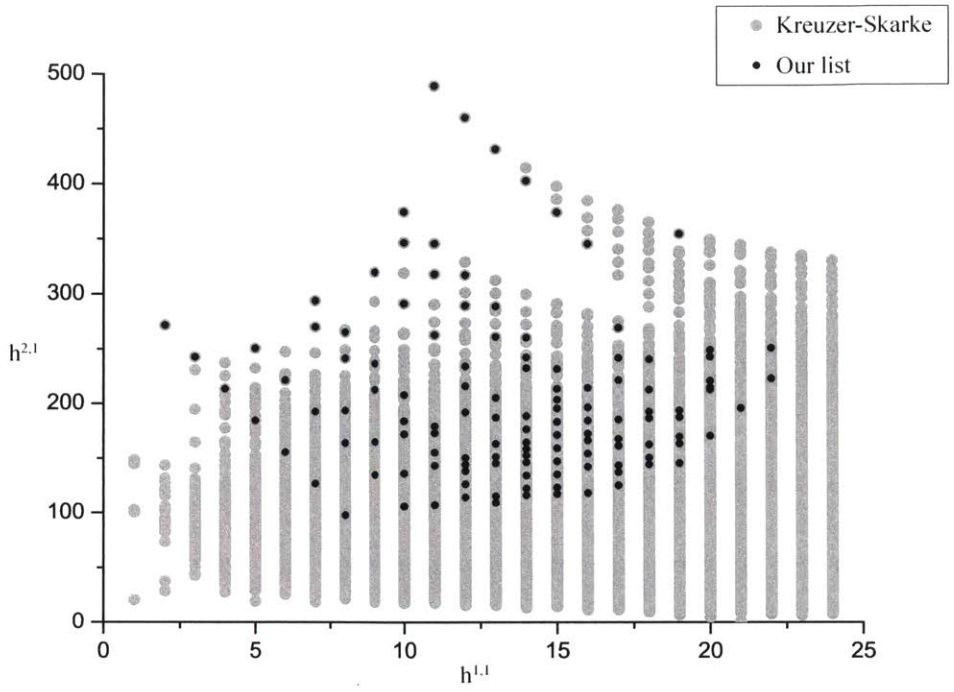

Figure 3-8: The Hodge numbers of the generic EFS (elliptically fibered with section) Calabi-Yau threefolds over all smooth complex surface bases with $h^{1,1}(S) < 8$ are represented by black dots. The 6D theories that result from compactification on these CY3s have $T < 7$ tensor supermultiplets. The Hodge numbers in the Kreuzer-Skarke database are represented by gray dots.

We plot these Hodge numbers in Figure 3-8.

Classification of all bases for elliptic Calabi-Yau threefolds with $h^{2,1} \geq 150$

Another set of bases that we can completely classify is the set of bases that support elliptic Calabi-Yau threefolds X with $h^{2,1}(X) \geq 150$. This subset is relatively easy to study, because it turns out that the difference between $|\text{Neg}(S)|$ and $\text{rk}(\text{Pic}(S))$ is small, hence the dual cone problem is easier to solve. Also, the situations in which three negative curves intersect each other or the dual of $\text{Neg}(S)$ contains a negative curve never happen, nor does an infinite number of negative curves ever arise. The only issue that could in principle make our list incomplete is the presence of special blow-ups, which is related to the existence of higher degree curves. However, for example, if we consider the bases from blowing up $\mathbb{F}_{12}$, the existence of the (-12)-curve strictly constrains the possible form of curves on S. The curve (3,-1,-1,-1,-1,-1,-1,-1,-2) will never appear since it intersects the (-12)-curve (-5,6,-1,...,0) negatively.

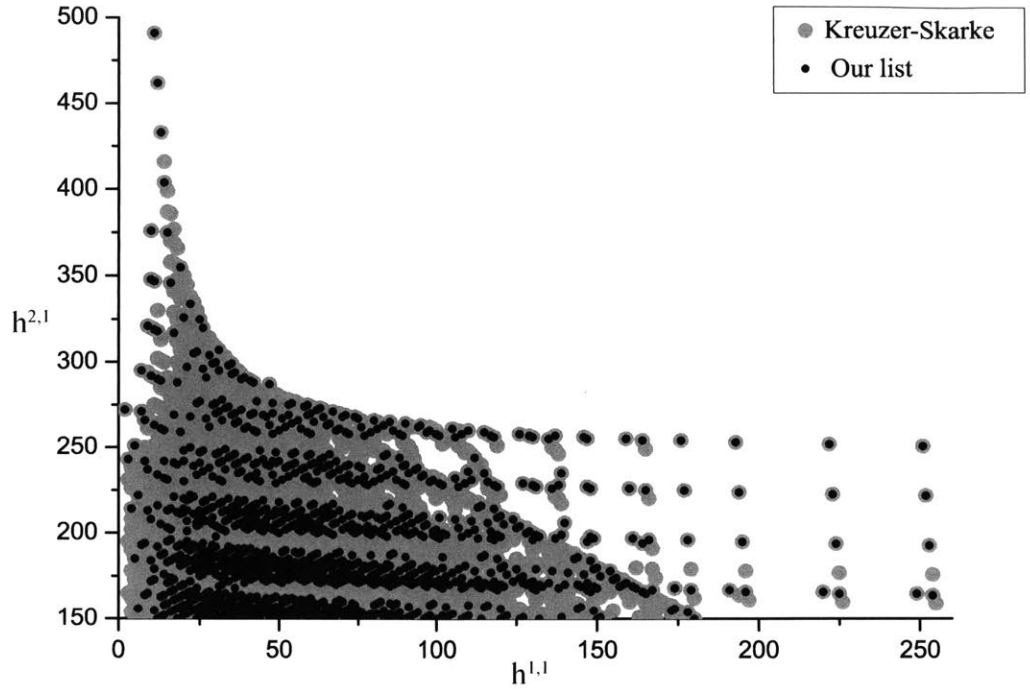

Figure 3-9: The Hodge numbers of all the EFS Calabi-Yau threefolds with $h^{2,1} \geq 150$ generated by generic elliptic fibrations over smooth surfaces are represented by black dots. The Hodge numbers in the Kreuzer-Skarke database are represented by gray dots.

The rational curve with degree $d > 0$ that intersects (-12)-curve non-negatively is the one with form $(6, -5, 0, \dots)$. And the base giving maximal $h^{2,1}(X)$ that contains a negative curve in this form is the one constructed from blowing up $\mathbb{F}_{12}$ at 13 generic points, with $h^{2,1}(X) = 491 - 13 \times 29 = 114 < 150$. Similar analysis can be done for the other cases, see Section 10.3 in [125] explicitly.

In total, our algorithm produces 6511 bases over which the generic elliptic Calabi-Yau threefold has $h^{2,1}(X) \geq 150$. This set of bases includes $\mathbb{P}^2$ and $\mathbb{F}_n$, with $n = 0 \sim 8$ or 12. All the 3871 toric and toric + semi-toric bases identified in [105, 97] giving threefolds with $h^{2,1} \geq 150$ can be found in our list (including ones generated from blowing up -9/-10/-11 curves at generic points). Hence the number of new bases that is not in the list of [97] is 2640.

We plot the Hodge numbers of the generic elliptic Calabi-Yau threefolds over this set of bases in Figure 3-9. Generic elliptic fibrations over the 6511 distinct bases give CY threefolds with 1278 distinct Hodge number pairs.

Among them, we have identified 15 bases that give rise to elliptic Calabi-Yau

threefolds with Hodge numbers that are not in the Kreuzer-Skarke database. Their Hodge numbers are:

$$\begin{aligned}(h^{1,1}, h^{2,1}) \;=\; & (29,299),(48,270),(30,270),(59,269),(41,269),(70,268),\\ & (31,241),(31,241),(66,240),(42,240),(89,239),(20,214),\\ & (84,210),(149,179),(104,152)\,.\end{aligned} \tag{3.3.54}$$

For example, the base giving $(h^{1,1}, h^{2,1}) = (29, 299)$ can be constructed by blowing up a generic point on the (-4)-curve of the toric base

$$((-12,-1,-2,-2,-3,-1,-4,-1,-3,-1,6,0)). \tag{3.3.55}$$

Since they typically have large $h^{2,1}(X)$, the number of Weierstrass moduli $W \gg 12$ and non-Higgsable U(1)s will not appear, see Chapter 5. Hence we have computed the correct Hodge numbers.

Chapter 4

Classification of complex base threefolds

4.1 Calabi-Yau fourfolds and 4D F-theory

A Calabi-Yau fourfold X is a Ricci flat Kähler manifold with holonomy group SU(4). The major topological invariants we are interested in are the Hodge numbers $h^{p,q}(0 \leq p, q \leq 4)$, which are the dimension of the linear space of harmonic (p, q)-form on X. There is a unique holomorphic (4,0)-form Ω on X, hence $h^{4,0} = 1$. Similarly, since the $(0, 0)$ form is just a complex number, we have $h^{0,0} = 1$. The Calabi-Yau condition implies that $h^{1,0} = h^{2,0} = h^{3,0} = 0$, and the K$\acute{}$ahler condition ensures $h^{p,q} = h^{q,p}$. Along with the Hodge duality relation $h^{p,q} = h^{4-p,4-q}$ on a complex fourfold, the Hodge diamond $h^{p,q}$ of X always takes the following form ($h^{p,q}$ is on the p-th row and q-th column):

$$\begin{array}{ccccc} 1 & 0 & 0 & 0 & 1 \\ 0 & h^{1,1} & h^{2,1} & h^{3,1} & 0 \\ 0 & h^{2,1} & h^{2,2} & h^{2,1} & 0 \\ 0 & h^{3,1} & h^{2,1} & h^{1,1} & 0 \\ 1 & 0 & 0 & 0 & 1 \end{array} \tag{4.1.1}$$

A corollary from Hirzebruch-Riemann-Roch index theorem gives us a relation between these Hodge numbers[84]:

$$h^{2,2} = 2(22 + 2h^{1,1} + 2h^{3,1} - h^{2,1}). \tag{4.1.2}$$

Hence there are only three indepedent Hodge numbers for a Calabi-Yau fourfold: $h^{1,1}$, $h^{2,1}$, $h^{3,1}$. $h^{1,1}$ counts the number of Kähler moduli T_A or the parameters that controls the size of different cycles on X. $h^{3,1}$ counts the number of complex structure moduli z_a, which is closely related to the number of Weierstrass monomials in the case of an elliptic fourfold.

We have the Euler number

$$\begin{aligned} \chi(X) &= \sum_{i=0}^{4}(-1)^i \sum_{j=0}^{i} h^{j,i-j} \\ &= 4 + 2h^{1,1} + 2h^{3,1} + h^{2,2} - 4h^{2,1} \\ &= 6(8 + h^{1,1} + h^{3,1} - h^{2,1}). \end{aligned} \tag{4.1.3}$$

Another useful topological number is the fourth betti number $b_4 = \dim(H^4(X))$:

$$\begin{aligned} b_4 &= 2 + 2h^{3,1} + h^{2,2} \\ &= 46 + 4h^{1,1} + 6h^{3,1} - 2h^{2,1} \end{aligned}. \tag{4.1.4}$$

To get a feeling of the Hodge numbers of Calabi-Yau fourfolds systematically generated in the literature, we plot the distribution of Hodge numbers for Calabi-Yau hypersurfaces in 5D weighted projective spaces in Figure 4-1. Although a large number of Calabi-Yau fourfolds lies in the region $h^{1,1}, h^{3,1} < 10,000$, the maximal value of $h^{1,1}$ and $h^{3,1}$ can be very high, up to 303,148.

These topological numbers are crucial for 4D F-theory on X because of the central importance of the G_4 flux. In the M-theory dual picture, the G_4 flux is the field strength of the C_3 form field that couples to M2-branes. The G_4 flux is integrally

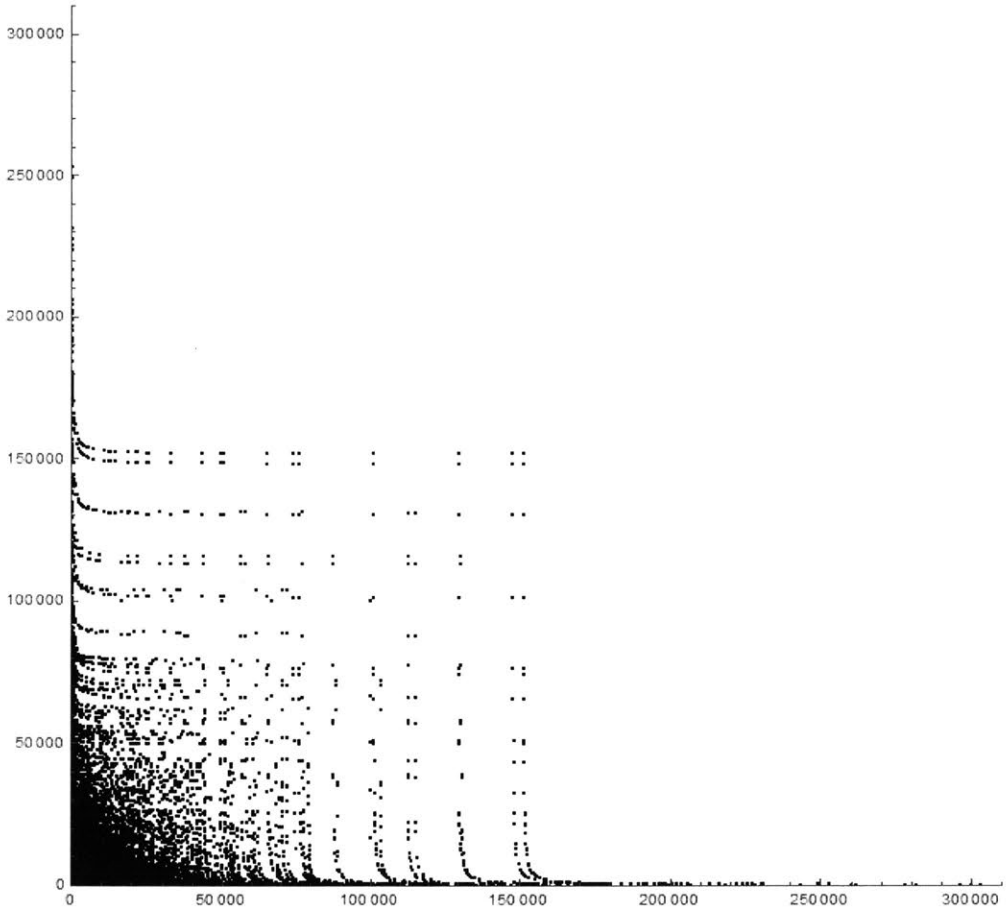

Figure 4-1: Distribution of Hodge numbers for Calabi-Yau fourfolds constructed as hypersurfaces in weighted projective space using reflexive polytopes [89].

quantized[135]:

$$G_4 - \frac{c_2(X)}{2} \in H^4(X, \mathbb{Z}). \tag{4.1.5}$$

c_2 is the second Chern class of X. Hence if $c_2(X)/2 \notin H^4(X, \mathbb{Z})$, then we cannot take $G_4 = 0$.

We can write down the low energy effective action of M-theory containing a higher derivative term:

$$S_M \propto \int d^{11}(X)\sqrt{-g}R - \frac{1}{2}\int G_4 \wedge *G_4 - \frac{1}{6}\int C_3 \wedge G_4 \wedge G_4 + \int C_3 \wedge X_8(R) + \sum_i \int_{M2_i} C_3, \tag{4.1.6}$$

where $X_8(R)$ is the 8-form[49]

$$X_8(R) = \frac{1}{(2\pi)^4}\left[-\frac{1}{768}(\mathrm{tr}R^2)^2 + \frac{1}{192}\mathrm{tr}R^4\right] = \frac{1}{192}(4p_2 - p_1^2). \tag{4.1.7}$$

p_1 and p_2 are the first and second Pontryagin class of X ($c_2(X) = \frac{1}{2}p_1(X)$). The crucial property of X_8 is that

$$\int_X X_8(R) = \frac{\chi(X)}{24}. \tag{4.1.8}$$

The final term in (4.1.6) is the coupling term of C_3 with N_{M2} copies of M2 branes $M2_i$.

The equation of motion for C_3 from (4.1.6) is

$$d * G_4 = \frac{1}{2}G_4 \wedge G_4 - X_8(R) + \sum_i \delta_{M2_i}. \tag{4.1.9}$$

Integrating this equation over X, we arrive at the "tadpole cancellation equation":

$$\frac{1}{2}\int_X G_4 \wedge G_4 + N_{M2} = \frac{\chi(X)}{24}. \tag{4.1.10}$$

Again, we see that if $\chi(X)/24$ is not integral, then there has to be a non-vanishing

G_4 flux in the background to make the theory self-consistent.

The set of possible quantized G_4 flux is called the "flux vacua", which represents a large number of F-theory/string theory solutions on a single geometry[47, 41, 11].

There are a number of physical constraints on G_4. The condition that the 4D low energy theory has SO(3,1) Lorentz symmetry put the following constraints on G_4[37]:

$$\int_{Z \bigcap B_i} G_4 = \int_{B_i \bigcap B_j} G_4 = 0, \tag{4.1.11}$$

where Z is the zero section of the elliptic fibration X, which is isomorphic to the base threefold B. B_i are "vertical divisors" in X constructed from the fibration of the base divisors. Z and B_i are all complex threefolds, and their intersection locus is a complex surface in the elliptic fourfold X over which we can integrate G_4.

If we require that the low energy theory preserves $\mathcal{N} = 1$ supersymmetry, there are D-term and F-term conditions involving Kähler moduli and complex structure moduli on X.

The D-term condition can be written as

$$G_4 \wedge J = 0 \in H^6(X, \mathbb{R}), \tag{4.1.12}$$

where J is the Kähler (1,1)-form of X.

The F-term condition is related to the superpotential in the 4D $\mathcal{N} = 1$ theory, which is the Gukov-Vafa-Witten superpotential[69]

$$W = \int_X G_4 \wedge \Omega, \tag{4.1.13}$$

where Ω is the unique holomorphic (4,0) form on X. The F-term conditions are[40]

$$W = 0 \tag{4.1.14}$$

and

$$D_a W = 0, \tag{4.1.15}$$

where D_a is a covariant derivative in the space of complex structure moduli

$$D_a = \partial_a - \partial_a \ln \int_X \Omega \wedge \bar{\Omega}. \tag{4.1.16}$$

These equations are crucial for the moduli stabilization, which is a procedure to determine the actual value of these Kähler moduli and complex structure moduli. For example, we need these information to actually compute the mass of massive particles in an F-theory model. It is not entirely clear if a general G_4 in the flux vacua will lead supersymmetric solution satisfying the D-term and F-term conditions. We will not consider these problems in detail in this thesis.

The space of G_4 flux can be decomposed into a vertical part $H_V^{2,2}$, a horizontal part H_H^4 and a remaining part $H_{RM}^{2,2}$[23, 131]:

$$H^4(X) = H_H^4(X) \oplus H_V^{2,2}(X) \oplus H_{RM}^{2,2}(X). \tag{4.1.17}$$

The vertical flux has the form of

$$G_4 = \sum_i F^i \wedge \omega_i \tag{4.1.18}$$

where ω_i is the (1,1)-form that is Poincaré dual to the exceptional divisor E_i(the exceptional $\mathbb{P}^1$ fibered over a base divisor with gauge group) in X. F^i is a (1,1)-form corresponding to the gauge flux on the 7-branes. The presence of vertical flux will break the gauge group on the divisor to the commutant of the Cartan generator corresponding to E_i. For example, this provides a mechanism to break the GUT SU(5) gauge group on a divisor to the standard model gauge group SU(3)×SU(2)×U(1)[46].

For this reason, the "non-Higgsable gauge groups" we compute in the 4D F-theory are only geometrically non-Higgsable. They can be broken by the vertical G_4 flux.

In constrast, the horizontal flux in H_H^4 is the space of G_4 flux that does not break any of the gauge groups. The remaining part is the non-vertical G_4 flux which breaks the gauge group, which is argued to be non-significant for a general elliptic Calabi-Yau fourfold[23].

The massless spectrum of particles in the 4D $\mathcal{N} = 1$ supergravity is not as constrained as the 6D case, since there is no pure gravitational anomaly in 4D. The supermultiplets are a unique supergravity multiplet with graviton $g_{\mu\nu}$ and gravitino ψ_μ^α, a number of vector multiplets with a vector field A_μ and a gaugino χ^α and a number of chiral multiplets with a scalar ϕ and a spinor ψ^α. Similar to the 6D case, there are charged chiral multiplets under gauge groups and neutral chiral multiplets.

The number of vector multiplets n_v and chiral multiplets n_c are related to the topological number of X and B in the following way[67].

The total rank of the gauge group equals to

$$\mathrm{rk}(G) = (h^{1,1}(X) - h^{1,1}(B) - 1) + h^{2,1}(B). \tag{4.1.19}$$

The first part $(h^{1,1}(X) - h^{1,1}(B) - 1)$ is given by the Shioda-Tate-Wazir formula (3.1.23). The second contribution $h^{2,1}(B)$ corresponds to a number of U(1)s from the decomposition of the R-R 4-form field C_4 in the IIB description:

$$C_4 = A_I \wedge \omega^I (I = 1, \ldots, h^{2,1}(B)), \tag{4.1.20}$$

where ω^I are the harmonic (2,1)-forms on B. The complete set of geometric gauge groups in 4D F-theory then has three components: the non-Abelian gauge groups on divisors, the U(1) gauge groups from additional rational sections of the elliptic fibration and the additional U(1)s from $h^{2,1}(B)$.

The total number of chiral multiplets equals to

$$n_c = h^{3,1}(X) + h^{1,1}(B) + (h^{2,1}(X) - h^{2,1}(B)). \tag{4.1.21}$$

$h^{3,1}(X)$ counts the number of complex structure moduli of X, $h^{1,1}(B)$ counts the number of Kähler moduli on B, which can be thought as the Hodge dual of the tensor multiplets in the 4D theory. The last term $(h^{2,1}(X) - h^{2,1}(B))$ comes from the "Wilson line scalars" used in M/F-theory duality[67].

The spectrum of charged chiral multiplets depends crucially on the G_4 flux. Let

us consider the localized matter on a curve C, which is the intersection of two divisors D_1 and D_2 that carry gauge groups G_1 and G_2. Suppose that on the curve C, the exceptional divisor forms an affine Dynkin diagram of a larger group $G \supset G_1 \times G_2$, then the matter representations on C is given by (R_1, R_2) in the following decomposition:

$$\text{adj}_G \to (\text{adj}_{G_1}, 1) \oplus (1, \text{adj}_{G_2}) \oplus \sum (R_1, R_2). \tag{4.1.22}$$

Suppose that the G_4 flux only contains the vertical parts (4.1.18), then the multiplicity of chiral multiplets on C is given by

$$N_C = h^0(C, [F] + \frac{1}{2}K_C), \tag{4.1.23}$$

and the multiplicity of anti-chiral multiplets is

$$\bar{N}_C = h^1(C, [F] + \frac{1}{2}K_C) = h^0(C, \frac{1}{2}K_C - [F]). \tag{4.1.24}$$

$[F]$ is a divisor class on the curve C that is Poincaré dual to the gauge flux (1,1)-form in (4.1.18). The identity $H^1(C, [F] + \frac{1}{2}K_C) = H^0(C, \frac{1}{2}K_C - [F])$ is a result of *Serré duality*[66] on a curve. The net chirality is then

$$\chi = h^0(C, [F] + \frac{1}{2}K_C) - h^1(C, [F] + \frac{1}{2}K_C) = \int_C F. \tag{4.1.25}$$

Hence if we set all the G_4 flux to be zero, there is no net chirality on any matter curve. Since $K_C = -2$ for rational curves with genus $g = 0$, there is no matter on rational curves if $G_4 = 0$. For more generic G_4 fluxes, the computation of matter spectrum is extremely involved, see [19, 20].

Besides the local matter fields, there are also charged matter on a divisor D carrying gauge group G. The chiral spectrum can be computed using an 8D topological twisted Yang-Mills theory on the 7-brane world volume[15].

Another new feature in 4D F-theory is the Yukawa coupling term from the intersection of three divisors on B[15]. It does not exist in the 6D case. As a summary,

we see that the 4D F-theory model contains all the different components of the real world physics. The problem is then how to realize the standard model in a natural way, and find out whether the standard model can be realized on a general geometry.

4.2 Classification of base geometry in 4D F-theory

In the regime of 4D F-theory, the traditional terminology of "string landscape" often corresponds to the set of flux vacua on a given elliptic Calabi-Yau fourfold X. However, we want to increase the territory of this string landscape to a broader "string geometric landscape" that includes all the possible geometries used in compactification. The classification program of 4D F-theory solutions then has the following three different layers:

- Classification of topologically distinct base threefolds B. Unlike the classification of base surfaces, there does not exist a mathematical theorem about what are the possible classes of base threefolds. Nonetheless, it was recently proved that the family of base threefolds and elliptic Calabi-Yau fourfolds are finite up to *flops*[44]. Flop is a birational map that is a combination of a blow up and a blow down, see Figure 4-3. In practice, we can also try to generate a large number of base threefolds connected to each other via blow up and blow down and study the properties of these bases, such as the topological numbers and the non-Higgsable gauge groups.

  Physically, these blow up/down process corresponds to tensionless string transitions that changes the base geometry in the very early universe. These physical transitions can be thought of quantum tunneling between states in a huge web[31], although we do not know anything concrete about the quantum mechanical process or what is the energy of each eigenstate.

- Classification of different fibrations on a given base B. A non-generic fibration will bring separated 7-branes together and give a larger gauge group than the non-Higgsable phase. Since f and g are tuned, the number of complex structure

moduli $h^{3,1}(X)$ will decrease. This will decrease the total number of flux vacua on the resulted geometry by a large exponential factor. For example, it was shown in [22, 131] that tuning an additional SU(5) GUT group on $\mathbb{P}^3$ will suppress the total number of flux vacua by a factor of $\sim 10^{-3,000}$. Following this logic, we may argue that the GUT construction is unnatural in constrast to the non-Higgsable phase. In this thesis, we only consider the generic fibration over a given base.

- Analyze each flux vacuum corresponding to a specific G_4, computing the particle spectrum and stablize the K$\acute{}$ahler and complex structure moduli.

In this thesis, we only focus on the classification of base threefolds. Analogous to the case of base surfaces, the set of rational threefolds that are birationally equivalent to $\mathbb{P}^3$ is a good family to be explored. For simplicity, we will only consider the toric threefolds due to the following three reasons:

- The crucial discrete data such as the effective cone and Mori cone are straight forward to read out on a toric threefold. They are simply generated by the toric divisors and toric curves. For a non-toric threefold, they are not so obvious.

- On a toric variety, the section of line bundles can be easily written out with the points in the dual polytope (2.4.67). On a non-toric variety, we do not know how to write down the section of $-4K_B$ and $-6K_B$ explicitly. So we do not know how to compute the order of vanishing of (f, g) on divisors and curves. For non-toric surfaces, we can compute them with Zariski decomposition. However, for non-toric threefolds, the Zariski decomposition method will not provide sufficient data to determine $\text{ord}(f, g)$.

  There exists formula to compute the coefficients f_k and g_k in the expansion near a divisor D_i given by the local equation $s = 0$[107]:

$$f = \sum_k f_k s^k \ , \ g = \sum_k g_k s^k, \tag{4.2.26}$$

using the normal bundle and canonical bundle of D_i[107]:

$$f_{k,i} \in \mathcal{O}(-4K_{D_i} + (4-k)N_{D_i} - \sum_{D_i \bigcap D_j \neq \varnothing} \phi_j C_{ij}), \tag{4.2.27}$$

$$g_{k,i} \in \mathcal{O}(-6K_{D_i} + (6-k)N_{D_i} - \sum_{D_i \bigcap D_j \neq \varnothing} \gamma_j C_{ij}). \tag{4.2.28}$$

ϕ_j, γ_j denotes the order of vanishing of f and g on D_j that intersects D_i. If $f_{k,i} \in \mathcal{O}(C_k)$ and C_k is ineffective for all $k < k_0$, then f vanishes to at least order k_0 on D_i. Similar statement holds for g.

However, it is not clear how to construct a definite algorithm to determine $\mathrm{ord}(f,g)$ on all the divisors since the formula (4.2.27, 4.2.28) involves $\mathrm{ord}(f,g)$ of the adjacent divisors as well. On the other hand, the non-adjacent divisors may enhance the order of vanishing of (f,g) and they cannot be read off by (4.2.27, 4.2.28).

- The only possible ways to blow up a toric threefold is to blow up a toric curve or a toric point, see Figure 4-2. More generally, one can blow up a curve on a threefold to produce a non-toric threefold. However, the classification of non-isomorphic irreducible curves on a threefold B is unknown, even if $B = \mathbb{P}^3$. So we do not really know how many non-toric threefolds are connected to a given threefold via a blow up/down.

The defining data for a smooth compact toric threefold is the set of rays $\Sigma(1) = \{v_i = (v_{i,x}, v_{i,y}, v_{i,z}) \in N = \mathbb{Z}^3\}$ and the set of 3D cones $\Sigma(3) = \{\sigma = v_i v_j v_k\}$. Denote $n = |\Sigma(1)|$, then we always have $|\Sigma(3)| = 2n - 4$. The set of toric curves $\Sigma(2) = \{v_i v_j | \exists \sigma \in \Sigma(3)\ ,\ v_i v_j \subset \sigma\}$ is completely determined by the data $\Sigma(3)$.

There are two kinds of blow up operations on toric bases B: one can either blow up a point that corresponds to a three-dimensional cone $\sigma = v_i v_j v_k$ or blow up a toric curve $v_i v_j$. In the first case, a new ray $\tilde{v} = v_i + v_j + v_k$ is introduced. The old three-dimensional cone σ is removed, and three new three-dimensional cones $\tilde{\sigma}_1 = v_i v_j \tilde{v}$, $\tilde{\sigma}_2 = v_j v_k \tilde{v}$, $\tilde{\sigma}_3 = v_k v_i \tilde{v}$ are included. For the second case, a new ray $\tilde{v} = v_i + v_j$ is

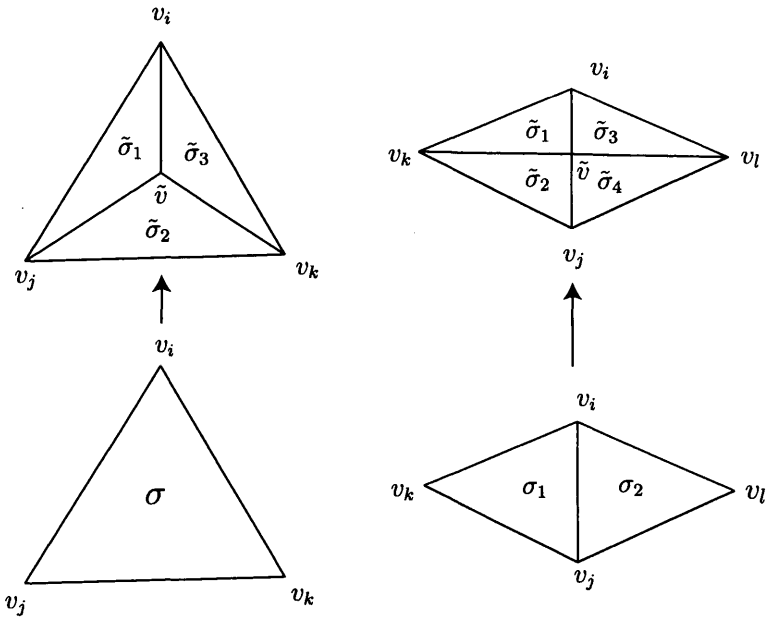

Figure 4-2: Illustration of two different kinds of blow ups, viewed from above. The left case corresponds to blowing up a point $v_iv_jv_k$. The right case corresponds to blowing up a curve v_iv_j.

introduced. Suppose that there are two old 3d cones $\sigma_1 = v_iv_jv_k$ and $\sigma_2 = v_iv_jv_l$ that contain the toric curve v_iv_j. They are removed after the blow up. Four new 3d cones $\tilde{\sigma}_1 = v_iv_k\tilde{v}$, $\tilde{\sigma}_2 = v_jv_k\tilde{v}$, $\tilde{\sigma}_3 = v_iv_l\tilde{v}$, $\tilde{\sigma}_4 = v_jv_l\tilde{v}$ are included. Note that v_iv_j is no longer a toric curve after the blow up. Similarly a blow down is described as the contraction and removal of a ray. Given a ray v, it may or may not be contracted depending on the neighboring rays. If there are only 3 neighboring rays v_i, v_j, v_k and they satisfy $v = v_i + v_j + v_k$, then v can be contracted into a point. If there are 4 neighboring rays v_i, v_k, v_j, v_l (in cyclic order around the curve), if $v = v_i + v_j$ or $v = v_k + v_l$, then v can be contracted into toric curve v_iv_j or v_kv_l respectively. For all the other cases, the ray v cannot be contracted to get another smooth toric threefold.

When there are rays v_i, v_j, v_k, v_l that satisfy the relation $v_i + v_j = v_k + v_l$, and there is a 2d cone v_iv_j, then there exists a "flop" operation, which is a combination of a blow up and a blow down; see Figure 4-3.

The Weierstrass polynomial f ang g for a generic elliptic fibration over B is defined

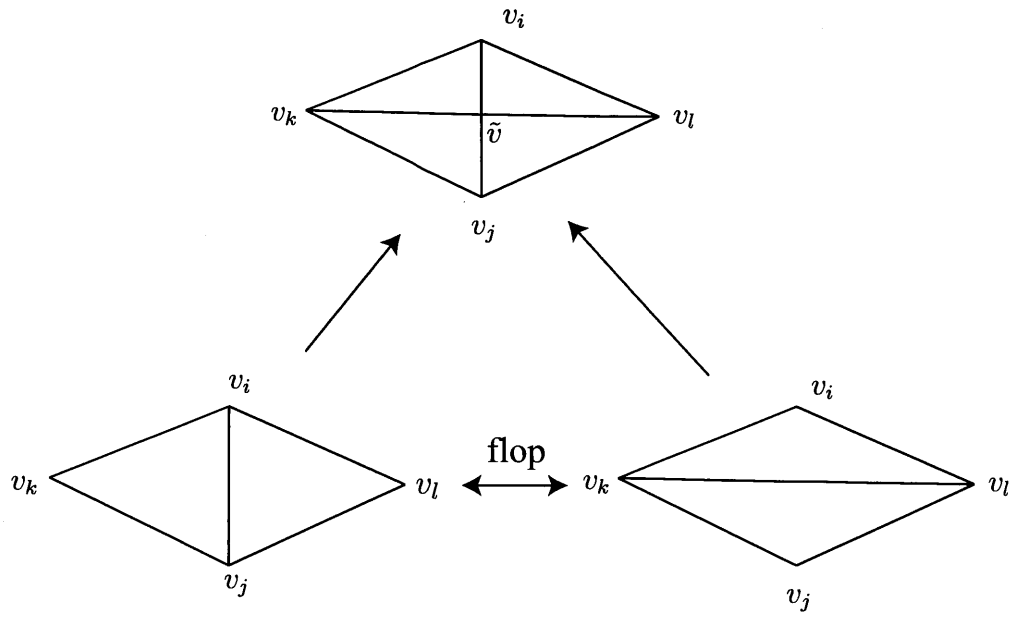

Figure 4-3: Illustration of the flop process, which can happen when $v_i + v_j = v_k + v_l$.

by the polytopes $\mathcal{F}$ and $\mathcal{G}$ as usual:

$$\mathcal{F} = \{u \in \mathbb{Z}^3 | \forall v_i, \langle u, v_i \rangle \geq -4\}, \tag{4.2.29}$$

$$\mathcal{G} = \{u \in \mathbb{Z}^3 | \forall v_i, \langle u, v_i \rangle \geq -6\}, \tag{4.2.30}$$

The order of vanishing of f and g on a toric divisor D_i is

$$\begin{aligned} \text{ord}_{D_i}(f) &= \min(\langle u, v_i \rangle + 4)|_{u \in \mathcal{F}}, \\ \text{ord}_{D_i}(g) &= \min(\langle u, v_i \rangle + 6)|_{u \in \mathcal{G}}. \end{aligned} \tag{4.2.31}$$

The order of vanishing of f and g on a toric curve $D_i D_j$ is:

$$\begin{aligned} \text{ord}_{D_i D_j}(f) &= \min(\langle u, v_i + v_j \rangle + 8)|_{u \in \mathcal{F}}, \\ \text{ord}_{D_i D_j}(g) &= \min(\langle u, v_i + v_j \rangle + 12)|_{u \in \mathcal{G}}. \end{aligned} \tag{4.2.32}$$

Note that $\text{ord}_{D_i D_j}(f, g)$ can be greater or equal to $\text{ord}_{D_i}(f, g) + \text{ord}_{D_j}(f, g)$. This is different from the case of 2d bases, where the order of vanishing on the intersection point of two divisors is always the sum of the orders of vanishing on those two divisors.

Similarly we can write down the order of vanishing of f, g and Δ on the point $D_iD_jD_k$:

$$\begin{aligned} \text{ord}_{D_iD_jD_k}(f) &= \min(\langle u, v_i + v_j + v_k\rangle + 12)|_{u\in\mathcal{F}}, \\ \text{ord}_{D_iD_jD_k}(g) &= \min(\langle u, v_i + v_j + v_k\rangle + 18)|_{u\in\mathcal{G}}. \end{aligned} \tag{4.2.33}$$

We can compute the non-Higgsable gauge groups following the general procedure in Chapter 2.

To exactly define the set of toric threefold bases we are going to classify, it is important to clarify the following issues:

- Codimension-two (4,6) locus.

When (f, g, Δ) vanish to order $(4, 6, 12)$ or higher over a codimension-two locus on B, we can try to blow up these loci and lower the degree of vanishing of (f, g) to be less than $(4, 6)$. If this blow-up process can be done without introducing a codimension-one (4,6) locus in the process, then we call this base B a "resolvable base". In fact, the polynomials $\mathcal{F}$ and $\mathcal{G}$ are unchanged after this resolution process. Since the points u that are removed in $\mathcal{F}/\mathcal{G}$ polytopes after blowing a curve D_iD_j are the ones satisfying $\langle u, v_i + v_j\rangle < -4/-6$.

As we have discussed in Chapter 3, the appearance of such a codimension-two (4,6) locus in 6D F-theory signify a (1,0) SCFT sector decoupled with gravity. In 4D F-theory, the correspondence between such codimension-two (4,6) loci and the 4D $\mathcal{N} = 1$ SCFT is not clear. After the usual resolution process of the singular Weierstrass model without blowing up the (4,6) curve on the base, there will be an exceptional 4-cycle such that the fibration is no longer flat. Wrapping a D5 brane on this 4-cycle will give us a 1D object in the IIB picture. Hence in the limit where this exceptional 4-cycle is shrunk to zero volume, we will have a tensionless string when we attempt to directly compactify F-theory over the base with a codimension-two (4,6) locus. It is not clear whether these tensionless string object will cause any problem in the 4D low energy effective theory, especially in the presence of non-zero G_4 flux.

- Terminal singularities on the Calabi-Yau fourfold.

Sometimes there are non-resolvable singularities on the CY 4-fold that cannot be resolved to a smooth Calabi-Yau geometry, which has nothing to do with the $(4,6)$ singularity. For example, we can write the Weierstrass equation in the following form using local coordinates (s,t,u):

$$y^2 = x^3 + (a_0 s + a_1 t)x + (b_0 s^2 + b_1 st + b_2 t^2), \tag{4.2.34}$$

where the coefficients a_0, a_1, b_0, b_1, b_2 are generic functions of u. Then there will be singularity over the locus $x = y = s = t = 0$. We cannot resolve this singularity without changing the canonical class of the CY 4-fold. This type of terminal singularity appears generically in the complex structure moduli space, but we treat these singularities as acceptable ones. In a recent paper on elliptic CY 3-fold[9], these terminal singularities are shown to be correspond to a finite number of neutral chiral matter fields. The impact of these terminal singularities in CY 4-fold is still not well-understood yet, but we expect that they will only alter the counting of the chiral multiplets.

- Codimension-three (4,6) locus

It is also a common feature that f and g vanishes to order (4,6) or higher over codimension-three locus in the base. They may lead to non-flat fibration in the resolution process if there is only one gauge group involved [94, 26]. For example, if there is an E_7 gauge group on $s = 0$:

$$y^2 = x^3 + (a_0 s^3 + a_1 s^4 + \dots) + (b_0 s^5 + b_1 s^6 + \dots), \tag{4.2.35}$$

then there is a codimension-three (4,6) locus at $a_0 = b_0 = s = 0$, which leads to non-flat fiber at this point[94].

A clearer classification of codimension-three (4,6) locus and their physical consequences should be done in further research, and we generally allow their appearance if (f,g) does not vanish to order $(8,12)$ or higher on this point.

Hence the allowed bases in this classification program are separated into two different classes:

(1) The *resolvable bases* with toric (4,6) curves, but they can be removed after a finite number of blow ups along these toric curves. A practical criterion for the resolvability is to check whether the origin $(0,0,0)$ lies on the boundary of $\mathcal{G}$. If the origin $(0,0,0)$ lies in the interior of $\mathcal{G}$, then after the resolution process where all the (4,6) curves are blown up, there will not be a codimension-one (4,6) locus on any divisor. This follows because if there exists such a divisor corresponding to the ray v, then all the points $u \in \mathcal{G}$ satisfying $\langle u, v\rangle < 0$ will vanish and the origin $(0,0,0)$ lies on the boundary plane $\langle u, v\rangle = 0$ of $\mathcal{G}$.

(2) The *good bases* without any toric (4,6) curves. We allow the non-toric (4,6) curves on divisors with E_8 gauge group in parallel to the 6D F-theory case where we allow the -9/-10/-11 curves in the counting of "toric" base surfaces. These non-toric (4,6) curves can be easily blown up to get rid of these codimension-two (4,6) singularity. We also have *strictly good bases* which are toric threefold bases without any (4,6) curves at all.

The appearances of terminal singularities and codimension-three (4,6) points are generally allowed in all of these classes.

For the generic elliptic fourfold X over a good base B, we can compute the Hodge number $h^{1,1}(X)$ using the Tate-Shioda-Wazir formula:

$$h^{1,1}(X) = h^{1,1}(B) + \mathrm{rk}(G) + 1 + N(blp), \tag{4.2.36}$$

where G is the non-Abelian gauge groups on B. $N(blp)$ is the number of additional blow ups to resolve the codimension-two (4,6) singularity on divisors with E_8 gauge groups. If this codimension-two (4,6) locus is irreducible, then it contributes 1 to $N(blp)$. If it is reducible, then its contribution to $N(blp)$ is the number of irreducible components.

We can also estimate the Hodge number $h^{3,1}(X)$ using an approximate Batyrev

type formula [124]:

$$h^{3,1}(X) \cong \tilde{h}^{3,1}(X)$$
$$= |\mathcal{F}| + |\mathcal{G}| - \sum_{\Theta\in\Delta,\dim\Theta=2} l'(\Theta) - 4 + \sum_{\Theta_i\in\Delta,\Theta_i^*\in\Delta^*,\dim(\Theta_i)=\dim(\Theta_i^*)=1} l'(\Theta_i)\cdot l'(\Theta_i^*). \tag{4.2.37}$$

Here Δ^* is the convex hull of $\{v_i\}$ and Δ is the dual polytope of Δ^*, defined to be

$$\Delta = \{u \in \mathbb{R}^3 | \forall v \in \Delta^* \ , \ \langle u, v\rangle \geq -1\}. \tag{4.2.38}$$

The symbol Θ denotes 2d faces of Δ. Θ_i and Θ_i^* denote the 1d edges of the polytopes Δ and Δ^*. $l'(\cdot)$ counts the number of integral interior points on a face. This formula is analogous to the formula (3.2.39) in the elliptic Calabi-Yau threefold case. Here $|\mathcal{F}| + |\mathcal{G}|$ counts the number of Weierstrass moduli, $\sum_{\Theta\in\Delta,\dim\Theta=2} l'(\Theta) + 3$ is the dimension of the automorphism group w_{aut} of the base B, and the final term in (4.2.37) is analogous to N_{-2}. This formula was not proven, but we have checked that it produces consistent results for many examples in [100].

Now we are going to present two different exploration results of the toric threefold bases.

4.3 Random walk on the set of toric threefold bases

4.3.1 Methodology

In [124], we restricted ourselves to the set of strictly good toric bases, which means that there is absolutely no (4,6) curves on the base. Under this constraint, we can probe a connected set $\mathcal{C}$ of strictly good toric bases that include $\mathbb{P}^3$. We start with starting point $\mathbb{P}^3$, and in each step of the random walk, the base may be blown up or blown down to get another base. In the performance, each valid blow-up or blow-down from a given base $B \in \mathcal{C}$ is given an equal probability. Following a basic result in graph theory, if we perform a random walk on a graph where each node V_i has n_i

neighbors, and the neighbors are chosen uniformly on each step of the walk, we will get a distribution of bases on nodes proportional to n_i.

In practice, we randomly choose from the set of all the $(6n-10)$ possible 3D cones, 2D cones, and rays at each step. Then we test the chosen move to see if it results in an allowed base. For the cases of 3D cones, 2D cones and rays, they correspond to blowing up a toric point, blowing up a toric curve and blowing down the toric divisor respectively. If the tested step does not lead to an allowed base, we try again. After a large number of steps, we expect a "thermal" distribution in which the probability of each base B in the set $\mathcal{C}$ is proportional to n_i, the number of valid neighbors to which B is connected by a single blow up/down. Hence in order to compute the statistical information using a uniform distribution on $\mathcal{C}$, we need to weight each base by the factor $1/n_i$. To reduce the computational complexity, we do not explicitly compute n_i for each base. We record the number t of attempts needed to identify an allowed neighbor instead. Naively the number of allowed neighbors of a given base B should be $(6n-10)/\langle t\rangle$, where $\langle t\rangle$ is the average number of tries needed to identify an allowed neighbor over many trials on the base B. The weighting factor $1/n_i$ can therefore be estimated as $\langle t\rangle/(6n-10)$, so we can get uniform statistics on $\mathcal{C}$ by weighting each base with the factor $t/(6n-10)$.

This factor is not correct if different neighbors of one base are equivalent. For example, consider a graph with only three nodes: $\mathbb{P}^3$, $\mathrm{blp}_{\mathrm{cone}}\mathbb{P}^3$ and $\mathrm{blp}_{\mathrm{curve}}\mathbb{P}^3$. $\mathrm{blp}_{\mathrm{cone}}\mathbb{P}^3$ and $\mathrm{blp}_{\mathrm{curve}}\mathbb{P}^3$ denote the bases that result from blowing up a 3D cone or a curve on $\mathbb{P}^3$ respectively, which are explicitly defined below:

$$\begin{aligned}\mathbb{P}^3 \ &: v_1=(1,0,0), v_2=(0,1,0), v_3=(0,0,1), v_4=(-1,-1,-1),\\ &\Sigma(3)=\{v_1v_2v_3, v_1v_2v_4, v_1v_3v_4, v_2v_3v_4\}\end{aligned} \tag{4.3.39}$$

$$\text{blp}_{\text{cone}}\mathbb{P}^3 \ : v_1 = (1,0,0), v_2 = (0,1,0), v_3 = (0,0,1), v_4 = (-1,-1,-1), v_5 = (1,1,1),$$
$$\Sigma(3) = \{v_1v_2v_4, v_1v_3v_4, v_2v_3v_4, v_1v_2v_5, v_1v_3v_5, v_2v_3v_5\} \tag{4.3.40}$$

$$\text{blp}_{\text{curve}}\mathbb{P}^3 \ : v_1 = (1,0,0), v_2 = (0,1,0), v_3 = (0,0,1), v_4 = (-1,-1,-1), v_5 = (1,1,0),$$
$$\Sigma(3) = \{v_1v_3v_4, v_2v_3v_4, v_1v_3v_5, v_1v_4v_5, v_2v_3v_5, v_2v_4v_5\} \tag{4.3.41}$$

There are four ways to get $\text{blp}_{\text{cone}}\mathbb{P}^3$ and six ways to get $\text{blp}_{\text{curve}}\mathbb{P}^3$ from blowing up a cone or curve on $\mathbb{P}^3$, since there are 4 3d-cones and 6 2d-cones in the toric fan of $\mathbb{P}^3$. This means that naively $\mathbb{P}^3$ has 10 neighbors, and the base is weighted by $1/10$. Now, if we perform a random walk on this graph, the expected probability ratio is $p(\mathbb{P}^3) : p(\text{blp}_{\text{cone}}\mathbb{P}^3) : p(\text{blp}_{\text{curve}}\mathbb{P}^3) = 10 : 4 : 6$. Then after we weight $p(\mathbb{P}^3)$ by a factor $1/10$, the expected probability ratio becomes $1 : 4 : 6$, which is still far from uniform. To fix this problem, we compute the symmetry factor F of each base, which is defined to be the order of the subgroup of the permutation group acting on the toric divisors of the base that preserves the cone structure. For example, for the base $\mathbb{P}^3$, since all the four rays v_1, v_2, v_3, v_4 can be permuted arbitrarily without changing the cone structure, $F(\mathbb{P}^3) = 24$. For the base $\text{blp}_{\text{cone}}\mathbb{P}^3$, the divisors corresponding to v_1, v_2 and v_3 can be permuted, hence $F(\text{blp}_{\text{cone}}\mathbb{P}^3) = 6$. For the base $\text{blp}_{\text{curve}}\mathbb{P}^3$, there are two symmetric divisor pairs: (v_1, v_2) and (v_3, v_4), hence $F(\text{blp}_{\text{curve}}\mathbb{P}^3) = 4$. After we multiply those symmetry factors by the ratio $1 : 4 : 6$, then we achieve a uniform distribution. In general, if we use the proper weighting factor

$$w(B) = \frac{t \cdot F(B)}{(6n-10)}, \tag{4.3.42}$$

then this problem will not bother us.

For a general base with a large number of rays, the probability of having a non-

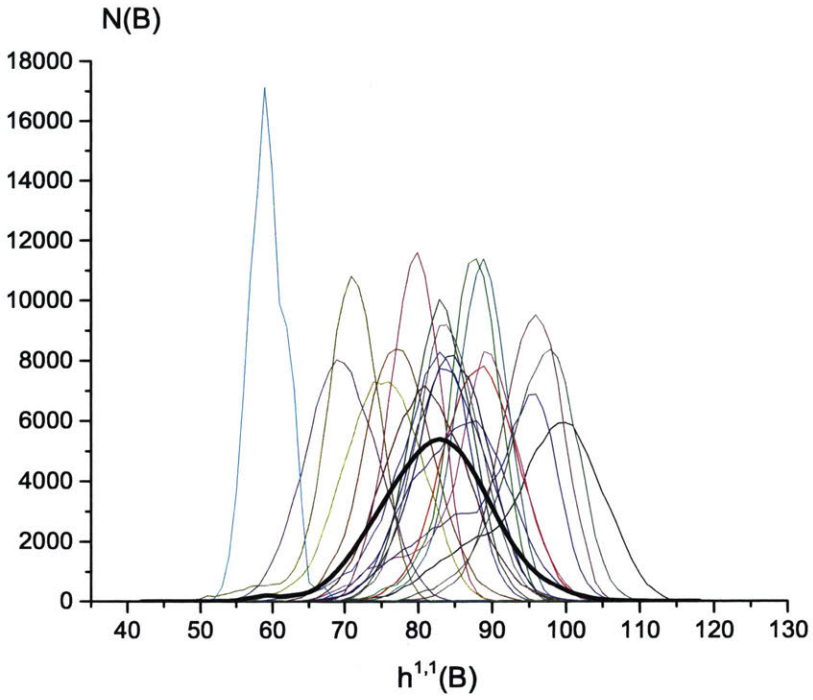

Figure 4-4: The distribution of $h^{1,1}(B)$ including weighting factors (4.3.42). Bold black curve is the average distribution among the 100 runs, while the colored curves are some example distributions from individual runs. The total number of samples in each run is normalized to 100,000.

trivial symmetry is negligible. Practically, the inclusion of symmetry factors only affects the statistics of bases with a number of rays $n \lesssim 10$.

4.3.2 Unbounded random walk

We have recorded 100 independent random walk sequences (runs), each of which starts from $\mathbb{P}^3$ and has 100,000 bases in it. They are refered as "unbounded" runs to distinguish them from the other runs with bounded $h^{1,1}(B)$ described in Section4.3.3. To compute the statistics of the each subregion of $\mathcal{C}$ probed by these runs, we remove the first 1000 bases since they have atypically small $h^{1,1}(B)$ and do not represent a typical base in the middle of $\mathcal{C}$.

The total distribution of $h^{1,1}(B)$ is plotted in Figure 4-4 and compared to the distributions for several individual runs.

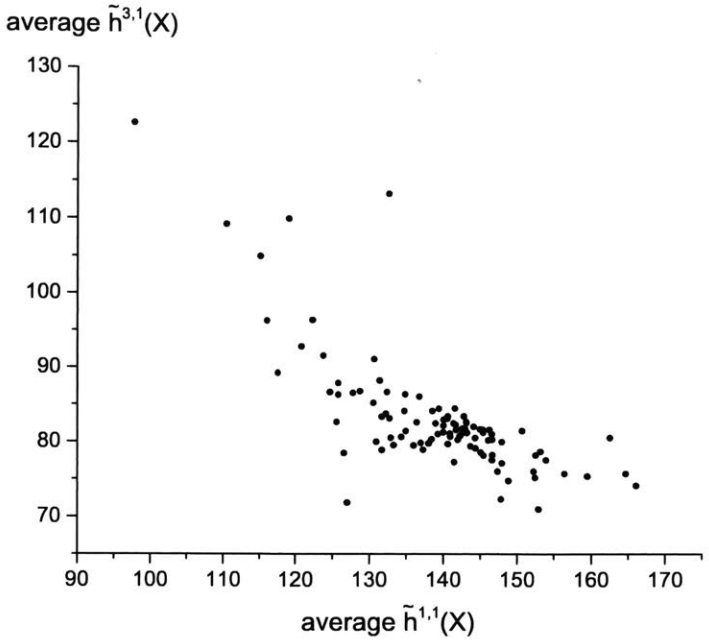

Figure 4-5: Average values of the (approximate) Hodge numbers for generic elliptic Calabi-Yau fourfolds over the threefold bases encountered in each of the independent random walk sequences.

We also plot the average Hodge numbers $(h^{1,1}(X), \tilde{h}^{3,1}(X))$ of the generic elliptic Calabi-Yau fourfolds X over the sets of bases B explored by the different random walk sequences in Figure 4-5. $\tilde{h}^{3,1}(X)$ is the approximate Hodge number computed by (4.2.37). These Hodge numbers locate at the corner close to the origin in the Figure 4-1.

For the geometric non-Higgsable gauge groups, it turns out that essentially all the bases found in the Monte Carlo runs had some divisors supporting non-Higgsable gauge factors. The only exceptions were in the first few bases encountered in each run. This is generally verified in [72, 71] as well.

For bases with $h^{1,1}(B)$ between 40 and 100, the fraction of divisors on any base that support a non-Higgsable gauge factor is roughly 35–40%.

We list the average numbers of times that each individual non-Higgsable gauge group factor arises on a typical base in Table 4.1. $\mathrm{SU}(2)_{III}$ and $\mathrm{SU}(2)_{IV}$ denotes the SU(2) non-Higgsable gauge group from type III and type IV Kodaira fiber type

$SU(2)_{III}$	$SU(2)_{IV}$	$SU(2)$	$SU(3)$	G_2
6.1 ± 1.7	7.5 ± 1.5	13.6 ± 1.6	2.0 ± 0.6	9.7 ± 1.8
$SO(7)$	$SO(8)$	F_4	E_6	E_7
$4 \times 10^{-6} \pm 2 \times 10^{-5}$	1.0 ± 0.6	2.8 ± 1.1	0.3 ± 0.4	0.2 ± 0.5

Table 4.1: Average number of times each non-Higgsable gauge group factor appears on a base, with standard deviation computed among the 100 runs.

$SU(2)$	$SU(3)$	G_2	$SO(7)$	$SO(8)$	F_4	E_6	E_7
99.999 ± 0.001	83 ± 11	99.93 ± 0.07	0.0004 ± 0.002	59 ± 21	94 ± 21	26 ± 31	18 ± 37

Table 4.2: Average percentage of bases with a specific gauge group factor, with standard deviation computed among the 100 runs.

respectively. We also list the percentage of bases with a specific gauge group factor in Table 4.2.

It turns out that the gauge factors SU(2) and G_2 are mostly dominant. The gauge factors F_4 and SU(3) also generally arise on a typical base, with an average number of appearances higher than 1 in each case. For the other gauge group factors, their appearance seems to characterize some "local feature" of the part of landscape covered by a particular run. For example, in a particular run, a large percentage of bases possess E_6 gauge group but they are not common for the other runs.

Along with the observation in Figure 4-4 and Figure 4-5, we see that each runs actually probe a local subregion of their own. Hence each of these random walk sequence is not a good global approximation of the whole set $\mathcal{C}$, and it really makes sense to perform a number of different runs rather than record a single sequence with a billion bases.

From these statistics, the SO(7) gauge group is the rarest and one should not expect the appearance of SO(7) on a typical base.

Since we do not allow the bases with divisors having E_8 and (4,6) curves on them, we never encounter a base with E_8 as they are effectively disconnected with $\mathcal{C}$. This phenomenon is not present in the other classes of bases.

For the pair of non-Higgsable gauge groups on adjacent divisors, the only possible

SU(2)×SU(2)	SU(3)×SU(2)	SU(3)×SU(3)	G_2×SU(2)	SO(7)×SU(2)
7.6 ± 1.9	2.4 ± 0.9	0.4 ± 0.4	14 ± 3	0 ± 0

Table 4.3: Average number of appearances of each gauge pair on a base, with standard deviation computed among the 100 runs.

SU(2)×SU(2)	SU(3)×SU(2)	SU(3)×SU(3)	G_2×SU(2)	SO(7)×SU(2)
98 ± 6	76 ± 14	28 ± 16	99.9 ± 0.7	0 ± 0

Table 4.4: Average percentage of bases with a specific gauge pair, with standard deviation computed among the 100 runs.

configurations are [107]:

$$SU(2) \times SU(2) \ , \ SU(3) \times SU(2) \ , \ SU(3) \times SU(3) \ , \ G_2 \times SU(2) \ , \ SO(7) \times SU(2) \tag{4.3.43}$$

This follows from the requirement that there is not a (4,6) singularity on the intersection of the two divisors, along with monodromy conditions. Such gauge pairs are naturally associated with codimension two singularities supporting (geometric) matter that transforms as a field charged under both gauge factors in presence of a non-vanishing G_4 flux.

We have listed the average number of times each gauge pair arises on a typical base in Table 4.3. We also list the percentage of bases with a specific gauge pair in Table 4.4.

An interesting feature in the statistics is that for a typical base, the gauge pair SU(3)×SU(2) appears more than once, and more than half of bases ($\sim 76\%$) support at least one SU(3)×SU(2) gauge pair. Such a non-Higgsable gauge pair could act as the non-Abelian part of the standard model gauge group in a non-GUT scenario [62]. It is not clear how to reproduce the standard model spectrum if a U(1) is tuned on that base.

4.3.3 Estimate the total number of bases in $\mathcal{C}$

To estimate the total number of bases, we have carried out a sequence of runs in which we have placed an artificial upper bound on the Picard number of the base. If a base in the sequence hits this upper bound, then it can only be blown down in the next step.

We have done 10 Monte Carlo runs of 30,000 steps each with upper bounds $h^{1,1}(B) \leq 5k + 2$ for each $k = 1, \ldots, 13$. We again ignore the first 1000 bases in all the statistical analyses. Using the appropriate weighting factors (4.3.42), this gives an estimate of the distribution of bases in each bounded range of $h^{1,1}(B)$.

To estimate the total number of bases in $\mathcal{C}$ we can combine the distributions from the bounded runs. We define

$$N(h) = |\{B \in \mathcal{C} : h^{1,1}(B) = h\}| . \tag{4.3.44}$$

We know that $N(1) = 1$ (from $B = \mathbb{P}^3$), and it is not hard to determine that $N(2) = 27$ (from $\mathbb{P}^1 \times \mathbb{P}^2$, 12 distinct nontrivial $\mathbb{P}^1$ bundles over $\mathbb{P}^2$ and 14 distinct nontrivial $\mathbb{P}^2$ bundles over $\mathbb{P}^1$.

The $\mathbb{P}^1$ bundles over $\mathbb{P}^2$ are typically called "generalized Hirzebruch threefold" $\tilde{\mathbb{F}}_n$, with the following toric data:

$$\begin{aligned} \Sigma(1) &= \{v_1 = (1,0,0), v_2 = (0,1,0), v_3 = (0,0,1), v_4 = (-1,-1,-n), v_5 = (0,0,-1)\} \\ \Sigma(3) &= \{\{v_1v_2v_3, v_1v_5v_3, v_2v_5v_3, v_1v_2v_4, v_1v_5v_4, v_2v_5v_4\}. \end{aligned} \tag{4.3.45}$$

The good generalized Hirzebruch threefold $\tilde{\mathbb{F}}_{18}$ with an E_8 gauge group and no (4,6) curves is not connected to $\mathcal{C}$. As a check on our methodology, the ratio $N(2)/N(1) = 27$ is correctly reproduced to good accuracy by Monte Carlo runs with a low bound on h.

We denote the number of bases with $h^{1,1}(B) = h$ encountered in the experiment $h^{1,1}(B) \leq m$ by $\mathcal{N}_m(h)$. The numbers are geometrically averaged among multiple

runs. Then the run at $k = 1$ gives an estimate of $N(7)$, using the experimental ratio $\mathcal{N}_7(7)/\mathcal{N}_7(2)$ and the fact that $N(2) = 27$:

$$N(7) \cong 27 \cdot \frac{\mathcal{N}_7(7)}{\mathcal{N}_7(2)}. \tag{4.3.46}$$

From the run at $k = 2$, we can use the experimental value $\mathcal{N}_{12}(12)/\mathcal{N}_{12}(7)$ to estimate $N(12)$. Repeating this process we can give a rough estimate for

$$N(h) \cong 27 \times \frac{\mathcal{N}_7(7)}{\mathcal{N}_7(2)} \times \frac{\mathcal{N}_{12}(12)}{\mathcal{N}_{12}(7)} \times \cdots \times \frac{\mathcal{N}_{h'}(h')}{\mathcal{N}_{h'}(h'-5)} \times \frac{\mathcal{N}_{h'+5}(h)}{\mathcal{N}_{h'+5}(h')}, \tag{4.3.47}$$

where $h' \equiv 2 \pmod 5$ and $h - 5 < h' \leq h$. Finally when $h \geq 67$, the proportion of bases at each h is significant enough that we can employ the data from the 100 unbounded runs, and $N(h)$ can be estimated by

$$N(h) \cong N(67) \cdot \frac{\mathcal{N}_{\text{unbounded}}(h)}{\mathcal{N}_{\text{unbounded}}(67)}. \tag{4.3.48}$$

The resulting estimations of $N(h)$ are graphed in Figure 4-6. We also plot $\log_{10}(N(h))$ in Figure 4-7, with the standard deviation. It turns out that in the region $h \leq 35$, the number of bases grows exponentially. In the region $35 \leq h \leq 60$, the exponential growth slows down. Finally the number of bases reaches a peak at $h \cong 82$, as a base with larger $h^{1,1}(B)$ typically has (4,6) curves.

Summing these approximate values, we have a very rough estimation

$$|\mathcal{C}| = \sum_{h=1}^{\infty} \mathcal{N}(h) \sim 10^{48 \pm 2}. \tag{4.3.49}$$

One possible explanation for the exponential growth of the number of bases with $h^{1,1}(B)$ is the existence of many flops (see Figure 4-3) on typical bases with large $h^{1,1}(B)$. Since a flop does not change the rays or the set of monomials, the geometric non-Higgsable gauge groups of the associated F-theory compactification does not change under a flop. Because $v_i + v_j = v_k + v_l$, f and g also vanish to the same order on the toric curves $v_i v_j$ and $v_k v_l$. Hence if $B_1 \in \mathcal{C}$, and B_2 can be related to B_1 by a

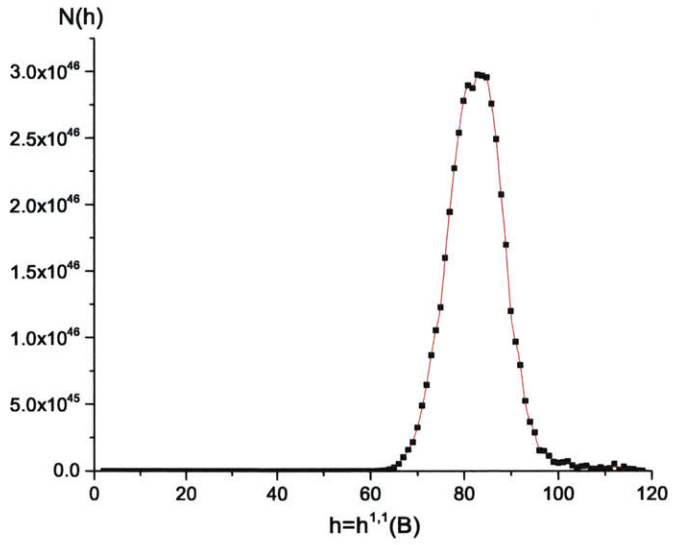

Figure 4-6: Rough estimation of the number of bases $B \in \mathcal{C}$ with $h^{1,1}(B) = h$.

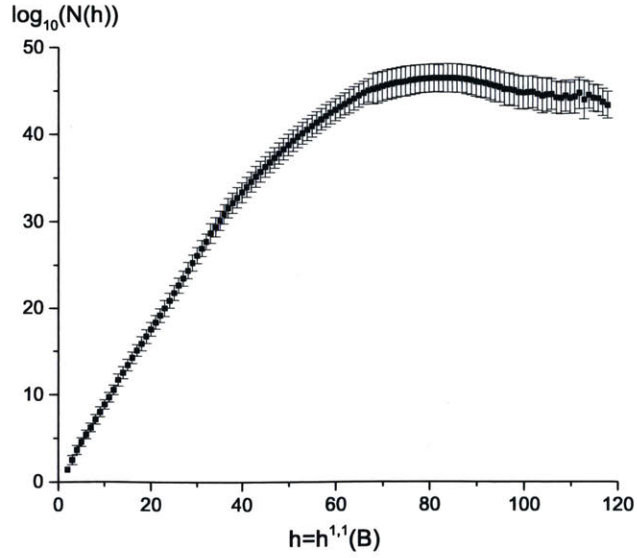

Figure 4-7: Rough estimation of $\log_{10}(N(h))$ with error bars, where $N(h)$ is the number of bases $B \in \mathcal{C}$ with $h^{1,1}(B) = h$.

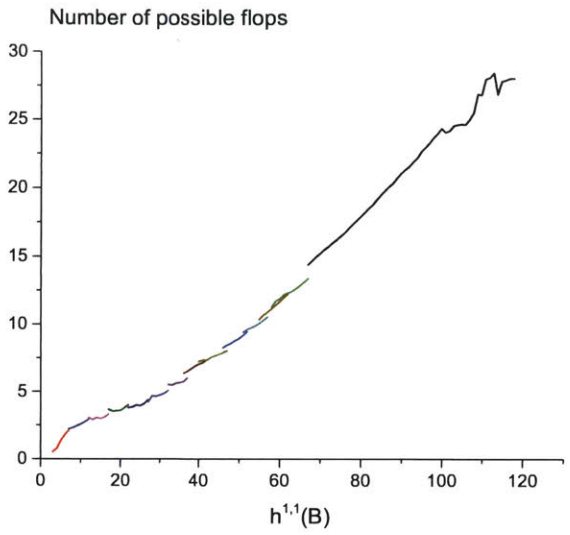

Figure 4-8: Average number of possible flops on B as a function of $h^{1,1}(B)$. For $h^{1,1}(B) > 67$, the numbers are computed from the 100 unbounded runs. For the lower values of $h^{1,1}(B)$, they are computed from the bounded runs.

flop, then $B_2 \in \mathcal{C}$ always holds. However, since the set of curves changes after a flop, the local matter spectrum on the curves will be different.

If there are n possible flops on a base $B \in \mathcal{C}$, and each flop is isolated, then there are approximately 2^n bases in $\mathcal{C}$ that can be related to B by a sequence of flops.

The average numbers of possible flops on bases with different $h^{1,1}(B)$ are plotted in Figure 4-8. The number of flops grows almost linearly from $h^{1,1}(B) = 50$ to $h^{1,1}(B) = 100$. Comparing to Figure 4-7, we can see that even if we divide the total number of bases for a given $h^{1,1}(B)$ by 2^n, where n is the average number of possible flops, the number of distinct triangulation types of bases still grows exponentially. Hence there are still approximately $10^{48}/2^{20} \sim 10^{42}$ distinct bases that cannot be related by flops.

4.4 Random blow up on the set of toric threefold bases

4.4.1 Methodology

In the last section, we have studied the statistical information in a subset of strictly good bases $\mathcal{C}$ with fairly small $h^{1,1}(B) \lesssim 120$ and give rise to elliptic Calabi-Yau fourfolds with $h^{1,1}(X) \lesssim 200$. This subset of bases could be very incomplete and do not represent a a typical base in the whole set of good bases. For example, none of them contains any E_8 gauge group, but the appearance of E_8 was argued to be common in [71].

In the case of classifying toric base surfaces, we allow the appearance of (4,6) points in the blow up process before they are blown up to a good base. If they are not allowed, then a large number of good bases will be leaved out, including the one giving rise to the elliptic Calabi-Yau threefold with the largest $h^{1,1} = 491$. This suggests that we should include resolvable bases with (4,6) curves in the classification of threefold bases as well.

If we only focus on the resolvable bases, then we can apply the random walk approach in a similar way. However, we want to generate good bases and estimate their total number as well. Because the number of good bases is negligible comparing to the vast number of resolvable bases, the possibility of finding a good base in a random walk is almost zero.

Instead of a random walk, we start from a base, say $a_1 = \mathbb{P}^3$, and then randomly generate a blow up sequence from it. Resolvable codimension-two singularities are allowed throughout the process, including the (4,6) singularities on toric curves and curves on E_8 divisors. The numbers of possible ways of blowing up and down from a base a_i are explicitly computed, which are called $N_{\text{out}}(a_i)$ and $N_{\text{in}}(a_i)$ respectively. At each step in the blow-up process, we pick one of the N_{out} possible blow ups, choosing each with equal probability $1/N_{\text{out}}$.

$N_{\text{out}}(a_i)$ can be evaluated by checking each possible blow up of toric curves and

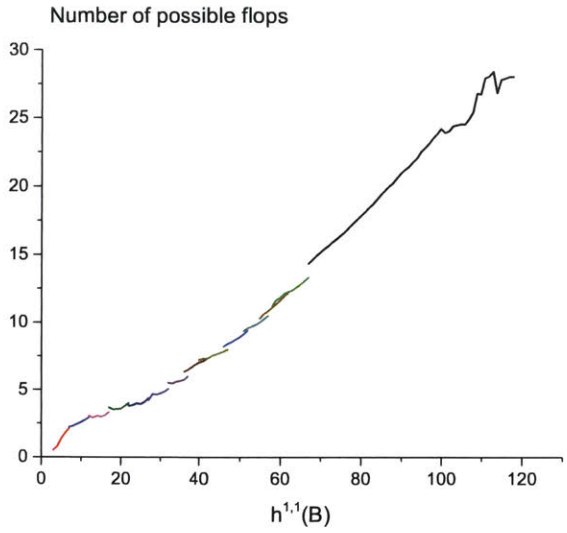

Figure 4-9: The blow up sequence as a probe of the set of resolvable bases. Different blow up sequences are different branches starting from the same starting point and end up with different end points.

points, and $N_{in}(a_i)$ is straight forward to read out because from the definition of resolvable bases, any blow down of a resolvable base gives another resolvable base. In the counting of $N_{\text{out}}(a_i)$ and $N_{\text{in}}(a_i)$, we only count the number of toric bases up to an $\text{SL}(3,\mathbb{Z})$ transformation on the toric fan. Instead of using the symmetry factor t, here we explicitly construct the bases after each possible blow up/downs and compare them[1].

Finally, this blow up sequence will end at an "end point" where there is no possible blow up to another resolvable base. This end point has to be good from definition, because there cannot be any toric (4,6) curve to be blown up, otherwise we can always blow up this toric (4,6) curve to get a base with exactly the same sets of $\mathcal{F}$ and $\mathcal{G}$. The whole picture of the blow up sequence as a probe of the whole set of resolvable bases is plotted in Figure 4-9.

To correctly take into account the unequal possibilities of entering each branch, we

[1]In the actual program, we only check the isomorphism among the bases after blow up/downs for the base with $h^{1,1} < 10$, since the isomorphism between the resulting bases is nearly impossible to happen for a general base with $h^{1,1} \geq 10$.

introduce a dynamic weight for each node a_n from the path $p = a_1 \to a_2 \to \cdots \to a_n$:

$$D(p = a_1 \to a_n) = \prod_{i=1}^{n-1} \frac{N_{\text{out}}(a_i)}{N_{\text{in}}(a_{i+1})}. \tag{4.4.50}$$

We call the subscript i of node a_i the "layer number" of a_i. We claim that (4.4.50) gives the correct weight of each node such that the weighted possibility of getting each node a_n sums up to 1, under the assumption that the whole graph can be scanned by moving up from one initial node a_1.

We prove this by induction. Assume that this holds for all the nodes with layer number less than or equal to $k-1$, so that

$$\sum_{p \to a_{k-1}} D(p \to a_{k-1}) \mathcal{P}(p \to a_{k-1}) = 1 \tag{4.4.51}$$

for all the nodes a_{k-1} with layer number $k-1$. Here the sum is over all the paths leading to the node a_{k-1}, and $\mathcal{P}(p \to a_{k-1})$ is the probability of this path.

Now suppose that a node a_k with layer number k has m_k nodes $a_{k-1,1}, a_{k-1,2}, \ldots, a_{k-1,m_k}$ linked to it. Then the sum

$$\begin{aligned}
&\sum_{p \to a_k} D(p \to a_k) \mathcal{P}(p \to a_k) \\
=&\sum_{q=1}^{m_k} \sum_{p \to a_{k-1,q}} D(p \to a_{k-1,q}) \cdot \frac{N_{\text{out}}(a_{k-1,q})}{N_{\text{in}}(a_k)} \cdot \mathcal{P}(p \to a_k) \\
=&\sum_{q=1}^{m_k} \sum_{p \to a_{k-1,q}} D(p \to a_{k-1,q}) \cdot \frac{N_{\text{out}}(a_{k-1,q})}{m_k} \cdot \mathcal{P}(p \to a_{k-1,q}) \cdot \frac{1}{N_{\text{out}}(a_{k-1,q})} \\
=&\sum_{p \to a_{k-1,q}} D(p \to a_{k-1,q}) \mathcal{P}(p \to a_{k-1,q}) \\
=&1.
\end{aligned} \tag{4.4.52}$$

Here we used the fact that $D(p \to a_k) = D(p \to a_{k-1,q}) \cdot \frac{N_{\text{out}}(a_{k-1,q})}{N_{\text{in}}(a_k)}$ and $\mathcal{P}(p \to a_k) = \mathcal{P}(p \to a_{k-1,q}) \cdot \frac{1}{N_{\text{out}}(a_{k-1,q})}$.

The identity (4.4.51) simply holds for $k - 1 = 1$, which completes the proof.

From the dynamical weight factor, we can estimate the average of quantities across the nodes on the same layer. For a given property $f(a_k)$ of a node in the graph, such as the number of outgoing edges, we can determine the sum of f across all nodes on the layer k as

$$\sum_{a_k} f(a_k) = \langle f(a_k) D(k) \rangle = \sum_{\text{paths } p=a_1 \to a_n} f(a_k) D(p \to a_k) \mathcal{P}(p \to a_k) \,. \tag{4.4.53}$$

In particular, we can directly estimate the number of nodes at level k in the graph as

$$N_{\text{nodes}}(k) = \langle 1 \cdot D(k) \rangle \approx \frac{1}{N(p)} \sum_{i=1}^{N(p)} D(p \to k), \tag{4.4.54}$$

where $N(p)$ is the total number of sampling branches and $D(p \to k)$ is the weight factor when a branch p reaches the layer k. If a branch never reaches layer k then we take $D(p \to k) = 0$.

We can estimate the average of a quantity $f(k)$ across all nodes a_k at level k by dividing the total by the number of nodes

$$\langle f(k) \rangle_D \equiv \frac{\langle f(a_k) D(k) \rangle}{\langle D(k) \rangle} \,. \tag{4.4.55}$$

This gives an alternative expression relating the total number of nodes in layer k to the total number of nodes in layer $k-1$,

$$N_{\text{nodes}}(k) = \frac{\langle N_{\text{out}}(k-1) \rangle_D}{\langle N_{\text{in}}(k) \rangle_D} \cdot N_{\text{nodes}}(k-1) \,. \tag{4.4.56}$$

Following through the definitions shows that this estimate is precisely equivalent to (4.4.54), even for a finite number of samples $N(p)$.

Finally, we can compute the number of good bases $N_{\text{good}}(k)$ out of the resolvable bases, simply by multiplying the relative weight factor on $N_{\text{nodes}}(k)$:

$$N_{\text{good}}(k) = N_{\text{nodes}}(k) \times \frac{\sum_{a_k \text{ is good}} D(p \to a_k)}{\sum_{a_k} D(p \to a_k)}. \tag{4.4.57}$$

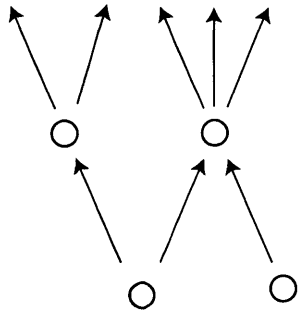

Figure 4-10: A typical graph where there are side branches entering the tree from the starting point. The $N_{\rm in}$ of the right node in the second layer should be 1 instead of 2, if we are interested in computing averages across the tree of nodes accessible from only the left starting point.

To estimate this quantity with a finite set of runs, we can simply use (4.4.54), where trajectories that do not reach a good base at level k contribute 0. This is equivalent to simply averaging the sampled value of $D(k)$ over the good bases at that level and multiplying by the fraction of trajectories that reach a good base at level k.

There are several reasons that the methodology described so far leads to a systematic underestimate of the number of bases. One key issue is that we have assumed in the analysis above that for each base a_k that is reached from a sequence of blow ups from the starting point a_1, every acceptable blow-down of a_k can also be reached by a sequence of blow ups from a_1. A problem arises, however, when the graph looks like the one shown in Figure 4-10. If there are side branches entering the tree from another starting point, the estimated number of nodes will be lower than the correct one, since the measured $\langle N_{\rm in}(k)\rangle$ will be higher than its correct value when considering only blow-ups of a_1.

Because we are counting the number of bases one can get from blowing up the starting point, one should only count the $N_{\rm in}(a_k)$ of a node for the blown down bases b_{k-1} of a_k that can be contracted to the starting point by a sequence of blow downs. This new $N'_{\rm in}(a_k)$ is always smaller or equal than $N_{\rm in}(a_k)$.

We can try to make a simple estimate of $N'_{\rm in}(a_k)$ by checking for each possible blow down whether the contracted ray is one of the rays on the starting point base or not. If it is not one of them, then we can add it into an estimated value $\tilde{N}'_{\rm in}(a_k)$,

but otherwise we do not. The motivation for dropping these contractable rays is that if we contract one of the rays on the starting point, then in general the base may no longer contain a set of rays that are linearly equivalent to the set of rays on the starting point by an $SL(3,\mathbb{Z})$ transformation. It is possible, however, that after we contract a ray that corresponds to a ray on the starting point, there may still exist another configuration of the starting base somewhere else to which the base may be contracted. Hence this estimated $\tilde{N}'_{\text{in}}(a_k)$ may be smaller than the actual value $N'_{\text{in}}(a_k)$. On the other hand, there can also be bases that still include the rays of the starting point base a_1 but cannot be contracted to a_1 for other reasons; these will cause $\tilde{N}'_{\text{in}}$ to overestimate N'_{in}. As we see in the next section, the distinction between N_{in} and $\tilde{N}'_{\text{in}}$ amounts to a fairly minor difference in numerical results in the one-way Monte Carlo computations, so this crude estimation does not detect any significant under or overcounting due to a misestimation of N'_{in}. On the other hand, as we discuss in more detail in Section 4.4.4, it seems that there are many other starting point bases possible at large $h^{1,1}(B)$ that are "dead ends" reached when we blow down along random incoming edges of the N_{in} possibilities for a_k, so that both N_{in} and $\tilde{N}'_{\text{in}}$ are likely substantially over estimating the correct value N'_{in} that would need to be used to correctly determine the number of nodes in the graph.

Finally, there is another systematic error in this one-way Monte Carlo approach that results in a smaller estimation of the total number of bases, even if there are no additional starting points possible or additional edges entering the tree. While in principle the estimate (4.4.54) gives an accurate estimate of the number of nodes when carried out over many runs of the one-way Monte Carlo, this estimate may only be accurate when enough runs are done to completely explore the set of possibilities, which is practically impossible as the number of trajectories through the graph grows exponentially in k. In practice, the most probable branches of the blow-up tree that we enter are the ones with small weight factors, which lead to a small estimated number of N_{nodes} and N_{good}. As an example, consider the red branch shown in Figure 4-11. If we only do one random blow up sequence through this graph, then we have a 60% possibility to enter this branch or the other two branches besides it. Applying (4.4.56)

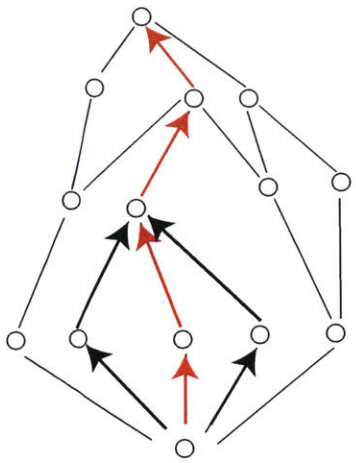

Figure 4-11: An example of a common branch in a random graph. Only from the information of N_{out} and N_{in} along this branch, we get a substantially underestimated total number of nodes in the top layer: $\frac{5}{27}$

repeatedly along this path, we get that the estimation of the number of nodes in the top layer is given by the weight factor $D = 5/27$ rather than 1. Thus, most of the time a random blow-up algorithm on this graph would give an expected number of nodes of < 0.2 at the top level. This is compensated by low-probability paths with large weight; for example, the path along the left side of the graph has probability 0.1 but gives a weight factor $D = 10/3$. While indeed one can check that the expectation value over all paths in this graph is indeed $\langle D \rangle = 1$, in a larger graph, such as one composed of many iterated copies of this graph, the distribution of D values becomes highly asymmetric, and typical paths will give much lower values of D than the idealized average. For a graph with regular fractal structure, D follows a lognormal distribution and we can compensate this systematic error by hand. However, this is not a proper approach to the actual experimental data.

4.4.2 Results about the end points

We have done 2,000 random blow up sequences starting from $\mathbb{P}^3$. We plot $\tilde{h}^{3,1}(X)$ of a generic elliptic fourfold over the base B (see (4.2.37)) for some example blow up sequences as a function of $h^{1,1}(B)$ in Figure 4-12. As we can see, the number of Weierstrass moduli quickly drops to a very small number after about 50 blow ups.

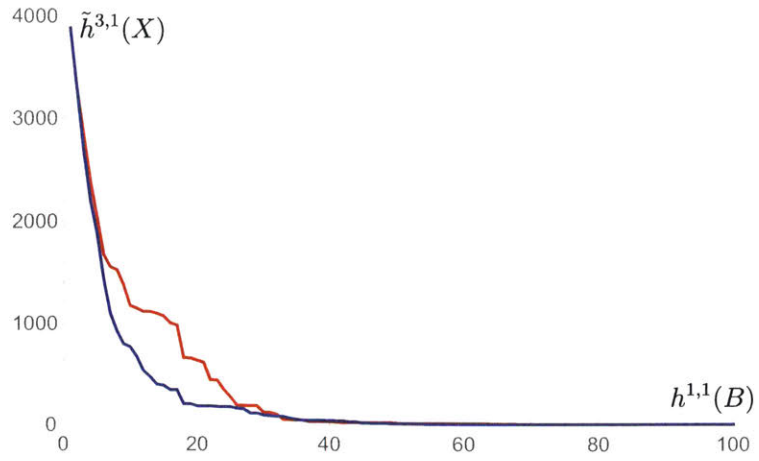

Figure 4-12: The change in $\tilde{h}^{3,1}(X)$ as a function of $h^{1,1}(B)$ for two random blow up sequences. The number of Weierstrass moduli drops quickly.

Usually the first 20 bases encountered in a blow up sequence are "good" bases without codimension-two (4, 6) loci. After this, all the sequences developed codimension-two (4, 6) toric curves, which continue to dominate the base geometry until the sequences terminate at an end point base that cannot be blown up further.

We list the unweighted number of good bases n_{good} encountered among the 2,000 runs at each layer k, with $h^{1,1}(B) = k$, in Table 4.5. For those values with $h^{1,1}(B) < 20$, the good bases are encountered near the beginning of the blow-up sequence, and these are never terminal end point bases. The number of good bases decreases when $h^{1,1}(B)$ increases, since codimension-two (4,6) loci appear during the blow up process. The remaining good bases arise as end points. These have very large $h^{1,1}(B)$ and are concentrated at sporadic values of $h^{1,1}(B)$.

We observe that about a half of the end point bases ends up at $h^{1,1}(B) = 1943$, 2249, 2303 or 2591, which shoule not be a coincidence. It turns out that for all the end point bases we found with each pecific value of $h^{1,1}(B)$, the non-Higgsable gauge group contents are the same. For $h^{1,1}(B) = 1943$, 2249, 2303 and 2591, the gauge groups are $G = E_8^{29} \times F_4^{81} \times G_2^{216} \times SU(2)^{324}$, $E_8^{33} \times F_4^{94} \times G_2^{250} \times SU(2)^{375}$, $E_8^{34} \times F_4^{96} \times G_2^{256} \times SU(2)^{384}$ and $E_8^{38} \times F_4^{108} \times G_2^{288} \times SU(2)^{432}$ respectively. This general structure is a common feature of the end point bases, since f almost always vanishes to degree 4 on every divisor (i.e. $\mathcal{F} = \{(0,0,0)\}$), so that the most common

$h^{1,1}(B)$	n_{good}	$h^{1,1}(B)$	n_{good}	$h^{1,1}(B)$	n_{good}	$h^{1,1}(B)$	n_{good}
1	2000	2	2000	3	2000	4	1900
5	1645	6	1259	7	846	8	545
9	283	10	129	11	48	12	26
13	13	14	8	15	4	16	1
1317	1	1727	17	1799	4	1882	1
1943	198	2015	41	2047	23	2057	139
2186	44	2199	10	2249	315	2303	306
2395	10	2399	31	2491	6	2591	205
2599	17	2623	64	2636	6	2661	29
2821	4	2824	16	2891	1	2915	2
2943	1	2961	21	2999	40	3037	9
3071	3	3086	112	3157	1	3247	2
3276	4	3295	2	3374	4	3401	4
3422	34	3498	3	3539	2	3599	2
3658	12	3686	55	3739	1	3741	2
3789	1	3811	3	3817	1	3887	27
3992	1	4049	4	4211	1	4274	1
4373	25	4375	3	4394	21	4468	4
4520	1	4741	1	4748	1	4913	5
4939	10	4946	1	5143	21	5356	1
5383	5	5503	2	5522	1	5623	1
5878	1	5989	6	6143	2	6440	2
6784	1	6802	5	6911	8	6945	1
7373	1	7498	2	7526	1	7909	7
8111	3	8230	1	8435	1	8938	1
8980	5	8999	1	10124	3	11341	2
12631	1	-	-	-	-	-	-

Table 4.5: The number of good bases encountered for each $h^{1,1}(B)$ among the 2,000 runs, without counting the weight factor. Bases at small $h^{1,1}(B) < 20$ are not end points, all bases with large $h^{1,1}(B) > 1000$ are end points of the algorithm.

non-Higgsable gauge group factors will be SU(2), G_2, F_4 and E_8, corresponding to the cases where g vanishes to order 2,3,4 and 5 respectively. The gauge groups SU(3) and SO(8) also appear infrequently, when the monodromy conditions are satisfied: if g vanishes to order 2 and g_2 is a complete square, then the gauge group is SU(3); if g vanishes to order 3 and g_3 is a complete cube, then the gauge group is SO(8). Similarly, if g vanishes to order 4 and g_4 is a complete square, then the gauge group should be E_6 rather than F_4. It turns out that we never found an E_6 in the scanning, although it could appear in principle.

The family with an SU(3) gauge group contains the bases with $h^{1,1} = 2999$ and gauge groups $G = E_8^{44} \times F_4^{125} \times G_2^{332} \times SU(3) \times SU(2)^{500}$.

An empirical formula for the number of gauge group factors SU(2), G_2, F_4 and E_8 in terms of $h^{1,1}(B)$ goes roughly as

$$N_{SU(2)} \cong \left[\frac{h^{1,1}(B)+1}{6}\right], N_{G_2} \cong \left[\frac{h^{1,1}(B)+1}{9}\right], N_{F_4} \cong \left[\frac{h^{1,1}(B)+1}{24}\right], N_{E_8} \cong \left[\frac{h^{1,1}(B)}{68}\right]. \tag{4.4.58}$$

While the non-Higgsable gauge groups appear to be quite uniform across end points with common $h^{1,1}(B)$, the non-Higgsable cluster structures on the bases with the same $h^{1,1}(B)$ are very different; this can be easily checked by looking at the different total number of non-Higgsable clusters and their different sizes. These bases also can have different convex hulls of the fan, hence they are not always related by a series of flops.

A potentially very interesting discovery is that the Hodge numbers of the elliptic Calabi-Yau fourfolds associated with end point bases at large $h^{1,1}(X)$ seem to give the mirror Hodge numbers to some simple Calabi-Yau fourfolds, which are constructed as generic elliptically fibered Calabi-Yau fourfolds over bases with small $h^{1,1}(B)$. For example, some of the bases with $h^{1,1}(B) = 2303$ give $h^{1,1}(X) = 3878$ and $h^{3,1}(X) = 2$. Since a generic elliptic fibration over $\mathbb{P}^3$ gives an X with $h^{1,1}(X) = 2$ and $h^{3,1}(X) = 3878$, these look exactly like mirror Calabi-Yau fourfold pairs[2]. There are also other bases with $h^{1,1}(B) = 2303$ that give $h^{1,1}(X) = 3877$ and $h^{3,1}(X) = 4$. They are

[2]The Hodge numbers of generic elliptic Calabi-Yau fourfolds are also computed in [100].

$h^{1,1}(B)$ (toric)	gauge group	$h^{1,1}(X)$	$h^{3,1}(X)$	Mirror base
1943	$E_8^{29} \times F_4^{81} \times G_2^{216} \times SU(2)^{324}$	3277	3	$\tilde{\mathbb{F}}_0$
2015	$E_8^{30} \times F_4^{84} \times G_2^{224} \times SU(2)^{336}$	3397	3	$\tilde{\mathbb{F}}_1$
2303	$E_8^{34} \times F_4^{96} \times G_2^{256} \times SU(2)^{384}$	3878	2	$\mathbb{P}^3$
2591	$E_8^{38} \times F_4^{108} \times G_2^{288} \times SU(2)^{432}$	4358	3	$\tilde{\mathbb{F}}_3$
3086	$E_8^{45} \times F_4^{129} \times G_2^{343} \times SU(2)^{513}$	5187	4	$\tilde{\mathbb{F}}_4$
3686	$E_8^{54} \times F_4^{153} \times G_2^{409} \times SU(2)^{615}$	6191	5	$\tilde{\mathbb{F}}_5$
4373	$E_8^{64} \times F_4^{180} \times SO(8) \times G_2^{486} \times SU(2)^{729}$	7341	7	$\tilde{\mathbb{F}}_6$
5143	$E_8^{75} \times F_4^{213} \times G_2^{571} \times SU(2)^{858}$	8629	7	$\tilde{\mathbb{F}}_7$
5989	$E_8^{87} \times F_4^{249} \times G_2^{664} \times SU(2)^{999}$	10045	7	$\tilde{\mathbb{F}}_8$
10124	$E_8^{145} \times F_4^{423} \times G_2^{1125} \times SU(2)^{1683}$	16959	10	$\tilde{\mathbb{F}}_{12}$
11341	$E_8^{162} \times F_4^{474} \times G_2^{1261} \times SU(2)^{1887}$	18994	12	$\tilde{\mathbb{F}}_{13}$
12631	$E_8^{180} \times F_4^{528} \times G_2^{1405} \times SU(2)^{2103}$	21151	12	$\tilde{\mathbb{F}}_{14}$

Table 4.6: A list of end point bases with the feature that the generic elliptic fibration over the base gives a Calabi-Yau fourfold with interesting Hodge numbers. In these cases the fourfolds seem to form mirror pairs with generic elliptic Calabi-Yau fourfolds over simple "mirror bases" with small $h^{1,1}(B)$. The $h^{1,1}(B)$ listed in the first column means the $h^{1,1}(B)$ of the toric base before the codimension-two (4,6) loci on divisors with E_8 are blown up.

also included in the dataset of Calabi-Yau fourfolds constructed as hypersurfaces in weighted projective space using reflexive polytopes [89]. For the bases with $h^{1,1}(B) = 1943$, the generic elliptic Calabi-Yau fourfold has $h^{1,1}(X) = 3277$ and $h^{3,1}(X) = 3$, which exactly looks like the dual of a generic elliptic fibration over the generalized Hirzebruch threefold $\tilde{\mathbb{F}}_0$, which is $\mathbb{P}_1 \times \mathbb{P}_2$. We list many of these interesting cases in Table 4.6. In this table, the generalized Hirzebruch threefold $\tilde{\mathbb{F}}_n$ is a $\mathbb{P}_1$ bundle over $\mathbb{P}_2$ given by toric data (4.3.45).

It is hard to directly prove that these Calabi-Yau fourfolds with large $h^{1,1}$ are actually the mirrors of the Calabi-Yau fourfolds with small $h^{1,1}$ and large $h^{3,1}$, because the Calabi-Yau fourfolds over specific threefold bases with large $h^{1,1}$ are generally hard to realize explicitly as hypersurfaces in reflexive polytopes. It is natural that the Calabi-Yau fourfolds with the same Hodge numbers could be isomorphic to each other. But it is still an open question how to check this isomorphism.

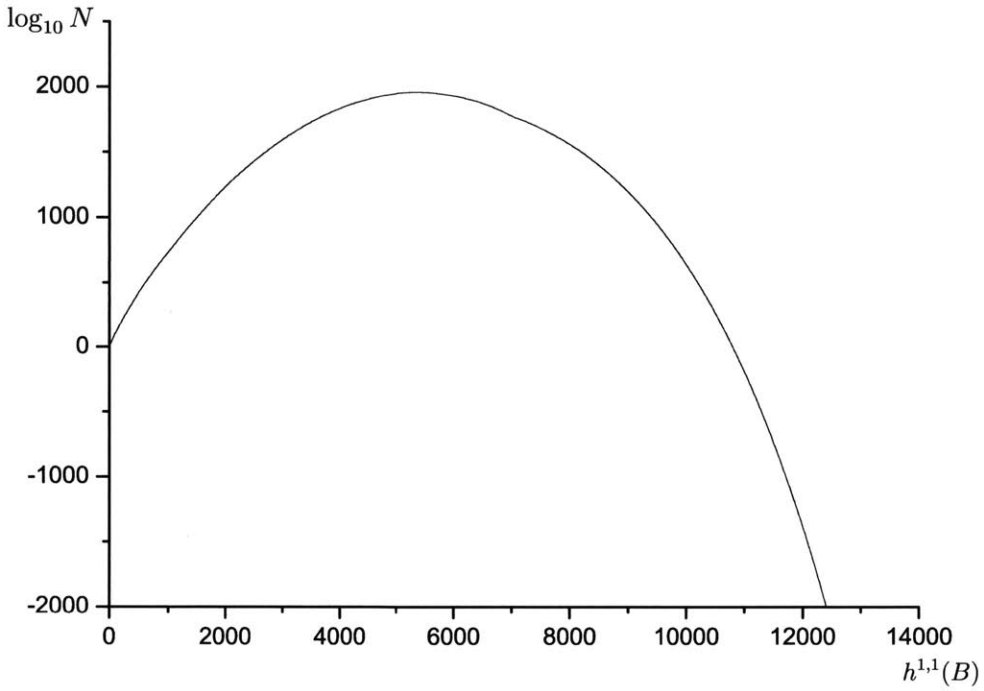

Figure 4-13: Logarithm of the estimated number of resolvable bases N_{nodes} as function of $h^{1,1}(B)$, from blowing up $\mathbb{P}^3$.

4.4.3 Estimating the total number of resolvable and good bases

Given the results of the 2,000 one-way Monte Carlo runs starting from $\mathbb{P}^3$, we can try to estimate the total number of resolvable and good bases that can be reached as blow-ups of $\mathbb{P}^3$ using (4.4.50), (4.4.54) and (4.4.57).

We plot the logarithm of the estimated number of resolvable bases and good bases in Figure 4-13 and Figure 4-14 respectively. As one may expect, the number of resolvable bases varies smoothly. As we have discussed above, however, the distribution of good bases consists of spikes. Because the weight factors typically has a large exponent and they vary in the exponent across different runs, the distribution of bases is effectively dominated by a single (or a few) run for a given k.

We can see from the figure that when $h^{1,1}(B) > 5,000$, the estimated number of good bases with that $h^{1,1}(B)$ is significantly smaller than 1, even though we found some good end point bases with much larger values of $h^{1,1}(B)$. Moreover, the estimated number of resolvable bases is smaller than 1 at $h^{1,1}(B) > 11,000$. For example,

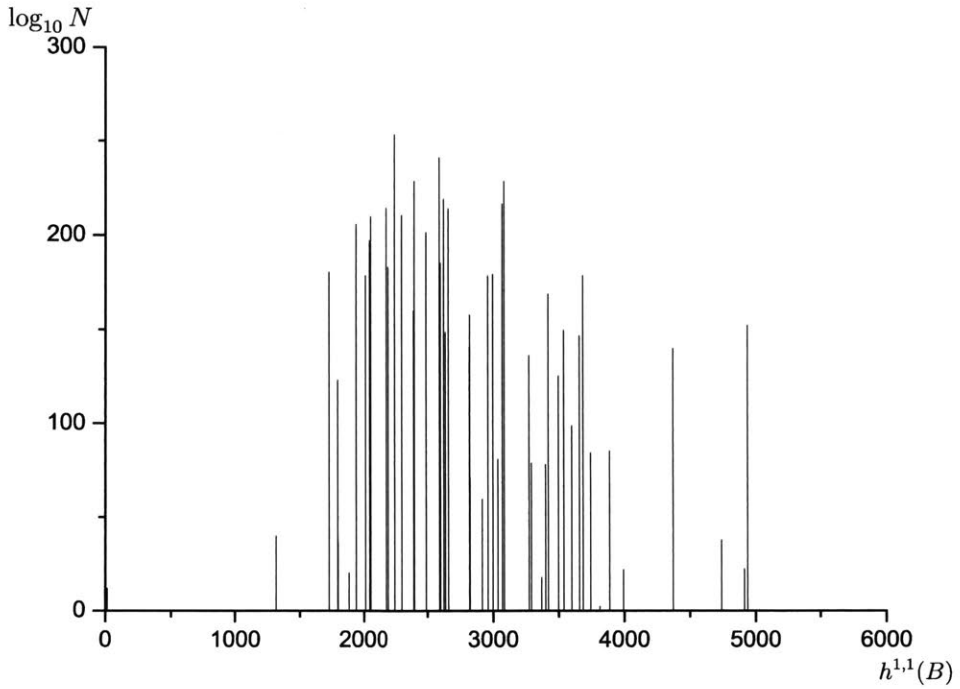

Figure 4-14: Logarithm of the estimated number of good bases N_{good} as function of $h^{1,1}(B)$, from blowing up $\mathbb{P}^3$.

for the base with biggest $h^{1,1}(B) = 12,631$, the total number of bases is estimated as 2.2×10^{-2474}. This fact verifies that we have indeed underestimated the total number of bases by a large exponential factor. Typically there are $\sim 10^3$ incoming edges for the bases near the end points but only a few outgoing edges, hence the situation is more extreme than Figure 4-11 shows.

Using the uncorrected $N_{\text{in}}(a_k)$ in (4.4.50), the estimated total number of resolvable bases is equal to 3.5×10^{1964} and the estimated number of good bases equals to 3.0×10^{253}. If we use the corrected estimation $\tilde{N}'_{\text{in}}(a_k)$, then the total number of resolvable bases is again estimated at to 3.5×10^{1964} and the number of good bases is estimated at 9.1×10^{253}. Hence from the experimental results, it seems that the different definition between $\tilde{N}'_{\text{in}}(a_k)$ and $N_{\text{in}}(a_k)$ does not much affect the estimation, so this mechanism does not capture the source of the underestimation.

As a cross-check, we also used other starting point bases with small $h^{1,1}(B)$, which are the generalized Hirzebruch threefold $\tilde{\mathbb{F}}_2$ with $h^{1,1}(B) = 2$ and a simple product space $\mathbb{P}^1 \times \mathbb{P}^1 \times \mathbb{P}^1$ with $h^{1,1}(B) = 3$. Similar to $\mathbb{P}^3$, these bases do not have non-

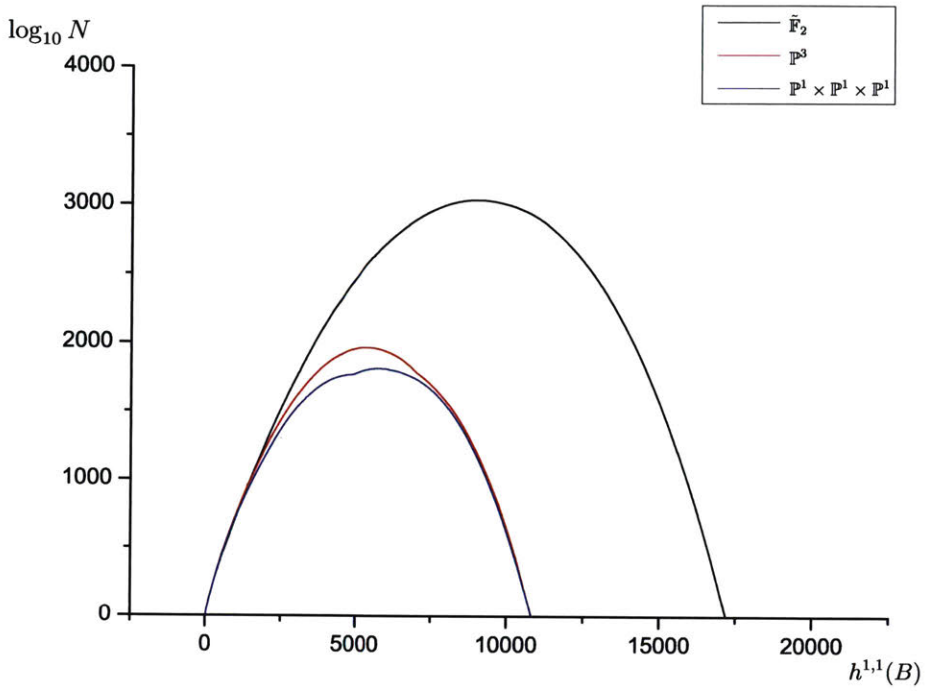

Figure 4-15: Logarithm of the estimated number of resolvable bases as function of $h^{1,1}(B)$ from blowing up $\mathbb{P}^3$, $\tilde{\mathbb{F}}_2$ and $\mathbb{P}^1 \times \mathbb{P}^1 \times \mathbb{P}^1$.

Higgsable gauge groups. After 1,000 random blow up sequences starting from $\tilde{\mathbb{F}}_2$, we found a larger fraction of end point bases with large $h^{1,1}(B)$ than when starting from $\mathbb{P}^3$. For $\tilde{\mathbb{F}}_2$, 1% of end points have $h^{1,1}(B) > 10,000$, while this percentage is 0.3% from the starting point $\mathbb{P}^3$. The largest $h^{1,1}(B)$ we got is 20,341, and the non-Higgsable gauge group on the resulting good endpoint base is $E_8^{290} \times F_4^{850} \times G_2^{2261} \times SU(2)^{3383}$. We estimate the total number of resolvable bases from $\tilde{\mathbb{F}}_2$ at 1.24×10^{3046} while the total number of good bases is estimated at 1.10×10^{254}, using weight factors with $N'_{\text{in}}(a_k)$. On the other hand, after 1,000 random blow up sequences from $\mathbb{P}^1 \times \mathbb{P}^1 \times \mathbb{P}^1$, the total number of resolvable bases is estimated to be 1.43×10^{1811} and the total number of good bases is estimated to be 1.80×10^{271}.

We plot the distribution of resolvable bases and good bases from the three starting points in Figures 4-15 and 4-16 respectively.

As another starting point with somewhat different structure, we have also tried blowing up the generalized Hirzebruch threefold $\tilde{\mathbb{F}}_{12}$, which has $h^{1,1}(B) = 2$ and a non-Higgsable gauge group E_7. After 100 random blow up sequences, the total

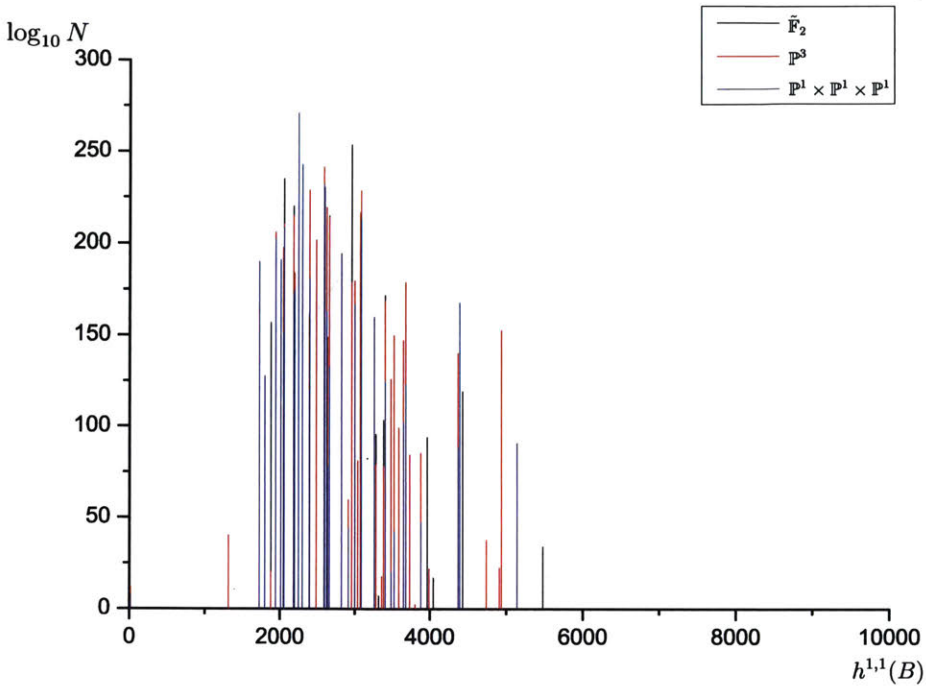

Figure 4-16: Logarithm of the estimated number of good bases as function of $h^{1,1}(B)$ from blowing up $\mathbb{P}^3$, $\tilde{\mathbb{F}}_2$ and $\mathbb{P}^1 \times \mathbb{P}^1 \times \mathbb{P}^1$.

number of resolvable bases is estimated as 1.77×10^{2130} while the total number of good bases is estimated as 2.02×10^7. On the end points, the E_7 gauge group has always disappeared since it is enhanced to E_8 after a sequence of blow ups.

Despite the difference of the starting point bases, the discrete peaks of good bases listed in Table 4.5 are universal, which shows that the set of resolvable bases is highly connected. Even if we start with an exotic base B_{max} which gives rise to the elliptic Calabi-Yau fourfold with the largest $h^{3,1} = 303,148$(see the next section), we still get peaks such as $h^{1,1}(B) = 7909$ and 8980, which are present in Table 4.5.

4.4.4 Global structure of the set of bases

As mentioned before, there are bases other than $\mathbb{P}^3$ that cannot be contracted to another smooth base. We know that $\mathbb{F}_n (n > 1)$ provides another class of these starting points, but the abundance of these starting points for larger $h^{1,1}(B)$ is unknown. To investigate this problem, we try to randomly blow down a typical good end point base until it hit a base that cannot be contracted to another smooth base. It turns

v_0	(0,0,1)	v_{16}	(0,-5,-1)	v_{32}	(2,-1,3)	v_{48}	(2,-1,4)
v_1	(0,1,0)	v_{17}	(-3,-5,-2)	v_{33}	(1,-1,2)	v_{49}	(1,-1,4)
v_2	(1,0,0)	v_{18}	(2,3,1)	v_{34}	(-7,-9,-5)	v_{50}	(-13,-26,-9)
v_3	(-1,-1,-1)	v_{19}	(2,-1,1)	v_{35}	(1,-1,3)	v_{51}	(1,-1,5)
v_4	(1,1,1)	v_{20}	(3,3,1)	v_{36}	(-1,-2,-1)	v_{52}	(-2,-7,-2)
v_5	(-1,-1,0)	v_{21}	(3,4,1)	v_{37}	(-10,-13,-7)	v_{53}	(-10,-20,-7)
v_6	(-2,-2,-1)	v_{22}	(0,1,-1)	v_{38}	(-4,-10,-3)	v_{54}	(-8,-19,-6)
v_7	(0,-1,0)	v_{23}	(0,2,-1)	v_{39}	(-3,-4,-2)	v_{55}	(-13,-25,-9)
v_8	(-1,-3,-1)	v_{24}	(-6,-7,-4)	v_{40}	(-9,-11,-6)	v_{56}	(-17,-35,-12)
v_9	(-1,0,-1)	v_{25}	(1,1,0)	v_{41}	(-7,-15,-5)	v_{57}	(-4,-9,-3)
v_{10}	(-2,-5,-2)	v_{26}	(1,-2,1)	v_{42}	(-3,-6,-2)	v_{58}	(-5,-13,-4)
v_{11}	(2,2,1)	v_{27}	(-1,-4,-1)	v_{43}	(-11,-25,-8)	v_{59}	(-11,-24,-8)
v_{12}	(0,4,-1)	v_{28}	(2,1,0)	v_{44}	(-5,-6,-3)	v_{60}	(-14,-29,-10)
v_{13}	(1,-1,1)	v_{29}	(-1,-5,-2)	v_{45}	(-12,-29,-9)	v_{61}	(-15,-33,-11)
v_{14}	(-3,-3,-2)	v_{30}	(2,-1,2)	v_{46}	(-12,-15,-8)		
v_{15}	(-4,-5,-3)	v_{31}	(4,4,1)	v_{47}	(-7,-16,-5)		

Table 4.7: The list of toric rays of the exotic starting point B_{ex}.

out that we will hit a base with fairly large $h^{1,1}(B) = 50$–200, even if we require that the original rays on the starting point are never removed. These "exotic starting points" have a complicated fan structure. Most of the rays in the fan have more than four neighbors, hence this base is clearly neither a $\mathbb{P}^1$ bundle over B_2 or a B_2 bundle over $\mathbb{P}^1$. An exotic starting point base typically has a lot of toric curves where f and g vanish to order (4,6) or higher. We explicitly present an example B_{ex} with $h^{1,1}(B_{\text{ex}}) = 59$, toric rays in Table 4.7 and the 3D cones in Table 4.8.

If we try to contract a $\mathbb{P}^2$ divisor on B_{ex}, for example the divisor corresponding to the ray v_{61}, then the volume of the new 3D cone $v_{58}v_{59}v_{60}$ is 2. Hence the resulting base after the contraction is singular.

This observation suggests that there is a large number of such exotic starting points, however at this point we neither have a good estimation of their total numbers or their general structures. If we want to extensively survey the set of resolvable bases, then these starting points should be taken into account. Knowing the distribution of these exotic starting points would also potentially help in resolving the underestimation issue. One possible approach would be to allow for singular bases, as suggested by Mori theory. These exotic starting points could be blown down further

(22,23,9)	(13,26,19)	(19,30,2)	(19,30,13)	(30,32,2)	(30,32,13)
(34,40,24)	(34,40,37)	(37,46,40)	(32,48,2)	(32,48,35)	(49,51,26)
(49,51,49)	(53,55,50)	(53,56,50)	(55,60,59)	(60,61,59)	(52,27,16)
(28,2,23)	(54,53,56)	(51,48,2)	(33,32,13)	(33,13,26)	(35,32,33)
(35,33,26)	(49,48,35)	(49,35,26)	(20,2,28)	(20,28,31)	(28,21,31)
(2,16,12)	(28,21,25)	(28,25,23)	(41,45,43)	(59,53,55)	(59,53,54)
(1,9,23)	(1,23,25)	(21,31,20)	(38,45,43)	(58,27,52)	(27,38,45)
(21,20,18)	(2,34,24)	(36,34,37)	(27,59,54)	(27,54,45)	(2,22,23)
(1,21,25)	(7,19,2)	(41,45,54)	(41,54,56)	(6,40,24)	(46,44,37)
(2,24,15)	(24,14,15)	(58,55,57)	(2,11,20)	(11,19,20)	(46,44,40)
(58,55,60)	(42,41,56)	(42,56,50)	(58,60,61)	(58,61,59)	(58,59,27)
(7,38,43)	(2,9,22)	(14,15,2)	(7,47,43)	(17,42,50)	(8,12,16)
(17,57,55)	(17,55,50)	(7,26,19)	(3,14,9)	(39,36,37)	(6,44,40)
(2,9,3)	(0,2,51)	(6,29,44)	(2,3,14)	(7,27,16)	(7,16,2)
(18,21,1)	(39,29,36)	(8,2,12)	(39,37,44)	(30,44,29)	(7,27,38)
(10,29,6)	(6,14,24)	(36,29,2)	(36,2,34)	(2,4,11)	(8,10,29)
(8,29,2)	(8,16,52)	(6,14,9)	(0,26,51)	(7,0,26)	(1,6,9)
(8,17,52)	(17,52,57)	(52,58,57)	(42,47,7)	(42,47,43)	(42,43,41)
(4,1,18)	(4,18,11)	(4,2,0)	(8,10,17)	(10,6,17)	(7,6,5)
(7,5,0)	(7,42,6)	(42,17,6)	(1,6,5)	(1,5,0)	(1,0,4)

Table 4.8: The list of 3D fans of the exotic starting point B_{ex}. We use (i, j, k) to denote the triple element set (v_i, v_j, v_k).

by allowing the contraction of rays associated with divisors other than $\mathbb{P}^2$, giving singular starting points.

For the set of good bases, it seems that they are isolated at disconnected "islands" among the big "ocean" of connected set of resolvable bases. Apart from connected component $\mathcal{C}$ and the end point bases we have discribed before, we can also construct a good base by only blowing up a resolvable base at the (4,6) curves before they are fully resolved. In this process, we can construct many good bases with $h^{1,1}(B)$ different from the list in Table 4.5. They are called intermediate good bases (which we denote by B_{int}), and their non-Higgsable gauge group structure is similar to the end points. The number of each gauge group factor SU(2), G_2, F_4 and E_8 can be approximated by the formula (4.4.58). One qualitative difference between these intermediate good bases and the end point bases is that the generic elliptic fourfold X over a base B_{int} typically has a larger $\tilde{h}^{3,1}(X)$, since we prefer blowing up codimension-two (4,6) loci, which does not reduce the number of Weierstrass monomials in f and g. For example, we can get an X with $h^{1,1}(X) = 7097$ and $\tilde{h}^{3,1}(X) = 1452$. We plot a rough picture of the set of resolvable bases and good bases in Figure 4-17

The intermediate bases are more sensitive to a small perturbation than the end point bases. If we randomly blow down a base B_{int} two times and then randomly blow it back up two times, then in general we will get a base with codimension-two (4,6) loci. On the other hand, if we blow down an end point base B_{end} with $h^{1,1}(B_{\text{end}}) = 2623$ two times and then randomly blow it up two times, we almost always return to the exact same base that we started at. The reason is that we only include the resolvable bases, which constrains the possible ways to blow up especially near the end point. Even if we randomly blow it down 2400 times and then randomly blow up 2400 times, we still always get another end point base with the same set of rays as B but different cone structure! Hence one may expect that a family of end point bases is much bigger than a family of intermediate bases, although it is not clear how to compare these two classes in the overall graph.

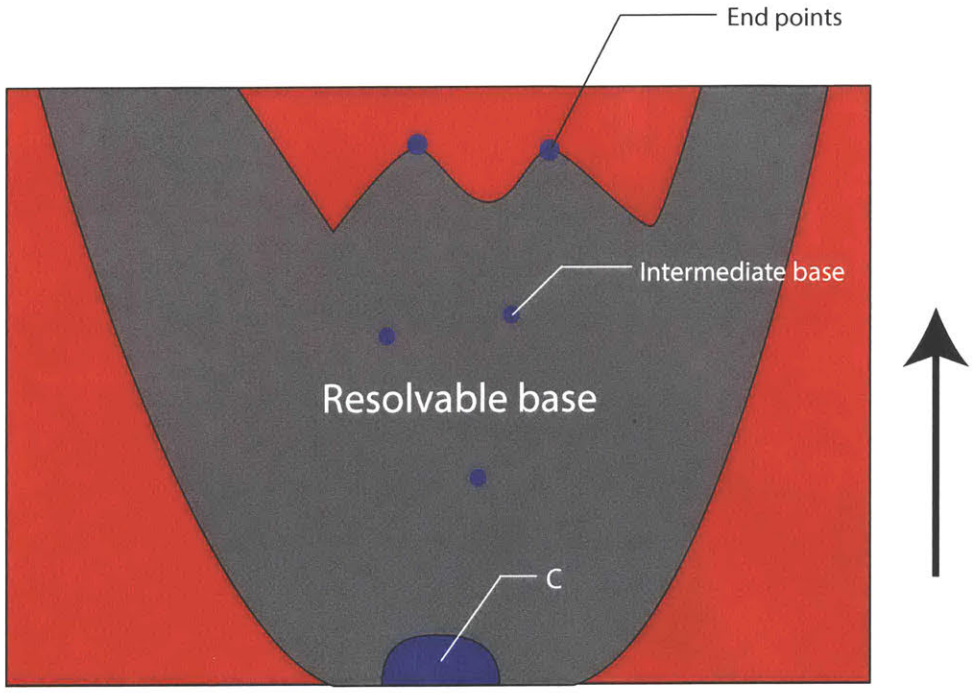

Figure 4-17: A rough picture of the set of toric threefold bases with red region as the non-resolvable bases with codimension-1 (4,6) locus, grey region as the resolvable bases and the blue region as the good bases. The black arrow on the right indicates the direction of blow up. The good bases consist of the end point bases, the intermediate bases and the bases in $\mathcal{C}$ that are connected to $\mathbb{P}^3$.

4.5 The geometry with most flux vacua

We have got a rough idea of how does the set of resolvable and good bases look like. In this section, we will present the geometry of the almost toric base threefold $B_{\max}$. The generic elliptic fibration over $B_{\max}$ leads to a particular elliptic Calabi-Yau fourfold $\mathcal{M}_{\max}$ with $h^{1,1} = 252$, $h^{2,1} = 0$ and the largest known $h^{3,1} = 303,148$, which lies exactly at the upperleft corner of Figure 4-1. This Calabi-Yau fourfold was originally identified in [84], but the base and fibration structure has not been written down before.

The base $B_{\max}$ is itself formed as a B_2 bundle over $\mathbb{P}^1$, where B_2 is a toric surface characterized by a closed cycle of toric divisors (curves, corresponding to rays in the toric fan) with self-intersections 0, +6, -12//-11//-12//-12//-12//-12//-12//-12//-12, where // denotes the sequence of self-intersections (-1, -2, -2, -3, -1, -5, -1, -3, -2, -2, -1), as we have mentioned before. B_2 itself supports a generic elliptic Calabi-Yau threefold that has Hodge numbers $(251, 251)$ [105, 121]. The toric fan of B_2 has the rays:

$$
\begin{aligned}
v_1 &= (-1,-12) && (4.5.59)\\
v_2 &= (0,1) && (4.5.60)\\
v_3 &= (1,6) && (4.5.61)\\
\vdots &\quad \vdots && (4.5.62)\\
v_{99} &= (0,-1)\,. && (4.5.63)
\end{aligned}
$$

The rays $v_4, \ldots, v_{98}$ are determined by the equation (3.2.27).

From the rays v_i we can construct the toric fan for $B_{\max}$, with rays

$$
\begin{aligned}
w_0 &= (0,0,1) && (4.5.64)\\
w_i &= (v_i, 0), \qquad 1 \leq i \leq 99 && (4.5.65)\\
w_{100} &= (84,492,-1) = (12v_{15}, -1)\,, && (4.5.66)
\end{aligned}
$$

where v_{15} corresponds to the curve in B_2 with self-intersection -11. The 3D cones for $B_{\max}$ are (w_0, w_i, w_{i+1}) and (w_{100}, w_i, w_{i+1}), including the cyclic case (w_0, w_{99}, w_1) and (w_{100}, w_{99}, w_1). This manifestly gives $B_{\max}$ the structure of a B_2 bundle over $\mathbb{P}^1$, where the toric projection onto the third axis corresponds to the fibration structure. The "twist" in this bundle is characterized by the offset $12v_{15}$ of the ray w_{100}. The 3D polytope containing the vertices w_i is defined by the tetrahedron spanned by w_0, w_1, w_2, w_{100}.

The divisors carrying non-Higgsable gauge groups on $B_{\max}$ are precisely the ones associated with curves in B_2 that carry non-Higgsable gauge factors in the corresponding 6d theory, where the -12 (and -11) curves carry E_8 factors, the -5 curves carry F_4 factors, and the $-3, -2, -2$ sequences each carry $G_2 \times SU(2)$ products with bifundamental matter. Thus, the geometrically non-Higgsable gauge group of a generic elliptic fibration over $B_{\max}$ is

$$G_{\max} = E_8^9 \times F_4^8 \times (G_2 \times SU(2))^{16} . \tag{4.5.67}$$

This group was originally associated with the elliptic Calabi-Yau fourfold $\mathcal{M}_{\max}$ in [30] using the method of "tops," which describe both Higgsable and non-Higgsable gauge group factors.

To count the total number of flux vacua on $\mathcal{M}_{\max}$, we use a simple estimation formula in [22, 23, 131] based on the tadpole cancellation (4.1.10)

$$\frac{1}{2}\int_X G_4 \wedge G_4 \leq \frac{\chi(X)}{24}. \tag{4.5.68}$$

Consider a fourfold X with $Q = \chi(X)/24$ and fourth Betti number $b_4 = \dim(H^4(X))$. Since a generic G_4 flux is an element of $H^4(X, \mathbb{Z}) + \frac{c_2(X)}{2}$, see (4.1.5), the problem of counting vacua can be simplified to problem of counting the number of lattice points in a b_4 dimensional sphere of radius $\sqrt{2Q}$. The assumption is that the metric of $\int_X G_4 \wedge G_4$ is positive definite and can be normalized to an identity matrix. In the case where $h^{3,1} \gg h^{1,1}, h^{2,1}$, we have $b_4 \approx \xi = 24Q$, see (4.1.4). In particular, for $\mathcal{M}_{\max}$, the Euler character $\xi = 1,820,448$ and $b_4 = 1,819,942$.

In this regime, the volume of this high dimensional sphere is not a good approximation. Instead, we are going to estimate the number of lattice points using the method of [99, 40].

It was proved that the exact number of lattice points in this sphere equals to

$$N(b_4, Q) = \frac{1}{2\pi i} \int \frac{dt}{t} e^{-Qt} Z(t), \tag{4.5.69}$$

where the contour is along the imaginary axis and passes the pole $t = 0$ on the left. (Note that with these conventions the integral runs from $i\infty$ to $-i\infty$.)

$$Z(t) = \sum_{\vec{n} \in \mathbb{Z}^b} e^{t\vec{n}^2/2} = \left(\sum_{n \in \mathbb{Z}} e^{tn^2/2} \right)^b \equiv \vartheta_3(0, e^{t/2})^b, \tag{4.5.70}$$

where ϑ_3 is the Jacobi theta function.

When b is large, this integration can be evaluated by saddle point approximation:

$$N(b_4, Q) \approx e^{S(t_*)}, \tag{4.5.71}$$

where t_* is the point where $S(t) = -\ln(-t) - Qt + b \ln \vartheta_3(0, e^{t/2})$ takes an extremal value.

For our case $Q \approx b/24$, $t_* = -6.18$ and

$$N(b_4, Q) \sim 10^{3.59 \times Q} \tag{4.5.72}$$

In the regime of $h^{1,1} \ll h^{3,1}$, $h^{2,1} = 0$, the number of flux vacua is approximately

$$N(h^{3,1}) \sim 10^{0.9 \times h^{3,1}} \tag{4.5.73}$$

Applying this analysis to $\mathcal{M}_{\max}$, the total number of flux vacua is estimated to be of order $10^{272,000}$.

Note that we have not imposed the Lorentz invariance conditions (4.1.11) yet, but they should not affect the order of magnitude by a large factor since $h^{1,1}(B) \ll$

$h^{3,1}(X)$, and there are only ~ 200 independent equations in (4.1.11). Another subtlety is that the metric on G_4 flux in the quadratic $\int_X G_4 \wedge G_4$ may not be positive definite[40]. The positive definiteness is guaranteed if the flux is self-dual: $G_4 = *G_4$. We can consider the subset of self-dual G_4 flux as well, where the dimension of the sphere becomes $b_4/2$, so that we need to evaluate $N(b_4/2, Q)$.

In this case the saddle point approximation gives $t_* = -4.61$ and

$$N(b_4/2, Q) \sim 10^{2.95 \times Q}, \tag{4.5.74}$$

hence approximately

$$N'(h^{3,1}) \sim 10^{0.74 \times h^{3,1}}. \tag{4.5.75}$$

Applying this formula to $\mathcal{M}_{\max}$, the total number of flux vacua$\sim 10^{224,000}$.

To get a feeling of the dominance of this set of flux vacua comparing to other geometry, we can compute the $h^{3,1}(X)$ on other B_2 bundles over $\mathbb{P}^1$. The second largest $h^{3,1}(X)$ we can get is $299,707$. Plug this into (4.5.73), we see that the number of flux vacua on this geometry is only a $10^{-3,000}$ fraction of the flux vacua on $\mathcal{M}_{\max}$. The other corners of the Figure 4-1 also contain much less flux vacua. For example, if we take another limit where $h^{1,1} \gg h^{3,1}$, then from (4.1.4), we see that the dimension of the ball $b_4 \approx 4h^{1,1}$, which is much smaller than the maximal number for the case of large $h^{3,1}$.

Since this number $10^{272,000}$ is much larger than the estimated total number of toric bases in the last section, it is possible that the flux ensemble on $\mathcal{M}_{\max}$ dominates the entire F-theory landscape if we assign each flux vacuum with equal weight. This weighting assumption may not be physically correct since the detailed dynamics of the early universe geometric transition are unknown.

If we assume that each flux vacuum solution across all the F-theory geometric solutions carries equal weight, then it is natural to conclude that we live in a flux vacuum on this geometry $\mathcal{M}_{\max}$. Now the problem is to construct the standard model on it. Since the non-Higgsable gauge groups are E_8, F_4 and $G_2 \times$ SU(2), it seems that the most probable way to realize the standard model gauge group is to embed

$\mathrm{SU}(3)\times\mathrm{SU}(2)\times\mathrm{U}(1)$ into a non-Higgsable E_8. Although we have $F_4 \supset \mathrm{SU}(3)\times\mathrm{SU}(2)\times\mathrm{U}(1)$, the matter representations from the branching rule are incorrect. It is also very hard to tune a larger gauge group on $B_{\max}$, since codimension-one or codimension-two (4,6) singularity will usually arise.

Hence a possible scenario to realize the standard model gauge group is to introduce four units of vertical flux in the form of (4.1.18) and breaks an E_8 down to SU(5). Then we need another Cartan flux to break down SU(5) into $\mathrm{SU}(3)\times\mathrm{SU}(2)\times\mathrm{U}(1)$. The problem is that since there is no local matter curve on the E_8 divisor D, we have to use the bulk matter on the divisor D. However, it was argued in Appendix E of [15] that the classical Yukawa coupling coefficient will vanish if D is a rational surface with effective anticanonical divisor. This could suggest that we do not really live on $\mathcal{M}_{\max}$, and the early universe thermodynamics disfavor $\mathcal{M}_{\max}$ despite of the largest flux ensemble on it.

Chapter 5

Bases with non-Higgsable U(1)s

5.1 Weierstrass models with additional rational sections

As we have briefly introduced in Section 2.3, the U(1) gauge groups in an F-theory setup correspond to additional rational sections, which are global holomorphic functions (λ,α,b) that satisfy

$$\alpha^2 = \lambda^3 + f\lambda b^4 + gb^6. \tag{5.1.1}$$

It is non-trivial to write out a Weierstrass model with such solutions $x = \lambda$, $y = \alpha$, $z = b$.

A useful special form of such Weierstrass models is the Morrison-Park form[102]:

$$y^2 = x^3 + (c_1c_3 - \frac{1}{3}c_2^2 - b^2c_0)xz^4 + (c_0c_3^2 + \frac{2}{27}c_2^3 - \frac{1}{3}c_1c_2c_3 - \frac{2}{3}b^2c_0c_2 + \frac{1}{4}b^2c_1^2)z^6. \tag{5.1.2}$$

In this chapter, we always denote the anticanonical divisor of B by $-K$. The coefficients b, c_0, c_1, c_2 and c_3 in (5.1.2) are defined as holomorphic sections of line bundles

L, $-4K-2L$, $-3K-L$, $-2K$ and $-K+L$ on B respectively:

$$\begin{aligned} b &\in \mathcal{O}(L) \\ c_0 &\in \mathcal{O}(-4K-2L) \\ c_1 &\in \mathcal{O}(-3K-L) \\ c_2 &\in \mathcal{O}(-2K) \\ c_3 &\in \mathcal{O}(-K+L) \end{aligned} \tag{5.1.3}$$

The rational section over B is then given by:

$$(x,y,z) = (\lambda,\alpha,b) = (c_3^2 - \frac{2}{3}b^2c_2, -c_3^3 + b^2c_2c_3 - \frac{1}{2}b^4c_1, b) \tag{5.1.4}$$

Apparently

$$\begin{aligned} \lambda &\in \mathcal{O}(-2K+2L) \\ \alpha &\in \mathcal{O}(-3K+3L). \end{aligned} \tag{5.1.5}$$

L is an effective bundle on B with holomorphic section b, which characterizes the particular way of tuning the U(1). For some bases with non-Higgsable clusters of high rank gauge groups, taking $L=0$ may lead to non-minimal singularities in the total space X that cannot be resolved [106]. We will discuss this issue explicitly for $B=\mathbb{F}_{12}$ in Section (5.2.2).

For c_0 and c_1, it is not clear whether their holomorphic sections exist. If the line bundle $-2K-L$ is effective, which is denoted by $-2K-L \geq 0$ or equivalently $L \leq -2K$, then c_0 and c_1 both have holomorphic sections. If $-2K-L$ is not effective, we can just take $c_0 \equiv 0$. In this special case, the discriminant of the Weierstrass form (5.1.2) is

$$\Delta = \frac{27}{16}b^4c_1^4 + b^2c_1^2c_2^3 - \frac{9}{2}b^2c_1^3c_2c_3 - c_1^2c_2^2c_3^2 + 4c_1^3c_3^3, \tag{5.1.6}$$

which means that an SU(2) gauge group exists on the curve $c_1=0$.

For the borderline case $L = -2K$, we have

$$c_0 \in \mathcal{O}(-4K - 2L) = \mathcal{O}(0). \tag{5.1.7}$$

Hence c_0 is a complex number in the Morrison-Park form (5.1.2). In this case, we have another rational section apart from (5.1.4):

$$(x, y, z) = (\frac{1}{4}c_1^2 - \frac{2}{3}c_0c_2, -\frac{1}{8}c_1^3 + \frac{1}{2}c_0c_1c_2 - c_0^2c_3, c_0^{1/2}), \tag{5.1.8}$$

and the gauge group is U(1)× U(1).

In this paper, we generally use the weaker constraint $-3K - L \geq 0$, or $L \leq -3K$.

Note that this condition $L \leq -3K$ cannot be further relaxed, otherwise $c_0 = c_1 = 0$, and the Weierstrass form (5.1.2) becomes

$$y^2 = x^3 - \frac{1}{3}c_2^2xz^4 + \frac{2}{27}c_2^3z^6, \tag{5.1.9}$$

which is globally singular over the base B.

To compute the charged matter under the U(1), a convenient way is to unHiggs the U(1) to SU(2) by setting $b = 0$ in (5.1.2). Then the Morrison-Park form becomes

$$y^2 = x^3 + (c_1c_3 - \frac{1}{3}c_2^2)xz^4 + (c_0c_3^2 + \frac{2}{27}c_2^3 - \frac{1}{3}c_1c_2c_3)z^6 \tag{5.1.10}$$

with discriminant

$$\Delta = 4f^3 + 27g^2 = c_3^2(-c_1^2c_2^2 + 4c_0c_2^3 + 4c_1^3c_3 - 18c_0c_1c_2c_3 + 27c_0^2c_3^3). \tag{5.1.11}$$

We can see that Δ vanishes to order 2 on the divisor $c_3 = 0$. From Table 4.1, there is an SU(2) on $c_3 = 0$. If we can compute the matter spectrum charged under the SU(2) in this phase, we will derive the U(1) charged matter in the original Morrison-Park form by a simple branching rule.

For example, if B is a complex surface, then the curve $c_3 = 0$ belongs in the divisor

class $-K+L$, which has self-intersection n and genus g:

$$n = K^2 - 2K \cdot L + L^2 \ , \ g = 1 + \frac{-K \cdot L + L^2}{2}. \tag{5.1.12}$$

From the 6D anomaly cancellation equations (3.1.6,3.1.7,3.1.8), we can derive the matter spectrum for SU(2) on such a curve[83]:

$$\text{matter} = (6n + 16 - 16g)\mathbf{2} + (g)\mathbf{3}. \tag{5.1.13}$$

After the SU(2) is broken to U(1), we have the branching rules $\mathbf{2} \to (1) + (-1)$, $\mathbf{2} \to (2) + (0) + (-2)$. Hence we have in total n_1 charge-(± 1) hypermultiplets and n_2 charge-(± 2) hypermultiplets:

$$n_1 = 12K^2 - 8K \cdot L - 4L^2 \ , \ n_2 = L^2 - K \cdot L. \tag{5.1.14}$$

The total number of charged hypermultiplet equals to

$$H_{\text{charged}} = n_1 + n_2 = 12K^2 - 9K \cdot L - 3L^2. \tag{5.1.15}$$

These formula can be cross-checked by the U(1) anomaly cancellation formula (3.1.11, 3.1.14) as well: for the case with a single U(1) and no non-Abelian gauge groups, we can assign

$$a = K \ , \ b_{11} = -2K + 2L. \tag{5.1.16}$$

Then the anomaly cancellation conditions involving n_i U(1) charged hypermultiplets with charge q_i are:

$$\begin{aligned} a \cdot b_{11} &= -\frac{1}{6}\sum_i n_i q_i^2 \\ b_{11} \cdot b_{11} &= \frac{1}{3}\sum_i n_i q_i^4. \end{aligned} \tag{5.1.17}$$

If there are only U(1) charged hypermultiplets with $q_1 = \pm 1$ and $q_2 = \pm 2$, these

equations become:

$$\begin{aligned} 2K^2 - 2K \cdot L &= \frac{1}{6}n_1 + \frac{2}{3}n_2 \\ 4K^2 - 8K \cdot L + 4L^2 &= \frac{1}{3}n_1 + \frac{16}{3}n_2, \end{aligned} \tag{5.1.18}$$

which exactly give the same result in (5.1.14).

The Calabi-Yau Morrison-Park form with sections (5.1.3) is by no mean the most general form. It only gives the cases where the U(1) charge (of massless hypermultiplet) $|q_i| \leq 2$. Various generalized forms have been written out[86, 103, 85, 115] with higher U(1) charges. In fact, the Morrison-Park form does not even produce all the U(1) models with charge $|q_i| \leq 2$. As an example, if we take the base to be the Hirzebruch surface $\mathbb{F}_0$ or equivalently $\mathbb{P}^1 \times \mathbb{P}^1$, with the effective divisor classes S and F:

$$S^2 = F^2 = 0 \ , \ S \cdot F = 1, \tag{5.1.19}$$

then the choice $L = 2S + 7F$ is not allowed in (5.1.2), as $L > -3K$ now. However, we can use a non-UFD (unique factorization domain) construction in [115]:

$$f = a_1 a_3 - \frac{1}{2}a_2^2 - b^2 a_0 \ , \ g = a_0 a_3^2 - \frac{1}{3}a_1 a_2 a_3 + \frac{2}{27}a_2^3 - \frac{2}{3}b^2 a_0 a_2 + \frac{1}{4}b^2 a_1^2, \tag{5.1.20}$$

where

$$a_3 = -\left(t + \frac{\bar{\phi}}{12}\frac{b_{(2)}\eta_a + b_{(1)}\eta_b}{\eta_b}b\right), \tag{5.1.21}$$

$$a_2 = \frac{1}{4}\left(h_{(2)}\eta_a^2 + 2h_{(1)}\eta_a\eta_b + h_{(0)}\eta_b^2 + \frac{\bar{\phi}^2}{36}(b_{(1)}^2 - b_{(0)}b_{(2)})\right) \tag{5.1.22}$$

$$+ \frac{\bar{\phi}}{4}\frac{t_{(3)}\eta_a^2 + 2t_{(2)}\eta_a\eta_b + t_{(1)}\eta_b^2}{\eta_b} + \frac{b_{(2)}\bar{\phi}^2}{96\eta_b^2}b, \tag{5.1.23}$$

$$\tag{5.1.24}$$

$$a_1 = -(\lambda_{(1)}\eta_a + \lambda_{(0)}\eta_b + \frac{\bar{\phi}}{24}\frac{h_{(2)}\eta_a + h_{(1)}\eta_b}{\eta_b} \tag{5.1.25}$$

$$+ \frac{\bar{\phi}^2}{48}\frac{t_{(3)}\eta_a + t_{(2)}\eta_b}{\eta_b^2} + \frac{b_{(2)}\bar{\phi}^3}{1728}\frac{b_{(2)}\eta_a + b_{(1)}\eta_b}{\eta_b^3}), \tag{5.1.26}$$

$$a_0 = -f_2 + \frac{\bar{\phi}}{12}\frac{\lambda_{(1)}}{\eta_b} + \frac{\bar{\phi}^2}{576}\frac{h_{(2)}}{\eta_b^2} + \frac{\bar{\phi}^3}{1728}\frac{t_{(3)}}{\eta_b^3} + \frac{\bar{\phi}^4}{82944}\frac{b_{(2)}^2}{\eta_b^4}, \tag{5.1.27}$$

$$\tag{5.1.28}$$

where

$$b = b_{(2)}\eta_a^2 + 2b_{(1)}\eta_a\eta_b + b_{(0)}\eta_b^2 \tag{5.1.29}$$

$$t = t_{(3)}\eta_a^3 + 3t_{(2)}\eta_a^2\eta_b + 3t_{(1)}\eta_a\eta_b^2 + t_{(0)}\eta_b^3. \tag{5.1.30}$$

The parameters are holomorphic sections of different line bundles listed in Table 5.1. Generally it is required that $\bar{\phi}, \eta_a, \eta_b \neq 0$. Now the unHiggsing from U(1) to SU(2) is given by the tuning

$$b_{(2)} = 2\beta_{(2)}\eta_b \ , \ b_{(1)} = -(\beta_{(2)}\eta_a + \beta_{(0)}\eta_b) \ , \ b_{(0)} = 2\beta_{(0)}\eta_a. \tag{5.1.31}$$

After this tuning, $b = 0$ and we have an SU(2) on the divisor $t = 0$. The crucial difference here is that the divisor $t = 0$ has triple point singularities at the locus $\eta_a = \eta_b = 0$, which gives the rank-3 symmetric tensor representation **4** of SU(2). After SU(2) is broken to U(1) again, we will get a number of charge-3 matter fields.

The matter multiplicity of U(1) charged hypermultiplets in this model is given by

$$n_3 = L_a \cdot L_b \ , \ n_2 = (-K + L) \cdot L - 6n_3 \ , \ n_1 = 12(-K + L)^2 - 81n_3 - 16n_2 \tag{5.1.32}$$

For our specific case $-K(\mathbb{F}_0) = 2S + 2F$, $L = 2S + 7F$, we can take $L_a = 2S$ and $L_b = 3S$. Then there is no matter with U(1) charge ± 3, but we still get a valid Weierstrass model that cannot be realized in the Morrison-Park form with sections (5.1.3).

Note that the form of f and g in (5.1.20) is similar to (5.1.2), but the coefficients a_i

Parameter	Line bundle	Parameter	Line bundle
b	L	$t_{(1)}$	$-K+L-L_a-2L_b$
t	$-K+L$	$t_{(2)}$	$-K+L-2L_a-L_b$
η_a	L_a	$t_{(3)}$	$-K+L-3L_a$
η_b	L_b	$h_{(0)}$	$-2K-2L_b$
$b_{(0)}$	$L-2L_b$	$h_{(1)}$	$-2K-L_a-L_b$
$b_{(1)}$	$L-L_a-L_b$	$h_{(2)}$	$-2K_2L_a$
$b_{(2)}$	$L-2L_a$	$\lambda_{(0)}$	$-3K-L-L_b$
ϕ	$-K-L+L_a+L_b$	$\lambda_{(1)}$	$-3K-L-L_a$
$t_{(0)}$	$-K+L-3L_b$	f_2	$-4K-2L$

Table 5.1: The parameters in the non-UFD model (5.1.20), which are holomorphic sections of various line bundles on B.

are taken as rational functions rather than holomorphic functions. The most general non-UFD formulation of Weierstrass form with U(1)s remains unknown.

In this thesis, we are still going to use the original Morrison-Park form with the sections (5.1.3). Despite that the Morrison-Park form does not reproduce all the F-theory U(1) models with matter fields $|q_i| \leq 2$, the following lemma should hold:

Lemma 4. *Any F-theory U(1) model without any massless charged matter field can be written in the Calabi-Yau Morrison-Park form (5.1.2) with sections (5.1.3).*

Such a U(1) gauge field without massless charged matter field is called "non-Higgsable U(1)", and the Weierstrass model should be completely smooth if the base is free of non-Higgsable gauge groups as well. As the discrepancy from the Morrison-Park form comes from the singularity structure of the divisor $c_3 = 0$ and $b = 0$ (see (5.1.29,5.1.30)), there will not be any issue for a smooth geometry.

The appearance of non-Higgsable U(1)s is a property of the base geometry B, just as the non-Higgsable non-Abelian gauge groups. If the generic Weierstrass model over B can be written in the Morrison-Park form (5.1.2), then we do not need any additional tuning to realize it.

The main focus of this chapter is to characterize the base geometry when non-Higgsable U(1)s appear. We provide a non-complete proof that non-Higgsable U(1) never appears on toric bases with any dimension. We are also going to construct some examples of (non-toric) threefold bases with non-Higgsable U(1)s.

5.2 Counting the Weierstrass moduli

Here we take our base manifold B to have d complex dimensions, and the generic elliptic Calabi-Yau manifold X over it has $d+1$ complex dimensions. Analogous to (3.2.39), we expect that $h^{d,1}(X)$ can be written as

$$h^{d,1}(X) = W - \omega_{\text{aut}} + N_{nW} - 1. \tag{5.2.33}$$

Here

$$W = h^0(-4K) + h^0(-6K) \tag{5.2.34}$$

is the number of Weierstrass moduli, or the total number of monomials in f and g. ω_{aut} is the dimension of the automorphism group of the base. N_{nW} is other non-Weierstrass contributions. For example, in the $d = 2$ case, $N_{nW} = N_{-2}$, the number of (-2)-curves on the base that are not in any non-Higgsable clusters, see (3.2.39).

ω_{aut} is determined by the properties of the base B, so it does not change when we tune a gauge group on B. N_{nW} does change in some rare cases. Taking a $d = 2$ example, if the degree of vanishing of the discriminant Δ goes from 0 to some positive number on a (-2)-curve, then this (-2)-curve is no longer counted in the term N_{-2} [82]. Hence after we have tuned a U(1) on B, the decrease in $h^{d,1}(X)$ is generally

$$-\Delta h^{d,1}(X) = -\Delta W - \Delta N_{nW}. \tag{5.2.35}$$

As the N_{nW} term is usually small, we neglect them in the discussion here and only consider the change in Weierstrass moduli. In the case of $d = 2$, we will never have a non-zero ΔN_{nW} from the rare case we presented before.

Now we want to count the number of independent Weierstrass moduli in the Morrison-Park form (5.1.2). The problem is that the functions b, c_0, c_1, c_2 and c_3 are not entirely independent. There may exist an infinitesimal transformation: $b \to b+\delta b$, $c_0 \to c_0 + \delta c_0$, $c_1 \to c_1 + \delta c_1$, $c_2 \to c_2 + \delta c_2$, $c_3 \to c_3 + \delta c_3$ such that the rational points

$\frac{\lambda}{b^2}$, $\frac{\alpha}{b^3}$ and f, g are invariant[1]. In fact, because of the relation (5.1.1):

$$\frac{\alpha^2}{b^6} = \frac{\lambda^3}{b^6} + \frac{f\lambda}{b^2} + g, \tag{5.2.36}$$

if $\frac{\lambda}{b^2}$, $\frac{\alpha}{b^3}$ and f are fixed, then g is also fixed. So we only need to guarantee the invariance of $\frac{\lambda}{b^2}$, $\frac{\alpha}{b^3}$ and f.

The number of such infinitesimal transformations then gives number of redundant variables in the Morrison-Park form, N_r.

If we can compute this number N_r, then the number of Weierstrass moduli in the Morrison-Park form equals to

$$W' = h^0(L)+h^0(-4K-2L)+h^0(-3K-L)+h^0(-2K)+h^0(-K+L)-N_r. \tag{5.2.37}$$

Comparing with (5.2.34), we see that the number of tuned Weierstrass moduli equals to

$$\begin{aligned} W - W' =& h^0(-4K) + h^0(-6K) - h^0(L) - h^0(-4K-2L) - h^0(-3K-L) - h^0(-2K) \\ & - h^0(-K+L) + N_r. \end{aligned} \tag{5.2.38}$$

We know that $N_r \geq 1$, since there is a trivial rescaling automorphism: $b \to tb$, $c_3 \to tc_3$, $c_2 \to c_2$, $c_1 \to t^{-1}c_1$, $c_0 \to t^{-2}c_0$ that keeps $\frac{\lambda}{b^2}$, $\frac{\alpha}{b^3}$, f and g invariant. However, other transformations may exist as well.

Now we study the simplest case $L = 0$ first. Since we have already taken the rescaling automorphism into account, we can set $b = 1$ for simplicity. The Morrison-Park form is reduced to

$$y^2 = x^3 + (c_1c_3 - \frac{1}{3}c_2^2 - c_0)xz^4 + (c_0c_3^2 + \frac{2}{27}c_2^3 - \frac{1}{3}c_1c_2c_3 - \frac{2}{3}c_0c_2 + \frac{1}{4}c_1^2)z^6. \tag{5.2.39}$$

[1]Similar redundancy issue also appears in the tuning of SU(7) gauge group[5].

The rational section is

$$(x, y, z) = (\lambda, \alpha, b) = (c_3^2 - \frac{2}{3}c_2, -c_3^3 + c_2c_3 - \frac{1}{2}c_1, 1). \tag{5.2.40}$$

If $\delta\lambda = 0$ under an infinitesimal transformation, then it is required that

$$\delta c_2 = 3c_3\delta c_3. \tag{5.2.41}$$

Plugging this equation into the requirement $\delta\alpha = 0$, we derive

$$\delta c_1 = 2c_2\delta c_3. \tag{5.2.42}$$

Then the explicit form of $\delta f = 0$ tells us

$$\delta c_0 = c_1\delta c_3. \tag{5.2.43}$$

Now one can easily check that under

$$\begin{aligned} \delta c_2 &= 3c_3\delta c_3, \\ \delta c_1 &= 2c_2\delta c_3, \\ \delta c_0 &= c_1\delta c_3, \end{aligned} \tag{5.2.44}$$

g is indeed invariant.

This infinitesimal transformation is parametrized by an arbitrary section $\delta c_3 \in \mathcal{O}(-K)$, which implies that the coefficient c_3 is actually a dummy variable. Hence the total number of redundant variables equals to

$$N_r = 1 + h^0(-K). \tag{5.2.45}$$

We have thus derived the formula for $(-\Delta W)$ in the case of $L = 0$:

$$-\Delta W_{L=0} = h^0(-6K) - h^0(-3K) - h^0(-2K). \tag{5.2.46}$$

Now we study the more general case $L > 0$. Similarly, the infinitesimal transformations parametrized by δc_3 and δb which leave $\frac{\lambda}{b^2}$, $\frac{\alpha}{b^3}$, f and g invariant are in the following form:

$$\begin{aligned}
\delta c_2 &= \frac{3c_3\delta c_3}{b^2} - \frac{3c_3^2\delta b}{b^3}, \\
\delta c_1 &= \frac{2c_2\delta c_3}{b^2} - \frac{c_1\delta b}{b} - \frac{2c_2c_3\delta b}{b^3}, \\
\delta c_0 &= \frac{c_1\delta c_3}{b^2} - \frac{c_1c_3\delta b}{b^3} - \frac{2c_0\delta b}{b}.
\end{aligned} \tag{5.2.47}$$

However, they are rational functions rather than holomorphic functions. Hence these infinitesimal transformations are not always legitimate. Nevertheless, we are guaranteed to have a subset of infinitesimal transformations:

$$\delta b \equiv 0 \ , \ b^2 | \delta c_3, \tag{5.2.48}$$

which indeed give holomorphic δc_2, δc_1 and δc_0. The condition $b^2|\delta c_3$ tells us that $\delta c_3' = \delta c_3/b^2$ is a holomorphic section of the line bundle $\mathcal{O}(-K-L)$. Hence we obtain a lower bound on N_r:

$$N_r \geq 1 + h^0(-K-L). \tag{5.2.49}$$

We have thus derived a lower bound for $(-\Delta W)$ for general L:

$$\begin{aligned}
-\Delta W \geq & h^0(-4K) + h^0(-6K) - h^0(L) - h^0(-4K-2L) - h^0(-3K-L) - h^0(-2K) \\
& - h^0(-K+L) + h^0(-K-L) + 1.
\end{aligned} \tag{5.2.50}$$

For base point free line bundles L (there is no base point x_0 on which every section $s \in \mathcal{O}(L)$ satisfies $s(x_0) = 0$), we claim that the above inequality is saturated, so we

get the exact formula:

$$\begin{aligned}-\Delta W =& h^0(-4K) + h^0(-6K) - h^0(L) - h^0(-4K-2L) - h^0(-3K-L) - h^0(-2K) \\ & - h^0(-K+L) + h^0(-K-L) + 1.\end{aligned} \tag{5.2.51}$$

Because L has no base point, for generic sections $c_3 \in \mathcal{O}(-K+L)$ and $b \in \mathcal{O}(L)$, they do not share any common factors after these polynomials are factorized to irreducible components (if they have). For δc_2 in (5.2.47) to be holomorphic:

$$\delta c_2 = \frac{3c_3 b \delta c_3 - 3c_3^2 \delta b}{b^3}, \tag{5.2.52}$$

it is required that $\delta b = tb$ where t is a complex number. But this form of δb is exactly the trivial rescaling isomorphism, so we want to substract this component and set $\delta b = 0$. Now

$$\delta c_2 = \frac{3c_3 \delta c_3}{b^2}. \tag{5.2.53}$$

Because c_3 does not share any common factor with b, the only possibility for δc_2 to be holomorphic is $b^2 | c_3$. Thus the only possible infinitesimal transformations keeping $\frac{\lambda}{b^2}$, $\frac{\alpha}{b^3}$, f and g invariant are given by (5.2.48), and

$$N_r = 1 + h^0(-K-L). \tag{5.2.54}$$

5.2.1 The minimal tuning of U(1)

Now we have the following key conjecture:

Conjecture 1. *The minimal value of $-\Delta h^{d,1}(X)$ and $-\Delta W$ on a given base B when a U(1) is tuned is given by the choice $L = 0$.*

In the above statement, we have not taken into account the possible bad singularities in the elliptic CY manifold X. If the choice $L = 0$ leads to (4,6) singularities of f and g over some codimension 1 or 2 base locus, then this choice is not acceptable.

Nonetheless, the acceptable values of $-\Delta h^{d,1}(X)$ and $-\Delta W$ are still lower bounded by (5.2.46).

We can construct a sufficient condition that implies the Conjecture 1 using formula (5.2.51). We only need to check that the following inequality holds

$$\begin{aligned} &h^0(-4K)+h^0(-6K)-h^0(L)-h^0(-4K-2L)-h^0(-3K-L)-h^0(-2K) \\ &-h^0(-K+L)+h^0(-K-L)+1 \geq h^0(-6K)-h^0(-3K)-h^0(-2K), \end{aligned} \tag{5.2.55}$$

However, this type of inequalities are not studied in the mathematical literature, hence we cannot formulate a rigorous proof to Conjecture (1).

For the class of generalized del Pezzo surfaces B without non-Higgsable non-Abelian gauge groups, the Conjecture (1) can be explicitly checked by an anomaly argument. Because of the gravitational anomaly cancellation

$$H_{\text{charged}}+H_{\text{neutral}}-V=273-29T, \tag{5.2.56}$$

after a U(1) is tuned, we get

$$-\Delta h^{2,1}(X)=-\Delta H_{\text{neutral}}=\Delta H_{\text{charged}}-1. \tag{5.2.57}$$

Here $\Delta H_{\text{charged}} = H_{\text{charged}}$ in (5.1.15) since there is no charged matter before the tuning. In order to prove Conjecture (1) in this case, we only need to prove

$$H_{charged}(L) \geq H_{charged}(0) \tag{5.2.58}$$

for any L that satisfies $-3K-L \geq 0$, or equivalently

$$-3K \cdot L - L^2 \geq 0. \tag{5.2.59}$$

We apply the Zariski decomposition of an effective divisor L in Section 3.1:

$$L = N + P, \tag{5.2.60}$$

where P is a nef divisor and N is a linear combination of negative self-intersection curves N_i:

$$N = \sum_i n_i N_i. \tag{5.2.61}$$

The intersection matrix $(N_i \cdot N_j)$ is negative definite, such that $N^2 \leq 0$.

Now

$$-3K \cdot L - L^2 = -3K \cdot N - N^2 - 3K \cdot P - P^2. \tag{5.2.62}$$

Because $-K$ is a nef divisor for generalized del Pezzo surfaces, $-3K \cdot N \geq 0$. We also have $-N^2 \geq 0$ from the negative definiteness of $(N_i \cdot N_j)$. The remaining two terms can be written as

$$-3K \cdot P - P^2 = (-3K - L + N) \cdot P. \tag{5.2.63}$$

$-3K - L + N$ is effective because $-3K - L$ is effective, and we can conclude $-3K \cdot P - P^2 \geq 0$ because P is nef.

We thus proved that

$$-3K \cdot L - L^2 \geq 0. \tag{5.2.64}$$

If there are charged hypermultiplets with charge ± 3 or higher, we denote the numbers of hypermultiplets with charge k by n_k. Then (5.1.18) is rewritten as:

$$\begin{aligned} 2K^2 - 2K \cdot L &= \frac{1}{6} n_1 + \frac{2}{3} n_2 + \frac{1}{6} \sum_{k \geq 3} k^2 n_k \\ 4K^2 - 8K \cdot L + 4L^2 &= \frac{1}{3} n_1 + \frac{16}{3} n_2 + \frac{1}{3} \sum_{k \geq 3} k^4 n_k. \end{aligned} \tag{5.2.65}$$

Now

$$\begin{aligned} n_1 &= 12K^2 - 8K\cdot L - 4L^2 - \frac{4}{3}\sum_{k\geq 3} k^2 n_k + \frac{1}{3}\sum_{k\geq 3} k^4 n_k \\ n_2 &= L^2 - K\cdot L + \frac{1}{12}\sum_{k\geq 3} k^2 n_k - \frac{1}{12}\sum_{k\geq 3} k^4 n_k. \end{aligned} \tag{5.2.66}$$

and the total number of charged hypermultiplets is

$$H_{\text{charged}} = n_1 + n_2 + \sum_{k\geq 3} n_k = 12K^2 - 9K\cdot L - 3L^2 - \frac{5}{4}\sum_{k\geq 3} k^2 n_k + \frac{1}{4}\sum_{k\geq 3} k^4 n_k + \sum_{k\geq 3} n_k. \tag{5.2.67}$$

Since

$$-\frac{5}{4}\sum_{k\geq 3} k^2 n_k + \frac{1}{4}\sum_{k\geq 3} k^4 n_k = \frac{1}{4}\sum_{k\geq 3} k^2(k^2-5) n_k \geq 0, \tag{5.2.68}$$

the value of H_{charged} is strictly larger than (5.1.15) when there are some hypermultiplets with charge ± 3 or higher.

We hence finished the proof of Conjecture 1 for 2D bases without non-Higgsable clusters.

5.2.2 6D F-theory examples

Now we check the formula (5.2.51) with some examples.

For the base $\mathbb{P}^2$, the tuning of a single was studied in Morrison and Park's original paper [102]. On $\mathbb{P}^2$, any effective line bundle can be written as $L = nH$, where H is the hyperplane class.

The linear system $|nH|$ is the vector space of degree-n homogeneous polynomials in 3 variables (for $n \geq 0$), hence

$$h^0(nH) = \frac{(n+1)(n+2)}{2}. \tag{5.2.69}$$

They are all base point free, hence we expect the exact formula (5.2.51) to hold.

Now our formula (5.2.51) gives

$$\begin{aligned}-\Delta W =& h^0(12H) + h^0(18H) - h^0(nH) - h^0((12-2n)H) - h^0((9-n)H) - h^0(6H) \\ & - h^0((3+n)H) + h^0((3-n)H) + 1.\end{aligned} \tag{5.2.70}$$

When $n \leq 5$, this expression can be reduced to

$$-\Delta W = -\Delta h^{2,1} = 107 + 27n - 3n^2 \tag{5.2.71}$$

Because of the appearance of a single U(1), $\Delta V = 1$, and we know that the number of charged hypermuliplets is

$$\begin{aligned}H_{\text{charged}} &= \Delta V - \Delta h^{2,1}(X) \\ &= 108 + 27n - 3n^2.\end{aligned} \tag{5.2.72}$$

From the anomaly computation (5.1.14), we get the numbers n_1, n_2 of charged hypermultiplets with U(1) charge ± 1 and ± 2:

$$(n_1, n_2) = (4(n+3)(9-n), n(n+3)). \tag{5.2.73}$$

The total number of charged hypermultiplets

$$H_{\text{charged}} = 108 + 27n - 3n^2 \tag{5.2.74}$$

exactly coincides with our formula (5.2.70) when $n \leq 5$.

When $n = 6$ or $L = 6H$, from (5.2.70) we can compute $-\Delta W = -\Delta h^{2,1}(X) = 160$. From the anomaly cancellation, the total number of charged hypermultiplets is $H_{\text{charged}} = 162$. Since $L = -2K$ in this case, as we have mentioned, two U(1)s emerge from this tuning: $\Delta V = 2$. Hence we still get consistent result.

When $n = 7$ or 8, $c_0 = 0$. In these cases, an additional SU(2) gauge group appears on the (irreducible) curve $c_1 = 0$. The total gauge groups in these cases are

$\mathrm{SU}(2)\times\mathrm{U}(1)$, $\Delta V = 4$.

The formula (5.2.70) for $n = 7$ and 8 gives $-\Delta W = -\Delta h^{2,1}(X) = 146$ and 128 respectively. On the other hand, the number of charged hypermultiplets from anomaly cancellation gives $H_{\text{charged}} = 150$ and 132 respectively. Hence our formula (5.2.70) exactly gives the correct number of tuned moduli.

We can also check $B = \mathbb{F}_{12}$, where the Picard group is generated by S and F:

$$S^2 = -12 \ , \ F^2 = 0 \ , \ S \cdot F = 1. \tag{5.2.75}$$

The anticanonical divisor is

$$-K(\mathbb{F}_{12}) = 2S + 14F, \tag{5.2.76}$$

and the section of various line bundles can be read out with the toric geometry methods in Section 2.4.

we denote the divisor S by $s = 0$, and F by $t = 0$. In the local coordinate patch SF, where s, t can vanish and the other local coordinates x_i are set to be 1, f and g can be written as:

$$f = \sum_{i=4}^{8} \sum_{j=0}^{12i-40} f_{i,j} t^j s^i \tag{5.2.77}$$

$$g = \sum_{i=5}^{12} \sum_{j=0}^{12i-60} g_{i,j} t^j s^i. \tag{5.2.78}$$

f and g vanish to order (4,5) on the curve S, which gives an E_8 gauge group. We can explicitly count

$$h^0(-4K) = 165 \ , \ h^0(-6K) = 344. \tag{5.2.79}$$

The Hodge numbers of the generically fibered elliptic Calabi-Yau threefold X over $\mathbb{F}_{12}$ are $h^{1,1} = 11$, $h^{2,1} = 491$.

Now we want to tune a U(1) on it. If we take $L = 0$, since $h^0(-2K) = 51$,

$h^0(-3K) = 100$, then

$$-\Delta W_{L=0} = h^0(-6K) - h^0(-3K) - h^0(-2K) = 193. \tag{5.2.80}$$

However, this choice of L is not allowed. The rational section $(x, y, z) = (\lambda, \alpha, 1)$ has to obey

$$\alpha^2 = \lambda^3 + f\lambda + g. \tag{5.2.81}$$

Now since $\lambda \in \mathcal{O}(-2K)$, $\alpha \in \mathcal{O}(-3K)$, they can be written as

$$\lambda = \sum_{i=2}^{4} \lambda_i s^i \ , \ \alpha = \sum_{i=3}^{6} \alpha_i s^i. \tag{5.2.82}$$

Plugging these into (5.2.81), we can see that the only term of order s^5 is the term $g_{5,0}s^5$. Hence this tuning of U(1) requires that $g_{5,0} = 0$, which leads to (4,6) singularity on $s = 0$.

One way of tuning U(1) on $\mathbb{F}_{12}$ is to take $c_3 \in \mathcal{O}(2\tilde{S})$. Since $2\tilde{S} = 2S + 24F = -K + 10F$, this corresponds to $L = 10F$. Now the equation (5.2.81) becomes

$$\alpha^2 = \lambda^3 + f\lambda b^4 + gb^6. \tag{5.2.83}$$

The functions $\lambda \in \mathcal{O}(-2K + 2L)$, $\alpha \in \mathcal{O}(-3K + 3L)$ can be written as

$$\lambda = \sum_{i=0}^{4} \lambda_i s^i \ , \ \alpha = \sum_{i=0}^{6} \alpha_i s^i. \tag{5.2.84}$$

The issue of (4,6) singularity no longer exists.

Now we can compute $-\Delta W$ using our formula (5.2.51). With $h^0(L) = 11$, $h^0(-4K-2L) = h^0(8S+36F) = 76$, $h^0(-3K-L) = h^0(6S+32F) = 63$, $h^0(-K+L) = h^0(2S + 24F) = 39$ and $h^0(-K - L) = h^0(4F) = 5$, the result is

$$-\Delta h^{2,1}(X)_{L=10F} = 275. \tag{5.2.85}$$

On the other hand, $-\Delta H_{\text{neutral}}$ matches the anomaly cancellation computation (5.1.14) as well.

5.3 Conditions on a base with a non-Higgsable U(1)

Now we are going to investigate the conditions for a base to have a non-Higgsable U(1). This means that we do not need to tune any complex structure moduli to get the Morrison-Park form. Assuming Conjecture1 holds, the equivalent conditon is that the minimal value of $-\Delta W$ in the formula (5.2.46) is non-positive:

$$-\Delta W_{L=0} = h^0(-6K) - h^0(-3K) - h^0(-2K) \leq 0 \tag{5.3.86}$$

This inequality imposes stringent constraint on the Newton polytopes A_n of $\mathcal{O}(-nK)$. For toric bases, they are the polytopes defined by the set of lattice points:

$$A_n = \{p \in \mathbb{Z}^d | \langle p, v_i \rangle \geq -n \ , \ \forall i\}. \tag{5.3.87}$$

Note that A_4 and A_6 corresponds to $\mathcal{F}$ and $\mathcal{G}$ defined in (2.4.69) and (2.4.70) respectively.

The notion of Newton polytopes can be generalized to arbitrary bases. For a point $p = (x_1, x_2, \ldots, x_d)$ in the Newton polytope A_n, it corresponds to a monomial $m_p = \alpha^n \prod_{i=1}^d \beta_i^{x_i}$, where α and β_i are some non-zero functions. Hence the product of two monomials is mapped to the vector sum of two points in $\mathbb{Z}^d$. For example, the expression of f and g for a semi-toric base with non-Higgsable U(1)s in Section 5.4.2 can be written as (5.4.112). In that case, we can assign $\alpha = \tilde{\eta}$, $\beta_1 = \eta\tilde{\eta}^{-1}$, and the Newton polytopes for f and g are one-dimensional. Note that the origin in the $\mathbb{Z}^d$ can be shifted.

We use the notation nP to denote the set of lattice points in the resized polytope

enlarged by a factor n:

$$nP = \{p | p = \sum_{i=1}^{n} p_i \ , \ \forall p_i \in P\}. \tag{5.3.88}$$

The lattice points in nP correspond to the monomials $m = \prod_{i=1}^{n} m_i$, where $m_i \in P$. $|A|$ denotes the number of lattice points in the Newton polytope A.

We denote the dimension of the Newton polytope A_n of $\mathcal{O}(-nK)$ by d_{An}. Clearly the dimension of any other $A_n (n < 6)$ is equal to or smaller than d_{A6}. We want to prove the following proposition:

Proposition 2. *For a base with a non-Higgsable U(1), the Newton polytopes $A_n (n \leq 6)$ are all one-dimensional. The number of lattice points in A_n satisfies*

$$|A_4| \leq 5, |A_6| \leq 7. \tag{5.3.89}$$

Note that regardless of d_{A2}, d_{A3} and d_{A6}, we always have

$$|2A_3| \geq 2|A_3| - 1 \ , \ |3A_2| \geq 3|A_2| - 2 \tag{5.3.90}$$

Then since $2A_3 \subseteq A_6$ and $3A_2 \subseteq A_6$,

$$\begin{aligned} -\Delta W_{L=0} &= |A_6| - |A_3| - |A_2| \\ &\geq |2A_3| - |A_3| - |A_2| \\ &\geq |A_3| - |A_2| - 1 \end{aligned} \tag{5.3.91}$$

and

$$\begin{aligned} -\Delta W_{L=0} &= |A_6| - |A_3| - |A_2| \\ &\geq |3A_2| - |A_3| - |A_2| \\ &\geq 2|A_2| - |A_3| - 2. \end{aligned} \tag{5.3.92}$$

If $-\Delta W_{L=0} \leq 0$ so that non-Higgsable U(1)s appear, we have constraints on $|A_3|$

$\lvert A_2\rvert$	1	1	2	2	3
$\lvert A_3\rvert$	1	2	2	3	4
$\lvert A_4\rvert$	1,2	1,2,3	3	3,4	5
$\lvert A_6\rvert$	2	3	4	5	7

Table 5.2: The possible values of the number of lattice points in the Newton polytope A_n of $\mathcal{O}(-nK)$, when non-Higgsable U(1)s exist.

and $|A_2|$:

$$|A_3| - |A_2| - 1 \leq 0 \ , \ 2|A_2| - |A_3| - 2 \leq 0. \tag{5.3.93}$$

The only possible values for $(|A_2|, |A_3|)$ satisfying these inequalities are $(1,1)$, $(1,2)$, $(2,2)$, $(2,3)$ and $(3,4)$. We list the possible values of $|A_6|$ for each of these cases in Table 5.2.

Now we argue that the dimension of Newton polytopes A_2, A_3 and A_6 cannot be higher than 1. The statement is trivial for $|A_6| = 2$ because these polytopes have at most 2 points. If $|A_6| = 3$, since $|A_6| = 2|A_3| - 1$, $|2A_3| \geq 2|A_3| - 1$ and $|2A_3| \leq |A_6|$ (see (5.3.90)), we know that $|2A_3| = 2|A_3| - 1$ and A_6 coincides with the polytope $2A_3$. Because A_3 is one-dimensional, we conclude that $d_{A6} = d_{A3} = 1$. If $|A_6| = 4$, since $|A_6| = |3A_2| = 3|A_2| - 2$, A_6 coincides with $3A_2$ and $d_{A6} = d_{A2} = 1$. If $|A_6| = 5$, similarly because $|A_6| = |2A_3| = 2|A_3| - 1$, A_6 coincides with the polytope $2A_3$. We have argued that if $d_{A3} > 1$, then $|2A_3| \geq 2|A_3|$. This does not happen here, hence the polytopes A_3 and A_6 are one-dimensional. When $|A_6| = 7$, similarly $|A_6| = |2A_3| = 2|A_3| - 1$, then A_6 coincides with the polytope $2A_3$ and they are both one-dimensional.

For the values of $|A_4|$ in Table 5.2, they are enumerated by the following method: we linearly transform the Newton polytopes A_n integral points on line segments $[na, nb]$, $a, b \in \mathbb{Q}, a < b$. This $\mathrm{SL}(d, \mathbb{Q})$ linear transformation is always possible because the Newton polytopes A_n are one-dimensional. Then for each $|A_6|$, we can try to find the pairs (a, b) that give all the possible value of $|A_4|$ with the correct values of $|A_2|$ and $|A_3|$. For $|A_6| = 2$, we can take $(a, b) = (0, \frac{1}{4})$ to get $|A_4| = 2$ and $(a, b) = (0, \frac{1}{6})$ to get $|A_4| = 1$. For $|A_6| = 3$, we can take $(a, b) = (-\frac{1}{4}, \frac{1}{4})$ to get $|A_4| = 3$, $(a, b) = (0, \frac{1}{3})$ to get $|A_4| = 2$ and $(a, b) = (\frac{1}{3}, \frac{2}{3})$ to get $|A_4| = 1$. For

$|A_6| = 4$, we can only take $(a, b) = (0, \frac{1}{2})$ to get $|A_4| = 3$. For $|A_6| = 5$, we can take $(a, b) = (0, \frac{3}{4})$ to get $|A_4| = 4$ and $(a, b) = (0, \frac{2}{3})$ to get $|A_4| = 3$. For $|A_6| = 7$, we can only take $(a, b) = (0, 1)$ to get $|A_4| = 5$.

Hence we have the proved the proposition.

This shows that the number of monomials in A_4 and A_6 are very small when non-Higgsable U(1)s exist. Recall the formula for $h^{d,1}$ (5.2.33), we expect the number of complex structure moduli of the elliptic Calabi-Yau manifold over this base to be small. In the 4D F-theory context, it means that the number of flux vacua is small.

Furthermore, the constraints on the Newton polytopes lead to the exclusion of non-Higgsable U(1)s on any toric bases:

Proposition 3. *For a resolvable (smooth compact) toric base in any dimension, the Newton polytopes A_n cannot satisfy Proposition 2.*

A simple argument is that if the origin of the Newton polytope $\mathcal{G} = A_6$ lies on the boundary of G, then there will be a (4,6) divisor with a toric ray perpendicular to the boundary. If there is not such a (4,6) divisor, it will always emerge after we resolved all the codimension-two (4,6) locus.

More precisely, for the case of 2D toric bases, we perform an $\mathrm{SL}(2, \mathbb{Z})$ transformation on the 2D toric fan, such that the monomials in g align along the y-axis. Now, we observe that there always exists a ray (1,0) in the fan. Otherwise, the only possible 2D cone for a smooth 2D toric base near the positive x-axis consists of a ray $(1, a)$ and a ray $(-b, -ab - 1)$, where $a \geq 1, b \geq 0$, see Figure 5-1.

If this is the case, suppose that (0,1) is in the Newton polytope A_6 for g, which means that there is no ray (x, y) in the fan with $y < -6$. Then from the structure of the fan, we can see that $(-1, 1)$ is also in the polytope A_6. This is because the other rays (x, y) with $x > 0$ all satisfy $y > ax$, hence they cannot satisfy $(x, y) \cdot (-1, 1) = -x + y < -6$. Then we conclude that A_6 is not a one-dimensional polytope, which contradicts our assumption. Hence $(0, 1) \notin A_6$. Similarly, we can exclude the existence of all points $(0, y > 0)$ in A_6. However, this implies that g vanishes to order 6 on the divisor corresponding to the ray $(-b, -ab - 1)$. Because $A_4 \subset A_6$ for toric

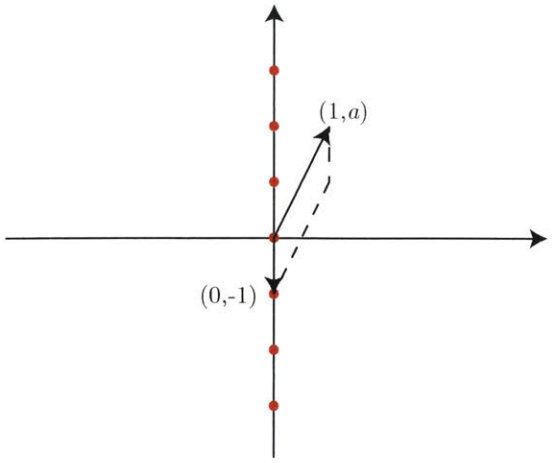

Figure 5-1: A fictional configuration of 2D toric base with monomials in g aligned along the y-axis. Suppose that there is no ray (1,0), then this is the only possibility up to a linear transformation.

bases, this excludes all the points $(0, y > 0)$ in A_4 as well. Hence (f, g) vanishes to order $(4, 6)$ on the divisor corresponding to the ray $(-b, -ab - 1)$, which is not allowed.

Hence we conclude that a ray (1,0) has to exist in the fan. However, because A_4 and A_6 aligns along the y-axis, it means that (f, g) vanishes to order $(4, 6)$ on the divisor corresponding to the ray (1,0). So this is not allowed, either.

Similar arguments can be applied to higher dimensional cases. For any smooth compact toric bases, there has to be a ray perpendicular to the line on which f and g aligns, but this will lead to (4,6) singularity on such a ray. If this ray does not exist, then there will be (4,6) singularities over codimension-two locus on the base that cannot be resolved by blowing up this locus.

We elaborate this statement for the case of toric threefold bases. We assume that the Newton polytopes A_4 and A_6 lie on the z-axis, and the fan of the toric base has no ray on the plane $z = 0$. Because the base is compact, there exists a 2D cone v_1v_2 in the fan such that $v_{1z} > 0$ and $v_{2z} < 0$ (v_{1z} and v_{2z} are the z-components of v_1 and v_2 respectively). Now we can analyze the degree of vanishing of (f, g) on this codimension-two locus v_1v_2 for each of the cases in Table 5.2. For example, if $|A_4| = 5$, $|A_6| = 7$, such that the points in A_4 are $(0, 0, -2) \sim (0, 0, 2)$ and the points in A_6 are $(0, 0, -3) \sim (0, 0, 3)$, then we have constraints on v_{1z} and v_{2z}: $2 \geq v_{1z} \geq 1$,

$-1 \geq v_{2z} \geq -2$. Now if $v_{1z} = -v_{2z} = 1$ or $v_{1z} = -v_{2z} = 2$, then it is easy to see that the degree of vanishing of (f, g) on this curve $v_1 v_2$ is $(8, 12)$. We cannot resolve this by blowing up the curve $v_1 v_2$, because the ray of the exceptional divisor will lie on the plane $z = 0$, which contradicts our assumptions. If $v_{1z} = 2$, $v_{2z} = -1$ or $v_{1z} = 1$, $v_{2z} = -2$, then the degree of vanishing of (f, g) on this curve $v_1 v_2$ is $(6, 9)$. If we try to resolve this by blowing up the curve $v_1 v_2$, then the exceptional divisor corresponds to a ray $v_3 = v_1 + v_2$ with $v_{3z} = \pm 1$. Then the $(4, 6)$ singularity issues remains on the curve $v_2 v_3$ or $v_1 v_3$. Hence we cannot construct a good toric threefold base with such Newton polytopes A_4 and A_6. Similarly we can explicitly apply this argument to all the other possible configurations of A_4 and A_6, showing that it is impossible to construct a toric threefold base with non-Higgsable U(1)s and without any codimension-one or codimension-two (4,6) singularities. This argument is independent of the dimension of the toric base, either.

This 1D feature of Weierstrass polynomials suggests that the bases with non-Higgsable U(1) always have the structure of a fibration over $\mathbb{P}^1$.

We have the following conjecture:

Conjecture 2. *Any n-dimensional base with non-Higgsable U(1) can be written as a resolution of a Calabi-Yau $(d-1)$-fold fibration over $\mathbb{P}^1$. The generic fiber is a smooth Calabi-Yau $(d-1)$-fold.*

The alignment of $f \in \mathcal{O}(-4K_B)$ and $g \in \mathcal{O}(-6K_B)$ on a line suggests that the base B is either a fibration of $F = -K_B$ or a blow up of such a $-K_B$ fibration. One can understand this from an analogous toric setup. If we take B to be a Hirzebruch surface $\mathbb{F}_n$, which is a $\mathbb{P}^1$ bundle over $\mathbb{P}^1$ with toric fan in Figure 3-3. From (2.4.67), we can see that any line bundle $\mathcal{O}(nF)$ on $\mathbb{F}_n$ has an one-dimensional Newton polytope. More generally, if we blow up $\mathbb{F}_n$ and the 0-curve F on $\mathbb{F}_n$ remains, the line bundle $\mathcal{O}(nF)$ still has an one-dimensional Newton polytope.

Now return to our case $F = -K_B$. From the adjunction formula, we can see that the canonical class of the fiber $F = -K_B$ vanishes:

$$K_F = (K_B + F)|_F = 0, \tag{5.3.94}$$

hence the fiber F is Calabi-Yau.

Additionally, the fiber F should not self-intersect, hence we have

$$F \cdot F = 0. \tag{5.3.95}$$

The elliptic Calabi-Yau $(d+1)$-fold X over this base B can be thought as resolution of the fiber product space, constructed below.

Take a rational elliptic surface A with section

$$\pi_A : A \to \mathbb{P}^1 \tag{5.3.96}$$

and a Calabi-Yau $(d-1)$-fold fibration B with section

$$\pi_B : B \to \mathbb{P}^1 \tag{5.3.97}$$

Then the elliptic Calabi-Yau $(d+1)$-fold X is the resolution of the fiber product

$$\tilde{X} = A \times_{\mathbb{P}^1} B = \{(u, v) \in A \times B | \pi_A(u) = \pi_B(v)\}. \tag{5.3.98}$$

In the case of $d = 2$, this is the generalized Schoen construction of fiber products of rational elliptic surfaces [104].

In the case of $d = 3$, the base B is a resolution of a K3 or T^4 fibration over $\mathbb{P}^1$.

Now we have an alternative interpretation of the relation between the fibration structure of B and the 1D feature of Weierstrass polynomials from the pullback of f and g over the elliptic surface A [104]:

$$\begin{aligned} f_{X'} &= \pi_B^\star(f_{\bar{A}}) \\ g_{X'} &= \pi_B^\star(g_{\bar{A}}). \end{aligned} \tag{5.3.99}$$

Here X' is the Weierstrass model over the base B, which is possibly singular. $\bar{A}$ is

the possibly singular Weierstrass model over $\mathbb{P}^1$. X' and $\bar{A}$ are related by

$$X' = \bar{A} \times_{\mathbb{P}^1} B = \{(\bar{u}, v) \in \bar{A} \times B | \pi_{\bar{A}}(\bar{u}) = \pi_B(v)\}. \tag{5.3.100}$$

Hence the 1D property of Weierstrass polynomials $f_{X'}$ and $g_{X'}$ over B is inherited from the 1D property of $f_{\bar{A}}$ and $g_{\bar{A}}$.

5.4 Examples of non-Higgsable U(1)s

5.4.1 A universal class

From Proposition 2, we need construct a base B where the Newton polytopes of $-4K_B$ and $-6K_B$ are one-dimensional. In fact, there exists a simple universal class of B satisfying this property. We start with a base B_0 whose $-K_{B_0}$ has no base point. Then we construct the base B by blowing up the intersection locus $D_1 \bigcap D_2$, where D_1 and D_2 are two different representative of the divisor class $-K_{B_0}$. We claim that such a base satisfies the requirements of Proposition 2.

The reason is fairly simple. Denotes the equation of D_1 and D_2 by $F_1 = 0$ and $F_2 = 0$ respectively. After the blow up, only the terms in f with the form $F_1^p F_2^q (p+q \geq 4)$ remain. Similarly only the terms in g with the form $F_1^p F_2^q (p+q \geq 6)$ remain. Since $F_1 = 0$ and $F_2 = 0$ are already holomorphic section of the line bundle $-K_{B_0}$, the only possible form of f and g after the blow up is

$$f = \sum_{i=0}^{4} f_i F_1^i F_2^{4-i} \ , \ g = \sum_{i=0}^{6} g_i F_1^i F_2^{6-i}, \tag{5.4.101}$$

where f_i and g_i are complex numbers. Indeed, f and g form one-dimensional Newton polytopes $\mathcal{F}$ and $\mathcal{G}$, and $|\mathcal{F}| = 5$, $|\mathcal{G}| = 7$.

As a more concrete example, if $B_0 = \mathbb{P}^2$, $-K_{B_0}$ is the divisor class of cubics on $\mathbb{P}^2$. Then the locus $D_1 \bigcap D_2$ is the collection of nine intersection points between two different cubics on $\mathbb{P}^2$. If we blow up these nine points, we get a good base B for 6D F-theory and non-Higgsable U(1)s. Since after the blow up we have $(-K_B) \cdot (-K_B) = 0$,

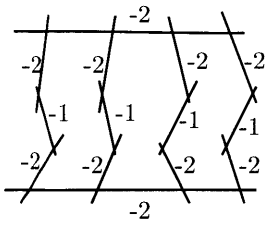

Figure 5-2: The geometric configuration of generalized del Pezzo surface gdP_{9st} with the negative curves on it. Note that there are two copies of (-2)-curve clusters that correspond to degenerate Kodaira fibers of type I_0^*.

we can think about B as a $-K_B$ fibration. This implies that B is an elliptic rational surface, which satisfies (5.3.94) and (5.3.95).

If $B_0 = \mathbb{P}^3$, $-K_{B_0} = 4H$ which is a K3 hypersurface inside $\mathbb{P}^3$. The locus $D_1 \bigcap D_2 = (4H) \bigcap (4H)$ is then the intersection locus of two different smooth K3 hypersurfaces in $\mathbb{P}^3$. After blowing up $(4H) \bigcap (4H)$, we get a good base B for 4D F-theory and non-Higgsable U(1)s that is a K3 fibration. Again (5.3.94) and (5.3.95) are satisfied and we find an example for Conjecture 2.

More generally, from the adjunction formula

5.4.2 Semi-toric generalized Schoen constructions

More generally, we can explicitly compute the form of Weierstrass polynomials for the semi-toric bases with non-Higgsable U(1)s constructed in [97], which are called generalized Schoen constructions[104].

As the first example, we choose the base to be the semi-toric generalized del Pezzo surface gdP_{9st} with $h^{1,1}(gdP_{9st}) = 10$, $T = 9$ and the set of negative rational curves in Figure 5-2.

Consider the general elliptic CY3 X over gdP_{9st}. In [97], it is computed that $h^{1,1}(X) = h^{2,1}(X) = 19$. There is a $U(1)^8$ abelian gauge group in the 6D low-energy effective theory, which explains the rank of the gauge group ($h^{1,1}(X) = h^{1,1}(gdP_{9st})+\text{rk}(G)+1 = 19$, $\text{rk}(G) = 8$). Using the anomaly cancellation in 6D:

$$273 - 29T = H - V = h^{2,1}(X) + 1 - V. \tag{5.4.102}$$

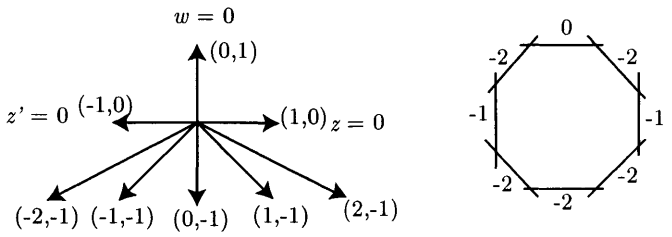

Figure 5-3: A toric generalized dP_5, with toric cyclic diagram $(0,-2,-1,-2,-2,-2,-1,-2)$, and the 2D toric rays shown on the left.

When $T=9$, $h^{2,1}(X)=19$, we get the correct number of vector multiplets $V=8$.

To write down the set of monomials in f and g for a general elliptic fibration over gdP_{9st}, we start with the 2D toric base with toric diagram in Figure 5-3.

We can compute the f and g with toric methods (2.4.69,2.4.70), and write down the general expression of f and g in the patch (z',w) and (z,w):

$$f = \sum_{i=0}^{8} f_{0,i} z^i z'^{8-i} + w \sum_{i=1}^{7} f_{1,i} z^i z'^{8-i} + w^2 \sum_{i=1}^{7} f_{2,i} z^i z'^{8-i} + w^3 \sum_{i=2}^{6} f_{3,i} z^i z'^{8-i} + w^4 \sum_{i=2}^{6} f_{4,i} z^i z'^{8-i} + w^5 \sum_{i=3}^{5} f_{5,i} z^i z'^{8-i} + w^6 \sum_{i=3}^{5} f_{6,i} z^i z'^{8-i} + w^7 f_{7,4} z^4 z'^4 + w^8 f_{8,4} z^4 z'^4. \tag{5.4.103}$$

$$g = \sum_{i=0}^{12} g_{0,i} z^i z'^{12-i} + w \sum_{i=1}^{11} g_{1,i} z^i z'^{12-i} + w^2 \sum_{i=1}^{11} g_{2,i} z^i z'^{12-i} + w^3 \sum_{i=2}^{10} g_{3,i} z^i z'^{12-i} + w^4 \sum_{i=2}^{10} g_{4,i} z^i z'^{12-i} + w^5 \sum_{i=3}^{9} g_{5,i} z^i z'^{12-i} + w^6 \sum_{i=3}^{9} g_{6,i} z^i z'^{12-i} + w^7 \sum_{i=4}^{8} g_{7,i} z^i z'^{12-i} + w^8 \sum_{i=4}^{8} g_{8,i} z^i z'^{12-i} + w^9 \sum_{i=5}^{7} g_{9,i} z^i z'^{12-i} + w^{10} \sum_{i=5}^{7} g_{10,i} z^i z'^{12-i} + w^{11} g_{11,6} z^6 z'^6 + w^{12} g_{12,6} z^6 z'^6 \tag{5.4.104}$$

In the above expressions, we have set all the local coordinates apart from z', z and w to be 1. From now on, we generally work in the patch (z,w), so we set $z'=1$. To recover the dependence on z', one just needs to multiply the factor z'^{8-i} to each

z^i term in f, and multiply z'^{12-i} to each z^i term in g. By the way, we will change the definition of coefficients f_{ij} and g_{ij} very often, they only mean general random complex numbers, for a generic fibration.

Now we blow up a point $z = 1$, $w = 0$, which is a generic point on the divisor $w = 0$. After the blow up, we assign new coordinates z_1, w_1 and ξ_1:

$$z - 1 = (z_1 - 1)\xi_1 \ , \ w = w_1\xi_1 \tag{5.4.105}$$

The divisor $w = 0$ becomes a (-1)-curve $w_1 = 0$. $\xi_1 = 0$ is the exceptional divisor of this blow-up, and $z_1 = 1$ is a new (-1)-curve. We plug (5.4.105) into the expression of f and g. Note that all the terms with ξ_1^m in f vanish for $m < 4$, similarly all the terms with ξ_1^m in g vanish for $m < 6$. This impose constraints on the coefficients f_{ij} and g_{ij}. Finally, we divide f by ξ_1^4, and g by ξ_1^6 after the process is done. The resulting f can be written as:

$$\begin{aligned} f = {} & (z_1 - 1)^4 \sum_{i=0}^{4} f_{0,i} z^i + (z_1 - 1)^3 w_1 \sum_{i=1}^{4} f_{1,i} z^i + (z_1 - 1)^2 w_1^2 \sum_{i=2}^{5} f_{2,i} z^i + (z_1 - 1) w_1^3 \sum_{i=2}^{5} f_{3,i} z^i \\ & + w_1^4 \sum_{i=2}^{6} f_{4,i} z^i + w_1^5 \xi_1 \sum_{i=3}^{5} f_{5,i} z^i + w_1^6 \xi_1^2 \sum_{i=3}^{5} f_{6,i} z^i + w_1^7 \xi_1^3 f_{7,4} z^4 + w_1^8 \xi_1^4 f_{8,4} z^4 \end{aligned} \tag{5.4.106}$$

g has similar structure, and we will not expand the details. Note that the divisor $z = 0$ and the local patch (z, w_1) still exist. In the patch (z, w_1), we can choose $\xi_1 = 1$, so that $z = z_1$. Then it is easy to rewrite f as a function only of z and w_1.

Then in the patch (z, w_1), we blow up a point $z = 2$, $w_1 = 0$, which is a generic point on divisor $w_1 = 0$. After the blow up, we assign new coordinates z_2, w_2 and ξ_2:

$$z - 2 = (z_2 - 2)\xi_2 \ , \ w = w_2\xi_2 \tag{5.4.107}$$

We draw the geometry of the base after this blow up in Figure 5-4.

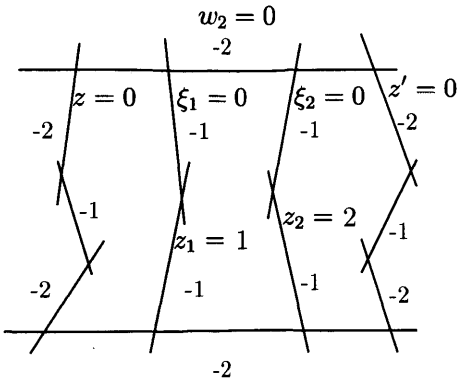

Figure 5-4: A semi-toric generalized dP_7, which is constructed by blowing up two points on the divisor $w = 0$ on the toric base given in Figure 5-3.

With a similar argument, after this blow up, f now takes the form of

$$\begin{aligned} f = {} & (z_1-1)^4(z_2-2)^4 + f_1(z_1-1)^3(z_2-2)^3 w_2 z + (z_1-1)^2(z_2-2)^2 w_2^2 z \sum_{i=0}^{2} f_{2,i} z^i \\ & + (z_1-1)(z_2-2) w_2^3 z^2 \sum_{i=0}^{2} f_{3,i} z^i + w_2^4 z^2 \sum_{i=0}^{4} f_{4,i} z^i + w_2^5 \xi_1 \xi_2 z^3 \sum_{i=0}^{2} f_{5,i} z^i \\ & + w_2^6 \xi_1^2 \xi_2^2 z^3 \sum_{i=0}^{2} f_{6,i} z^i + w_2^7 \xi_1^3 \xi_2^3 f_{7,4} z^4 + w_2^8 \xi_1^4 \xi_2^4 f_{8,4} z^4 \end{aligned} \tag{5.4.108}$$

g has the similar structure. Note that the shape of the Newton polytopes for f and g has become a rhombus from a triangle.

Finally, to get the gdP_{9st}, we need to blow up the points $z_1 = 1$, $\xi_1 = 0$ and $z_2 = 2$, $\xi_2 = 0$. After the blow-ups, we introduce new coordinates z_1', ξ_1', ζ_1 and z_2', ξ_2', ζ_2:

$$z_1 - 1 = (z_1' - 1)\zeta_1 \ , \ \xi_1 = \xi_1' \zeta_1 \ , \ (z_2 - 2) = (z_2' - 2)\zeta_2 \ , \ \xi_2 = \xi_2' \zeta_2 \tag{5.4.109}$$

We draw the corresponding equations for the divisors on gdP_{9st} in Figure 5-5.

The requirement that ζ_1 and ζ_2 vanish to at least degree 4 in f puts additional constraints on the coefficients in f. For example, the term $f_1(z_1-1)^3(z_2-2)^3 w_2 z$ in (5.4.108) has to vanish, since there is no way to have $\zeta_1^4 \zeta_2^4$ in that term. Similar things happen for g. After this analysis, we divide f by $\zeta_1^4 \zeta_2^4$ and g by $\zeta_1^6 \zeta_2^6$. The final

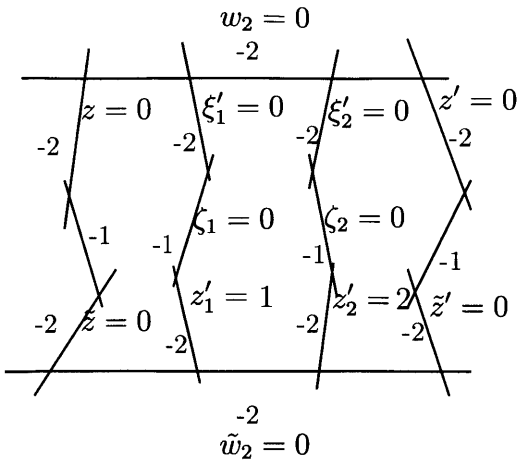

Figure 5-5: The local equations of divisors on gdP_{9st}.

expressions for f and g on gdP_{9st} are:

$$f = f_0(z_1'-1)^4(z_2'-2)^4 + f_1(z_1'-1)^3(z_2'-2)^3 w_2^2 z\xi_1'\xi_2' + f_2(z_1'-1)^2(z_2'-2)^2 w_2^4 z^2 \xi_1'^2\xi_2'^2 + f_3(z_1'-1)(z_2'-2)w_2^6 z^3\xi_1'^3\xi_2'^3 + f_4 w_2^8 z^4\xi_1'^4\xi_2'^4 \tag{5.4.110}$$

$$g = g_0(z_1'-1)^6(z_2'-2)^6 + g_1(z_1'-1)^5(z_2'-2)^5 w_2^2 z\xi_1'\xi_2' + g_2(z_1'-1)^4(z_2'-2)^4 w_2^4 z^2\xi_1'^2\xi_2'^2 + g_3(z_1'-1)^3(z_2'-2)^3 w_2^6 z^3\xi_1'^3\xi_2'^3 + g_4(z_1'-1)^2(z_2'-2)^2 w_2^8 z^4\xi_1'^4\xi_2'^4 + g_5(z_1'-1)(z_2'-2)w_2^{10} z^5\xi_1'^5\xi_2'^5 + g_6 w_2^{12} z^6\xi_1'^6\xi_2'^6 \tag{5.4.111}$$

We can restore the dependence on z' by multiplying $z'^{8-m-n-p}$ factors to each term $z_1'^m z_2'^n z^p$ for f, and multiplying $z'^{12-m-n-p}$ factors to each term $z_1'^m z_2'^n z^p$ for g. The final expressions of f and g are:

$$f = \sum_{i=0}^{4} f_i \eta^i \tilde{\eta}^{4-i} \ , \ g = \sum_{i=0}^{6} g_i \eta^i \tilde{\eta}^{6-i} \ , \ \eta \equiv w_2^2 z z' \xi_1'\xi_2', \tilde{\eta} \equiv \tilde{w}_2^2 (z_1'-1)(z_2'-2)\tilde{z}\tilde{z}'. \tag{5.4.112}$$

Indeed, the monomials in f and g lie on a line. Moreover, the number of monomials in f and g are respectively 5 and 7, which exactly saturates the bound (5.3.89).

Similarly, we can explicitly compute the form of f and g for the other semi-toric

bases in [97] with non-Higgsable U(1)s. Generally semi-toric bases are generated by blowing up Hirzebruch surfaces $\mathbb{F}_n$, in a way that the curves on it form chains between two specific curves D_0 and D_∞, which correspond to the $(-n)$-curve S and the $(+n)$-curve $\tilde{S}$ in the original $\mathbb{F}_n$. They are listed below, where n_0 and n_∞ denotes the self-intersection number of D_0 and D_∞. The chains are connected to D_0 at the front, and to D_∞ at the end. Here η, ξ and χ denote products of monomials, which are different from the notations in (5.4.112) and will not be specified.

We also list the rational sections in form of $(x, y, z) = (\lambda, \alpha, 1)$.

Mordell-Weil rank $r = 8$: $n_0 = -2, n_\infty = -2$, $T = 9$, $h^{1,1} = 19$, $h^{2,1} = 19$.

chain 1: $(-2, -1, -2)$

chain 2: $(-2, -1, -2)$

chain 3: $(-2, -1, -2)$

chain 4: $(-2, -1, -2)$

$$f = f_0\xi^4 + f_1\xi^3\eta + f_2\xi^2\eta^2 + f_3\xi\eta^3 + f_4\eta^4 \tag{5.4.113}$$

$$g = g_0\xi^6 + g_1\xi^5\eta + g_2\xi^4\eta^2 + g_3\xi^3\eta^3 + g_4\xi^2\eta^4 + g_5\xi\eta^5 + g_6\eta^6 \tag{5.4.114}$$

$$\lambda = \lambda_0\xi^2 + \lambda_1\xi\eta + \lambda_2\eta^2 \tag{5.4.115}$$

$$\alpha = \alpha_0\xi^3 + \alpha_1\xi^2\eta + \alpha_2\xi\eta^2 + \alpha_3\eta^3 \tag{5.4.116}$$

Mordell-Weil rank $r = 6$: $n_0 = -2, n_\infty = -6$, $T = 13$, $h^{1,1} = 35$, $h^{2,1} = 11$.

chain 1: $(-2, -1, -3, -1)$

chain 2: $(-2, -1, -3, -1)$

chain 3: $(-2, -1, -3, -1)$

chain 4: $(-2, -1, -3, -1)$

$$f = f_0\xi^2\eta^2 + f_1\xi\eta^3 + f_2\eta^4 \tag{5.4.117}$$

$$g = g_0\xi^4\eta^2 + g_1\xi^3\eta^3 + g_2\xi^2\eta^4 + g_3\xi\eta^5 + g_4\eta^6 \tag{5.4.118}$$

$$\lambda = \lambda_0\xi\eta + \lambda_1\eta^2 \tag{5.4.119}$$

$$\alpha = \alpha_0\xi^2\eta + \alpha_1\xi\eta^2 + \alpha_2\eta^3 \tag{5.4.120}$$

Mordell-Weil rank $r = 6$: $n_0 = -1, n_\infty = -2$, $T = 10$, $h^{1,1} = 24$, $h^{2,1} = 12$.

chain 1: $(-3, -1, -2, -2)$

chain 2: $(-3, -1, -2, -2)$

chain 3: $(-3, -1, -2, -2)$

$$f = f_0\xi^2\eta^2 + f_1\xi\eta^5 + f_2\eta^8 \tag{5.4.121}$$

$$g = g_0\xi^4 + g_1\xi^3\eta^3 + g_2\xi^2\eta^6 + g_3\xi^3\eta^9 + g_4\eta^{12} \tag{5.4.122}$$

$$\lambda = \lambda_0\xi\eta + \lambda_1\eta^4 \tag{5.4.123}$$

$$\alpha = \alpha_0\xi^2 + \alpha_1\xi\eta^3 + \alpha_2\eta^6 \tag{5.4.124}$$

Mordell-Weil rank $r = 5$: $n_0 = -1, n_\infty = -8$, $T = 16$, $h^{1,1} = 51$, $h^{2,1} = 3$.

chain 1: $(-3, -1, -2, -3, -2, -1)$

chain 2: $(-3, -1, -2, -3, -2, -1)$

chain 3: $(-3, -1, -2, -3, -2, -1)$

$$f = f_0\xi^2\eta^2\chi^2 + f_1\xi^5\eta\chi^3 \tag{5.4.125}$$

$$g = g_0\eta^4\chi^2 + g_1\xi^3\eta^3\chi^3 + g_2\xi^6\eta^2\chi^4 \tag{5.4.126}$$

$$\lambda = \lambda_0\xi\eta\chi \tag{5.4.127}$$

$$\alpha = \alpha_0\eta^2\chi + \alpha_1\xi^3\eta\chi^2 \tag{5.4.128}$$

Mordell-Weil rank $r = 4$: $n_0 = -2, n_\infty = -4$, $T = 13$, $h^{1,1} = 35$, $h^{2,1} = 11$.

chain 1: $(-2, -2, -1, -4, -1)$

chain 2: $(-2, -2, -1, -4, -1)$

chain 3: $(-2,-2,-1,-4,-1)$

$$f = f_0\xi^4 + f_1\xi^2\eta + f_2\eta^2 \tag{5.4.129}$$
$$g = g_0\xi^6 + g_1\xi^4\eta + g_2\xi^2\eta^2 + g_3\eta^3 \tag{5.4.130}$$

$$\lambda = \lambda_0\xi^2 + \lambda_1\eta \tag{5.4.131}$$
$$\alpha = \alpha_0\xi^3 + \alpha_1\xi\eta \tag{5.4.132}$$

Mordell-Weil rank $r = 4$: $n_0 = -6, n_\infty = -6$, $T = 17$, $h^{1,1} = 51$, $h^{2,1} = 3$.

chain 1: $(-1,-3,-1,-3,-1)$

chain 2: $(-1,-3,-1,-3,-1)$

chain 3: $(-1,-3,-1,-3,-1)$

chain 4: $(-1,-3,-1,-3,-1)$

$$f = f_0\xi^2\eta^2 \tag{5.4.133}$$
$$g = g_0\xi^4\eta^2 + g_1\xi^3\eta^3 + g_2\xi^2\eta^4 \tag{5.4.134}$$

$$\lambda = \lambda_1\xi\eta \tag{5.4.135}$$
$$\alpha = \alpha_0\xi^2\eta + \alpha_1\xi\eta^2 \tag{5.4.136}$$

Mordell-Weil rank $r = 4$: $n_0 = -1, n_\infty = -5$, $T = 14$, $h^{1,1} = 40$, $h^{2,1} = 4$.

chain 1: $(-2,-1,-3,-1)$

chain 2: $(-4,-1,-2,-2,-3,-1)$

chain 3: $(-4,-1,-2,-2,-3,-1)$

$$f = f_0\xi^4 + f_1\xi^2\eta^2 \tag{5.4.137}$$
$$g = g_0\xi^6 + g_1\xi^4\eta^2 \tag{5.4.138}$$

$$\lambda = \lambda_0\xi^2 \tag{5.4.139}$$

$$\alpha = \alpha_0\xi^3 \text{ or } \xi^2\eta \tag{5.4.140}$$

Mordell-Weil rank $r = 4$: $n_0 = -1, n_\infty = -2$, $T = 11$, $h^{1,1} = 25$, $h^{2,1} = 13$.

chain 1: $(-2, -1, -2)$

chain 2: $(-4, -1, -2, -2, -2)$

chain 3: $(-4, -1, -2, -2, -2)$

$$f = f_0\xi^4 + f_1\xi^2\eta^2 + f_2\eta^4 \tag{5.4.141}$$

$$g = g_0\xi^6 + g_1\xi^4\eta^2 + g_2\xi^2\eta^4 + g_3\eta^6 \tag{5.4.142}$$

$$\lambda = \lambda_0\xi^2 + \lambda_1\eta^2 \tag{5.4.143}$$

$$\alpha = \alpha_0\xi^3 + \alpha_1\xi\eta^2 \text{ or } \alpha_0\xi^2\eta + \alpha_1\eta^3 \tag{5.4.144}$$

Mordell-Weil rank $r = 3$: $n_0 = -4, n_\infty = -8$, $T = 19$, $h^{1,1} = 62$, $h^{2,1} = 2$.

chain 1: $(-1, -4, -1, -2, -3, -2, -1)$

chain 2: $(-1, -4, -1, -2, -3, -2, -1)$

chain 3: $(-1, -4, -1, -2, -3, -2, -1)$

$$f = f_0\xi^2 + f_1\xi\eta^2 \tag{5.4.145}$$

$$g = g_0\xi^3 + g_1\xi^2\eta^2 \tag{5.4.146}$$

$$\lambda = \lambda_0\xi \tag{5.4.147}$$

$$\alpha = \alpha_0\xi\eta \tag{5.4.148}$$

Mordell-Weil rank $r = 2$: $n_0 = -2, n_\infty = -6$, $T = 18$, $h^{1,1} = 46$, $h^{2,1} = 10$.

chain 1: $(-2, -1, -3, -1)$

chain 2: $(-2, -2, -2, -1, -6, -1, -3, -1)$

chain 3: $(-2,-2,-2,-1,-6,-1,-3,-1)$

$$f = f_0\xi^4 + f_1\xi^2\eta \tag{5.4.149}$$
$$g = g_0\xi^6 + g_1\xi^4\eta + g_2\xi^2\eta^2 \tag{5.4.150}$$

$$\lambda = \lambda_0\xi^2 \tag{5.4.151}$$
$$\alpha = \alpha_0\xi^3 + \alpha_1\xi\eta \tag{5.4.152}$$

Mordell-Weil rank $r = 2$: $n_0 = -5, n_\infty = -6$, $T = 21$, $h^{1,1} = 61$, $h^{2,1} = 1$.

chain 1: $(-1,-3,-1,-3,-1)$

chain 2: $(-1,-3,-2,-2,-1,-6,-1,-3,-1)$

chain 3: $(-1,-3,-2,-2,-1,-6,-1,-3,-1)$

$$f = f_0\xi^2\eta^2 \tag{5.4.153}$$
$$g = g_0\xi^2 + g_1\xi^4\eta^6 \tag{5.4.154}$$

$$\lambda = \lambda_0\eta\xi \tag{5.4.155}$$
$$\alpha = \alpha_0\xi + \alpha_1\eta^2\xi^3 \tag{5.4.156}$$

Mordell-Weil rank $r = 2$: $n_0 = -1, n_\infty = -2$, $T = 12$, $h^{1,1} = 24$, $h^{2,1} = 12$.

chain 1: $(-2,-1,-2)$

chain 2: $(-3,-1,-2,-2)$

chain 3: $(-6,-1,-2,-2,-2,-2,-2)$

$$f = f_0\xi\eta + f_1\eta^4 \tag{5.4.157}$$
$$g = g_0\xi^2 + g_1\xi\eta^3 + g_2\eta^6 \tag{5.4.158}$$

$$\lambda = \lambda_0 \eta^2 \tag{5.4.159}$$

$$\alpha = \alpha_0 \xi + \alpha_1 \eta^3 \tag{5.4.160}$$

Mordell-Weil rank $r = 1$: $n_0 = -2, n_\infty = -3$, $T = 15$, $h^{1,1} = 34$, $h^{2,1} = 10$.

chain 1: $(-2, -1, -2)$

chain 2: $(-2, -2, -1, -4, -1)$

chain 3: $(-2, -2, -2, -2, -2, -1, -8, -1, -2)$

$$f = f_0 \xi \eta + f_1 \eta^4 \tag{5.4.161}$$

$$g = g_0 \xi \eta^3 + g_1 \eta^6 \tag{5.4.162}$$

$$\lambda = \lambda_0 \eta^2 \tag{5.4.163}$$

$$\alpha = \alpha_0 \eta^3 \tag{5.4.164}$$

Chapter 6

Conclusions and outlook

Through this thesis, we have constructed a grand picture of the base classification program of 6D and 4D F-theory. For the base surfaces used in 6D F-theory, one can systematically blow up $\mathbb{P}^2$ and $\mathbb{F}_n$ in all the possible ways. For the base threefolds, the set of starting points is not known. Nonetheless, we have still managed to probe a subset of toric threefolds and generated a large number of sample bases. We will summarize the findings and discuss their physical implications and future directions.

Classification of base surfaces While the classification of toric and semi-toric base surfaces in 6D F-theory has been finished, the classification of general non-toric surfaces is still incomplete. We have constructed a finite algorithm in Section 3.3.1 to systematically construct all the base surfaces from blowing up $\mathbb{P}^2$ and $\mathbb{F}_n$, but it may not cover all the examples. A crucial geometric subtlety is the distinction between three lines intersecting at a single point and three lines intersecting at three points, see Figure 3-6. In an example of Pappus's theorem, see Figure 3-7, the three lines are forced to intersect at a single point. There is not a criterion to tell when does this happen for a general geometric configuration. If we see three lines intersect each other in the computation of intersection numbers, then this ambiguity will always arise and we get two different base surfaces with the same intersection and cone structure. The physics of 6D F-theory on these two base surfaces are different. Although the particle spectra are identical in the non-Higgsable phase of the 6D low energy supergravity theory, if we tune three SU(2) gauge groups on these three lines, the matter spectrum

will be different. In the case of three lines intersecting at a single point, there will be a rank-3 symmetric tensor representation **4** of SU(2) localized at this point. While in the other case, there will only be fundamental representations **2** at the intersection points. The tensionless string transition, which is the blow up of the base, also leads to different bases and low energy physics for the two cases in Figure 3-6. Other unresolved issues include the problem of infinite generators of the effective cone and the "special blow ups" of cubic curve at a double point to get a (-2)-curve.

Apart from these subtleties, we have still managed to completely classify all the bases with $h^{1,1}(S) \leq 7$ and the bases giving rise to elliptic Calabi-Yau threefolds with $h^{2,1} \geq 150$. In these regimes, it seems that the total number of non-toric bases are on the same magnitude of the total number of toric bases. For the entire set of base surfaces, we cannot give an estimation on the total number of bases, although it is known that this number is finite[68].

The set of base threefolds

Because of our ignorance about the general properties of base threefolds that support an elliptic Calabi-Yau fourfold, we restrict ourselves to the class of rational threefolds. Just as in the classification program of the base surfaces, we start from the subset of toric threefolds as a first step. It turns out that this subset is already extremely huge and it has rich structure. To obtain a clearer picture, we have separated the allowed bases in 4D F-theory into two classes: the resolvable bases and the "good" bases. The resolvable bases have codimension-two (4,6) singularities, which could give rise to 4D $\mathcal{N} = 1$ SCFTs with 4D conformal matter in parallel to the 6D conformal matter in [39]. The good bases do not have codimension-two (4,6) singularities, and should generally describe a 4D $\mathcal{N} = 1$ supergravity model. For the good bases, we still allow the appearance of codimension-three (4,6) singularities, or points where (f, g) vanish to at least order $(4, 6)$ but not as high as $(8, 12)$. In this case, we cannot blow up this point while not changing the number of complex structure moduli or $h^{3,1}$ of the elliptic Calabi-Yau fourfold. The physical implications of these codimension-three points are not entirely clear. Although there could be non-flat fibers after the resolution[94], they may not cause any problem in the 4D

effective theory because of the G_4 flux or other quantum effects[6]. Similarly, for the cases of resolvable bases with codimension-two (4,6) singularities, it is also not clear if the superconformal symmetry is actually unbroken. We will leave these important physical questions to future research.

From our random walk and random blow up approaches, we can see the global set of resolvable bases form a huge connected "ocean" while the good bases are isolated "islands" in this ocean. A big island of good bases is the set of good bases connected to $\mathbb{P}^3$ via a sequence of blow up/downs that only pass through good bases. If we take the restriction where the good bases mean the strictly good toric bases without any (4,6) curves, then we have estimated the total number of topologically distinct bases in this subset $\mathcal{C}$ to be $10^{48\pm2}$. The bases in $\mathcal{C}$ generally have no or a small number of gauge groups with high rank, such as E_6 and E_7. However, a local pair SU(3)$\times$ SU(2) is common on a typical base in $\mathcal{C}$. It is not clear how to construct an actual standard model particle spectrum on these bases using a non-GUT construction. The problem comes from the tuning of U(1) on it, since a general tuning in Morrison-Park form [102] may bring in codimension-two (4,6) singularity. This should be investigated in a future project.

If we allow the appearance of non-toric (4,6) curves on a divisor that supports an E_8 gauge group, then we can have many more examples for toric good bases. Among these good bases, there are the end point bases where any additional (toric) blow up will lead to codimension-one (4,6) singularity. It seems that the $h^{1,1}(B)$ of the end point bases are concentrated at specific values, and the generic elliptic Calabi-Yau fourfold over them have Hodge numbers that are mirrors of some simple Calabi-Yau fourfolds. This may imply that the set of Hodge numbers for Calabi-Yau fourfolds are highly constrained. The physical implication of this finding is not clear, since the mirror symmetry of Calabi-Yau manifolds in the F-theory paradigm does not correspond to any physical duality. Apart from the end point bases, there are also intermediate bases which can still be blown up. However, they are more isolated since we will generally get a resolvable base with toric (4,6) curves if they are randomly blow up or down once.

Unlike the classification of complex surfaces, we still have not obtained a complete list of smooth starting point threefold bases, even for the toric case. From the discovery of exotic starting points, it seems that there are a large number of resolvable bases with random structure that cannot be contracted to another smooth base. If we really want to get a precise estimation of the total number of resolvable toric bases, we need to count the number of these exotic starting points and correct the underestimation in Section 4.4.3. The current estimation $N_{\text{resolvable}} \sim 10^{3,000}$ seems to be an imprecise lower bound. Similarly, we expect the calculated total number of good bases $N_{\text{good}} \sim 10^{250}$ has a large error which cannot even be estimated.

Of course, we should finally investigate the set of non-toric rational bases as well. Since the total number of toric bases is not under control, it is even harder to say anything about the non-toric bases. Nonetheless, it will be good if we can develop some geometric tools and algorithms in parallel to the non-toric surface project.

Even more generally, we have not tried to relax the smoothness and compactness conditions. As suggested by the minimal model program of complex threefolds, adding singular threefolds can improve the connectivity of this graph. Physically, singular bases can describe an SCFT coupled to gravity in the 6D F-theory setups[38]. However, this has not been discussed for general singular 2D bases or any 3D bases. For non-compact 2D bases, they could describe an SCFT decoupled to gravity if the base is contractable[77]. It would be interesting if a similar classfication program of non-compact threefold bases can be carried over to classify 4D $\mathcal{N} = 1$ SCFTs.

Flux vacua and model building

Now we want to ask how many of these 4D F-theory models contain a subsector of our standard model, if any of them does. To get a quantative result, we need to enumerate the flux vacua associated to a single geometry and compute the particle spectrum using (4.1.25) and other formula in [15, 19]. We also need to stablize the K$\acute{\text{i}}$ahler and complex structure moduli to fix the volume of different cycles of the compact manifold, which correspond to energy scales in the 4D effective theory. Since the F-term conditions (4.1.14) and (4.1.15) contain one more equation than the number of complex structure moduli, we may expect that the supersymmetry is

broken in the moduli stablization process. This could actually be good for the model building because of the absence of low energy supersymmetry at LHC, but there have not been many detailed constructions following this possibility. It is also interesting to construct cosmology models under this setup.

The geometric structure is universal on many good bases we found, for example, the end point bases, many intermediate bases and the base $B_{\max}$ which supports the elliptic Calabi-Yau fourfold $\mathcal{M}_{\max}$ with the largest ensemble of flux vacua. The non-Higgsable gauge groups are mostly SU(2), G_2, F_4 and E_8, and it is almost impossible to tune the Weierstrass model to get a bigger gauge group without introducing codimension-one or two (4,6) singularities. However, it is universally hard to construct the standard model subsector on all these geometries. Since the tuning of SU(5) is impossible, the only way to get an SU(5) GUT gauge group is by breaking the non-Higgsable E_8 with vertical G_4 flux. However, the conventional local SU(5) constructions[15, 16] do not work as there is no local matter curve on a divisor with E_8 gauge group. We do not know yet how to produce the desired chirality and Yukawa coupling in the absence of matter curve. Another route is to use a non-GUT type construction with a local SU(2)$\times$ SU(3) or breaking the SU(2)$\times G_2$. It is hard to get a U(1) gauge group and the correct U(1) charges.

In the worst case scenario, it may be possible that the vast geometric landscape we have discovered is unfavored and that nature chose an alternative or simpler construction. Even if this is the case, we can still get some hints about the early universe geometric transition process. Another type of questions to ask is:

Despite that we get a lot of solutions that do not describe our world, how many of these solutions describe a physical universe with stars, large scale structure or intellegent life.

For example, the QCD gauge group may be replaced by a G_2, but the confinement behavior still exists and we can still get a similar chemistry if the masses of quarks have large enough gaps.

Swampland and string universality

As an potential application of the F-theory geometric classification program, we

can find supergravity models which seem to be self-consistent but do not have any F-theory/string theory realization. These low energy models are currently put into the "swampland" where we need to either:

(1) find a UV completion;

(2) find a hidden inconsistency in the low energy theory;

(3) decides that the constraint is actually a UV constraint from string theory that cannot be seen in the low energy theory.

The swampland problems involving U(1) gauge groups are particularly interesting. Recently, it was discovered that there exists an anomaly free 6D (1,0) supergravity spectrum with infinitely high U(1) charges[122]. If we take $T = 0$, a=$\{3\}$, $b_{11} = p^2 + pq + q^2$, and the matter spectrum of the single U(1) to be $54 \cdot (\pm\mathbf{p}) + 54 \cdot (\pm\mathbf{q}) + 54 \cdot (\pm\mathbf{p} + \mathbf{q})$ for any $p, q \in \mathbb{Z}$, then the anomaly cancellation equations (3.1.11, 3.1.12) are satisfied. From the finiteness of elliptic Calabi-Yau threefolds, apparently not all of these U(1) charged spectrum can be realized in 6D F-theory.

Another type of swampland problem or quantum gravity constraint problem, the weak gravity conjecture, has attracted a lot of attention recently[8]. It states that gravity is always weaker than the electric magnetic force. More precisely, in the weakest version of weak gravity conjecture, there always exists a U(1) charged particle with mass $m \leq qm_{pl}$. The initial argument is based on the thought experiment that a non-BPS extremal black hole must be able to decay into a smaller black hole. If the weak gravity conjecture is not satisfied, then this decay is impossible. Various versions of weak gravity have been tested on a number of string models[80, 79] and applied to axion inflation cosmology[116, 78, 28, 12, 75]. It was also argued that if a stronger weak gravity conjecture holds: the equality $m = qm_{pl}$ is satisfied if and only if the theory is supersymmetric and such a particle is BPS, then the AdS/CFT correspondence cannot be applied to a non-supersymmetric theory without higher spin particles[111].

Our example of non-Higgsable U(1) models in Chapter 5 provide a test set for various different versions of weak gravity conjecture. It is uncommon for a string theory model to have a U(1) gauge group but no massless charged matter. To compute the

mass spectrum of massive charged matter, we need to explicitly compute the moduli stabilization problem for different G_4 flux. We expect that some of the weak gravity conjectures may be ruled out, although the detailed calculation can be technically hard.

Apart from the swampland problem for supergravity, we can also ask the similar question for non-gravitational quantum field theory:

can every superconformal/supersymmetric field theory in a certain dimension be realized in a string/F-theory setup?

There is not a good a priori reason for this to hold, since superconformal field theories do not need any UV completion. However, we have seen that all the known 6D (2,0) SCFTs can be realized by compactifying type IIB superstring theory on a K3 surface with ADE type singularity. One may ask this question for other classes of theories, such as 6D (1,0), 4D $\mathcal{N} = 2$ and 4D $N = 1$ SCFTs as well [39, 76, 77].

In general, it is extremely hard to prove any string universality result, since we do not know what is the global set of "theories" of a particular type. However, we will learn the structure of quantum field theory/quantum gravity during the pursuit of this principle.

Appendix A

Notation for supersymmetry

In this appendix, we briefly explain the supersymmetry related terminologies used in the thesis. For more details, one can read [58] and the appendix of [114], Volume 2.

The Clifford algebra in D real space-time dimensions are generated by d-dimensional complex matrices $\gamma^\mu (\mu = 0, \ldots, D-1)$ that satisfies

$$\gamma^\mu \gamma^\nu + \gamma^\nu \gamma^\mu = 2\eta^{\mu\nu} I, \tag{A.0.1}$$

where $\eta^{\mu\nu}$ is the Minkowski metric in D dimensions and I is the identity matrix.

The minimal dimension of the γ matrices is $d = 2^{\lfloor D/2 \rfloor}$, hence the untruncated *Dirac spinors* in D dimensions have $d = 2^{\lfloor D/2 \rfloor}$ complex components. The Clifford algebra acts on a Dirac spinor, and the commutator

$$\Sigma^{\mu\nu} = \frac{1}{4}[\gamma^\mu, \gamma^\nu] \tag{A.0.2}$$

generates the Lorentz rotation.

For some D, the spinor representation can be truncated to shorter representations. For even $D = 2m$, the matrix

$$\gamma_{D+1} = (-i)^{m+1} \gamma_0 \gamma_1 \cdots \gamma_{D-1} \tag{A.0.3}$$

can take the following block diagonal form:

$$\gamma_{D+1} = \begin{pmatrix} I & 0 \\ 0 & -I \end{pmatrix}. \tag{A.0.4}$$

Hence we can introduce projection operators

$$P_L = \frac{1+\gamma_{D+1}}{2}\ ,\ P_R = \frac{1-\gamma_{D+1}}{2} \tag{A.0.5}$$

on the Dirac spinors to project them into left-handed and right-handed *Weyl spinors* with real dimension 2^m.

For dimensions $D \equiv 0, 1, 2, 3, 4 (\text{mod } 8)$, we can take the Dirac spinor to be real, which leads to a *Majorana spinor* with real dimension $2^{\lfloor D/2 \rfloor}$ that satisfies

$$\psi = \psi^C \tag{A.0.6}$$

where ψ^C is the charge conjugation acting on a spinor.

In dimensions $D \equiv 2 (\text{mod } 8)$, the Weyl and Majorana conditions are compatible with each other, and we can define a *Majorana-Weyl spinor* that is both chiral and real, with real dimension $2^{D/2-1}$.

In dimensions $D \equiv 5, 6, 7 (\text{mod } 8)$, we cannot reduce the dimension of spinor representation by the Majorana condition, but we can introduce a *symplectic Majorana* condition that applies on an even number of spinors $\psi^i (i = 1, \ldots, 2k)$:

$$\psi^i = \epsilon^{ij} (\psi^j)^C. \tag{A.0.7}$$

ϵ^{ij} is the antisymmetric symplectic matrix with block diagonal form

$$\epsilon = \begin{pmatrix} 0 & -I \\ I & 0 \end{pmatrix}. \tag{A.0.8}$$

In dimensions $D \equiv 6 (\text{mod } 8)$, this symplectic Majorana condition is compatible with

D	min. rep.	min. real components
2	MW	1
3	M	2
4	M or W	4
5	D(S)	8
6	W(SW)	8
7	D(S)	16
8	M or W	16
9	M	16
10	MW	16
11	M	32

Table A.1: The minimal spinor representations in dimensions $D = 2 \sim 11$. M, W, MW, D, S, SW denotes Majorana, Weyl, Majorana-Weyl, Dirac, symplectic Majorana and symplectic Majorana-Weyl representations respectively. For the cases $D = 5, 6, 7$, we can choose to impose symplectic Majorana condition. Although it will not reduce the number of spinor components, it is useful for understanding the supermultiplet structure.

the Weyl condition.

We summarize the minimal number of real components and the spinor representations for $D = 2 \sim 11$ in Table A.1

The supersymmetry algebra is an extension of Poincaré algebra including of a number of fermionic generators $Q^i_\alpha (i = 1, \ldots, \mathcal{N})$. These Q^i_αs are $\mathcal{N}$ copies of *supercharges*, which transforms in the minimal spinor representation in Table A.1 with spinor indices α. In $D = 0, 1, 3 (\text{mod } 4)$, we always use Majorana or Dirac spinors, and use a single integer $\mathcal{N}$ to label the amount of supersymmetry in the theory. In $D = 2 (\text{mod } 4)$, we use Weyl or Majorana-Weyl spinors, and use two integers $(\mathcal{N}_L, \mathcal{N}_R)$ to count the copies of left-handed and right-handed supercharges.

For example, theories with 32 supercharges include 11D $\mathcal{N} = 1$, 10D $(1, 1)$, $(2, 0)$, 9D $\mathcal{N} = 2$ and 4D $\mathcal{N} = 8$. 16 supercharges theories include 10D $(1, 0)$, 8D $\mathcal{N} = 1$, 6D $(2, 0)$, 5D $\mathcal{N} = 2$ and 4D $\mathcal{N} = 4$. 8 supercharges theories include 6D (1,0), 5D $\mathcal{N} = 1$, 4D $\mathcal{N} = 2$ and 3D $\mathcal{N} = 4$. 4 supercharges theories include 4D $\mathcal{N} = 1$ and 3D $\mathcal{N} = 2$.

The representations of supersymmetry algebra are usually called supermultiplets, which are combinations of bosonic and fermionic fields that transform into each other

with the action of supercharges. For massless particles with energy-momentum vector

$$p^\mu = (E, 0, \ldots, 0, E), \tag{A.0.9}$$

the states are labeled by the representation of the little group $\mathrm{SO}(D-2)$, which is the subgroup of the Lorentz group leaving p^μ invariant:

$$R(\mathrm{SO}(D-2)) : (h_1, \ldots, h_{\lfloor D/2 \rfloor - 1}). \tag{A.0.10}$$

The usual terminology of "spin" often corresponds to the sum of these h_is.

The supermultiplets are constructed by starting with a state with representation $(h_1, \ldots, h_{\lfloor D/2 \rfloor - 1})$, and then acting supercharges $Q_\alpha^{\dagger i}$ on this state to reduce the helicity h_α by $\frac{1}{2}$ (in a proper spinor representation). Since $\{Q_\alpha^{\dagger i}, Q_\beta^{\dagger j}\} = 0$, this procedure will finally ends.

For example, in $D = 4$, there is only a single quantum number for the representations of the little group $\mathrm{SO}(2)$, which we called spin or helicity in the massless case. If $\mathcal{N} = 1$, then this process will always terminate after one step. We have the following supermultiplets:

- Supergravity multiplet with a spin-2 graviton $g_{\mu\nu}$ and a spin-3/2 gravitino ψ_α^μ
- Rarita-Schwinger multiplet with a spin-3/2 rarita-schwinger field ψ_α^μ and a spin-1 vector field A_μ
- Vector multiplet with a spin-1 gauge boson A_μ and a spin-1/2 gaugino χ_α
- Chiral multiplet with a spin-1/2 spinor ψ_α and a spin-0 complex scalar ϕ

For $\mathcal{N} = 2$, we have

- Supergravity multiplet with a spin-2 graviton, two gravitinos and a spin-1 vector field
- Vector multiplet with a spin-1 gauge boson, two spin-1/2 gauginos and a spin-0 scalar

- Hypermultiplet with a spin-1/2 spinor and two spin-0 complex scalars

For 5D $\mathcal{N} = 2$ theory, we still only need one quantum number to label the representation under the little group SO(3). The supermultiplets are the same as the 4D $\mathcal{N} = 2$ theory.

For 6D $(1, 0)$ theory, one should think that there exists two copies of left-handed supercharges because of the existence of symplectic Majorana-Weyl spinor representation. Hence the action of supercharges $Q_\alpha^{\dagger i}$ will only end after two steps despite the minimal supersymmetry. We need to quantum numbers (h_1, h_2) to label the states under the little group SO(4), and the action of $Q_\alpha^{\dagger i}$ reduces h_1 by 1/2. The supermultiplets are

- Supergravity multiplet with a (1,1) graviton, a gravitino in $(1/2, 1)$ and a tensor field in representation $(0, 1)$

- Tensor multiplet with a rank-2 antisymmetric tensor in representation $(1, 0)$, a spinor field in $(\frac{1}{2}, 0)$ and a complex scalar field in (0,0)

- Vector multiplet with a gauge boson in $(\frac{1}{2}, \frac{1}{2})$ and a gaugino in $(0, \frac{1}{2})$.

- Hypermultiplet with a left-handed spinor in $(\frac{1}{2}, 0)$ and two complex scalars in $(0, 0)$

In $D = 11$, the only supermultiplet is the self-CPT-conjugate supergravity multiplet. In $D > 11$, every supermultiplet will contain a higher spin state, hence we cannot have a supergravity theory in 12 or more space-time dimensions respecting the super Poincaré algebra.

The supersymmetry algebra can also be extended to the superconformal algebra including the bosonic dilation D, special conformal transformation K^μ and another set of fermionic generators S^μ. A quantum field theory with superconformal symmetry and no supergravity multiplets is called superconformal field theory (SCFT). The scaling invariance can be broken by giving scalar fields a non-zero vacuum expectation value (vev).

For 6D (1,0) SCFT, if the scalar in the tensor multiplet has a non-zero vev, then the superconformal symmetry is broken and the theory is deformed into the "tensor branch" gauge theory. As we have mentioned in Section3.1, this corresponds to blowing up a (4,6)-point on the base in the F-theory picture. On the other hand, if the scalar in the hypermultiplet has a non-zero vev, then the theory is deformed into the "Higgs branch".

In 4D or 5D $\mathcal{N} = 2$ SCFT, there is no tensor branch since the absence of tensor multiplet. However, one can give the scalar in the vector multiplet a non-zero vev, and deform the theory into the "Coulomb branch". This deformation will break the non-Abelian gauge group into the Abelian subgroup. Such a Coulomb branch does not exist for 6D (1,0) SCFT. The Higgs branches are present for all these cases.

Finally, for 4D $\mathcal{N} = 1$ SCFT, only the Higgs branch exists. This fact makes 4D $\mathcal{N} = 1$ the hardest to study among all the SCFTs in dimension $D \geq 4$.

Bibliography

[1] Allan Adams, Washington Taylor, and Oliver DeWolfe. String universality in ten dimensions. *Physical review letters*, 105(7):071601, 2010.

[2] Ofer Aharony, Amihay Hanany, and Barak Kol. Webs of (p, q) 5-branes, five dimensional field theories and grid diagrams. *Journal of High Energy Physics*, 1998(01):002, 1998.

[3] G. Aldazabal, L. E. Ibanez, F. Quevedo, and A. M. Uranga. D-branes at singularities: A bottom-up approach to the string embedding of the standard model. *Journal of High Energy Physics*, 08:002, 2000.

[4] Luis Alvarez-Gaume and Edward Witten. Gravitational anomalies. *Nuclear Physics B*, 234(2):269–330, 1984.

[5] Lara B Anderson, James Gray, Nikhil Raghuram, and Washington Taylor. Matter in transition. *Journal of High Energy Physics*, 2016(4):80, 2016.

[6] Fabio Apruzzi, Jonathan J Heckman, David R Morrison, and Luigi Tizzano. 4D gauge theories with conformal matter. *arXiv preprint arXiv:1803.00582*, 2018.

[7] Nima Arkani-Hamed, Luboš Motl, Alberto Nicolis, and Cumrun Vafa. The string landscape, black holes and gravity as the weakest force. *Journal of High Energy Physics*, 2007(06):060, 2007.

[8] Nima Arkani-Hamed, Luboš Motl, Alberto Nicolis, and Cumrun Vafa. The string landscape, black holes and gravity as the weakest force. *Journal of High Energy Physics*, 2007(06):060, 2007.

[9] Philipp Arras, Antonella Grassi, and Timo Weigand. Terminal singularities, Milnor numbers, and matter in F-theory. *Journal of Geometry and Physics*, 123:71–97, 2018.

[10] Michela Artebani and Antonio Laface. Cox rings of surfaces and the anticanonical Iitaka dimension. *Advances in Mathematics*, 226(6):5252–5267, 2011.

[11] Sujay K Ashok and Michael R Douglas. Counting flux vacua. *Journal of High Energy Physics*, 2004(01):060, 2004.

[12] Thomas C Bachlechner, Cody Long, and Liam McAllister. Planckian axions and the weak gravity conjecture. *Journal of High Energy Physics*, 2016(1):91, 2016.

[13] W. Barth and Ch. Peters. Automorphisms of Enriques surfaces. *Inventiones mathematicae*, 73(3):383–411, 1983.

[14] Victor V Batyrev. Dual polyhedra and mirror symmetry for Calabi-Yau hypersurfaces in toric varieties. *arXiv preprint alg-geom/9310003*, 1993.

[15] Chris Beasley, Jonathan J Heckman, and Cumrun Vafa. GUTs and exceptional branes in F-theory-I. *Journal of High Energy Physics*, 2009(01):058, 2009.

[16] Chris Beasley, Jonathan J Heckman, and Cumrun Vafa. GUTs and exceptional branes in F-theory-II. Experimental predictions. *Journal of High Energy Physics*, 2009(01):059, 2009.

[17] Katrin Becker, Melanie Becker, and John H. Schwarz. *String theory and M-theory: A modern introduction.* Cambridge University Press, 2006.

[18] David S Berman, Chris DA Blair, Emanuel Malek, and Felix J Rudolph. An action for F-theory: exceptional field theory. *Classical and Quantum Gravity*, 33(19):195009, 2016.

[19] Martin Bies, Christoph Mayrhofer, Christian Pehle, and Timo Weigand. Chow groups, Deligne cohomology and massless matter in F-theory. *arXiv preprint arXiv:1402.5144*, 2014.

[20] Martin Bies, Christoph Mayrhofer, and Timo Weigand. Algebraic cycles and local anomalies in F-theory. *Journal of High Energy Physics*, 2017(11):100, 2017.

[21] Julie D Blum and Keith R Dienes. Duality without supersymmetry: the case of the SO (16)× SO (16) string. *Physics Letters B*, 414(3-4):260–268, 1997.

[22] Andreas P Braun and Taizan Watari. Distribution of the number of generations in flux compactifications. *Physical Review D*, 90(12):121901, 2014.

[23] Andreas P Braun and Taizan Watari. The vertical, the horizontal and the rest: anatomy of the middle cohomology of Calabi-Yau fourfolds and F-theory applications. *Journal of High Energy Physics*, 2015(1):47, 2015.

[24] AP Braun, Arthur Hebecker, and H Triendl. D7-brane motion from M-theory cycles and obstructions in the weak coupling limit. *Nuclear physics B*, 800(1-2):298–329, 2008.

[25] V. Braun, Y.H. He, B.A. Ovrut, and T. Pantev. The exact MSSM spectrum from string theory. *Journal of High Energy Physics*, 05:043, 2006.

[26] Volker Braun, Thomas W Grimm, and Jan Keitel. Geometric engineering in toric F-theory and GUTs with U(1) gauge factors. *Journal of High Energy Physics*, 2013(12):69, 2013.

[27] T Daniel Brennan, Federico Carta, and Cumrun Vafa. The String Landscape, the Swampland, and the Missing Corner. *arXiv preprint arXiv:1711.00864*, 2017.

[28] Jon Brown, William Cottrell, Gary Shiu, and Pablo Soler. On axionic field ranges, loopholes and the weak gravity conjecture. *Journal of High Energy Physics*, 2016(4):17, 2016.

[29] W. Buchmller, Hamaguchi, O. K., Lebedev, and M. Ratz. Supersymmetric standard model from the heterotic string. *Physical review letters*, 96(12):121602, 2006.

[30] Philip Candelas, Eugene Perevalov, and Govindan Rajesh. Toric geometry and enhanced gauge symmetry of F-theory/heterotic vacua. *Nuclear physics B*, 507(1-2):445–474, 1997.

[31] Jonathan Carifio, William J Cunningham, James Halverson, Dmitri Krioukov, Cody Long, and Brent D Nelson. Vacuum selection from cosmology on networks of string geometries. *arXiv preprint arXiv:1711.06685*, 2017.

[32] Sidney Coleman and Jeffrey Mandula. All possible symmetries of the S matrix. *Physical Review*, 159(5):1251, 1967.

[33] David A Cox. The homogeneous coordinate ring of a toric variety. *arXiv preprint alg-geom/9210008*, 1995.

[34] David A Cox, John B Little, and Henry K Schenck. *Toric varieties*. American Mathematical Soc., 2011.

[35] Mirjam Cvetič, Gary Shiu, and Angel M. Uranga. Three-family supersymmetric standardlike models from intersecting brane worlds. *Physical Review Letters*, 87(20):201801, 2001.

[36] Vladimir Ivanovich Danilov. The geometry of toric varieties. *Russian Mathematical Surveys*, 33(2):97–154, 1978.

[37] Keshav Dasgupta, Govindan Rajesh, and Savdeep Sethi. M-theory, orientifolds and G-flux. *Journal of High Energy Physics*, 1999(08):023, 1999.

[38] Michele Del Zotto, Jonathan J Heckman, David R Morrison, and Daniel S Park. 6D SCFTs and gravity. *Journal of High Energy Physics*, 2015(6):158, 2015.

[39] Michele Del Zotto, Jonathan J Heckman, Alessandro Tomasiello, and Cumrun Vafa. 6D conformal matter. *Journal of High Energy Physics*, 2015(2):54, 2015.

[40] Frederik Denef. Les Houches lectures on constructing string vacua. *arXiv preprint arXiv:0803.1194*, 2008.

[41] Frederik Denef and Michael R Douglas. Distributions of flux vacua. *Journal of High Energy Physics*, 2004(05):072, 2004.

[42] Ulrich Derenthal. *Geometry of universal torsors.* PhD thesis, PhD thesis, 2006.

[43] Ulrich Derenthal. Singular Del Pezzo surfaces whose universal torsors are hypersurfaces. *Proceedings of the London Mathematical Society*, 108(3):638–681, 2014.

[44] Gabriele Di Cerbo and Roberto Svaldi. Log birational boundedness of Calabi-Yau pairs. *arXiv preprint arXiv:1608.02997*, 2016.

[45] Keith R Dienes. Statistics on the heterotic landscape: Gauge groups and cosmological constants of four-dimensional heterotic strings. *Physical Review D*, 73(10):106010, 2006.

[46] Ron Donagi, Martijn Wijnholt, et al. Breaking GUT groups in F-theory. *Advances in Theoretical and Mathematical Physics*, 15(6):1523–1603, 2011.

[47] Michael R Douglas. The statistics of string/M theory vacua. *Journal of High Energy Physics*, 2003(05):046, 2003.

[48] Michael R Douglas and Miao Li. D-brane realization of N=2 super Yang-Mills theory in four dimensions. *arXiv preprint hep-th/9604041*, 1996.

[49] Michael J Duff, James T Liu, and R Minasian. Eleven-dimensional origin of string/string duality: A one-loop test. *Nuclear Physics B*, 452(1-2):261–282, 1995.

[50] Jens Erler. Anomaly cancellation in six dimensions. *Journal of Mathematical Physics*, 35(4):1819–1833, 1994.

[51] Mboyo Esole, Shu-Heng Shao, and Shing-Tung Yau. Singularities and gauge theory phases. *arXiv preprint arXiv:1402.6331*, 2014.

[52] Mboyo Esole, Shu-Heng Shao, and Shing-Tung Yau. Singularities and gauge theory phases II. *arXiv preprint arXiv:1407.1867*, 2014.

[53] Mboyo Esole, Shing-Tung Yau, et al. Small resolutions of SU(5)-models in F-theory. *Advances in Theoretical and Mathematical Physics*, 17(6):1195–1253, 2013.

[54] Sergio Ferrara, Ruben Minasian, and Augusto Sagnotti. Low-energy analysis of M- and F-theories on Calabi-Yau threefolds. *Nuclear Physics B*, 474(2):323–342, 1996.

[55] Pasquale Foggia. The vflib graph matching library, version 2.0, 2001.

[56] Sebastián Franco, Amihay Hanany, Dario Martelli, James Sparks, David Vegh, and Brian Wecht. Gauge theories from toric geometry and brane tilings. *Journal of High Energy Physics*, 2006(01):128, 2006.

[57] Sebastián Franco, Amihay Hanany, David Vegh, Brian Wecht, and Kristian D Kennaway. Brane dimers and quiver gauge theories. *Journal of High Energy Physics*, 2006(01):096, 2006.

[58] Daniel Z Freedman and Antoine Van Proeyen. *Supergravity*. Cambridge University Press, 2012.

[59] William Fulton. *Introduction to toric varieties*. Number 131. Princeton University Press, 1993.

[60] Paul H. Ginsparg and C. Vafa. Toroidal Compactification of Nonsupersymmetric Heterotic Strings. *Nucl. Phys.*, B289:414, 1987.

[61] Antonella Grassi. On minimal models of elliptic threefolds. *Mathematische Annalen*, 290(1):287–301, 1991.

[62] Antonella Grassi, James Halverson, Julius Shaneson, and Washington Taylor. Non-Higgsable QCD and the standard model spectrum in F-theory. *Journal of High Energy Physics*, 2015(1):86, 2015.

[63] Antonella Grassi and David R Morrison. Anomalies and the Euler characteristic of elliptic Calabi-Yau threefolds. *arXiv preprint arXiv:1109.0042*, 2011.

[64] M. B. Green, John H. Schwarz, and Edward Witten. *Superstring theory: volume 1,2*. Cambridge university press, 1987.

[65] Michael B Green, John H Schwarz, and Peter C West. Anomaly-free chiral theories in six dimensions. *Nuclear Physics B*, 254:327–348, 1985.

[66] Phillip Griffiths and Joseph Harris. *Principles of algebraic geometry*. John Wiley & Sons, 2014.

[67] Thomas W Grimm. The N=1 effective action of F-theory compactifications. *Nuclear Physics B*, 845(1):48–92, 2011.

[68] Mark Gross. A finiteness theorem for elliptic Calabi-Yau threefolds. *arXiv preprint alg-geom/9305002*, 1993.

[69] Sergei Gukov, Cumrun Vafa, and Edward Witten. CFT's from Calabi-Yau four-folds. *Nuclear Physics B*, 584(1-2):69–108, 2000.

[70] Rudolf Haag, Jan T Lopuszański, and Martin Sohnius. All possible generators of supersymmetries of the S-matrix. *Nuclear Physics B*, 88(2):257–274, 1975.

[71] James Halverson, Cody Long, and Benjamin Sung. Algorithmic universality in F-theory compactifications. *Physical Review D*, 96(12):126006, 2017.

[72] James Halverson and Washington Taylor. $\mathbb{P}^1$-bundle bases and the prevalence of non-Higgsable structure in 4d F-theory models. *Journal of High Energy Physics*, 2015(9):86, 2015.

[73] Brian Harbourne. Anticanonical rational surfaces. *Transactions of the American Mathematical Society*, 349(3):1191–1208, 1997.

[74] Robin Hartshorne. *Algebraic geometry*, volume 52. Springer Science & Business Media, 2013.

[75] Arthur Hebecker, Fabrizio Rompineve, and Alexander Westphal. Axion monodromy and the weak gravity conjecture. *Journal of High Energy Physics*, 2016(4):157, 2016.

[76] Jonathan J Heckman, David R Morrison, Tom Rudelius, and Cumrun Vafa. Atomic classification of 6D SCFTs. *Fortschritte der Physik*, 63(7-8):468–530, 2015.

[77] Jonathan J Heckman, David R Morrison, and Cumrun Vafa. On the classification of 6D SCFTs and generalized ADE orbifolds. *Journal of High Energy Physics*, 2014(5):28, 2014.

[78] Ben Heidenreich, Matthew Reece, and Tom Rudelius. Weak gravity strongly constrains large-field axion inflation. *Journal of High Energy Physics*, 2015(12):1–41, 2015.

[79] Ben Heidenreich, Matthew Reece, and Tom Rudelius. Evidence for a lattice weak gravity conjecture. *arXiv preprint arXiv:1606.08437*, 2016.

[80] Ben Heidenreich, Matthew Reece, and Tom Rudelius. Sharpening the weak gravity conjecture with dimensional reduction. *Journal of High Energy Physics*, 2016(2):140, 2016.

[81] P. Hořava and E. Witten. Heterotic and type I string dynamics from eleven dimensions. *Nuclear Physics B*, 460(3):506, 1996.

[82] Samuel B Johnson and Washington Taylor. Calabi-Yau threefolds with large $h^{2,1}$. *Journal of High Energy Physics*, 2014(10):23, 2014.

[83] Samuel B Johnson and Washington Taylor. Enhanced gauge symmetry in 6D F-theory models and tuned elliptic Calabi-Yau threefolds. *Fortschritte der Physik*, 64(8-9):581–644, 2016.

[84] A Klemm, B Lian, S-S Roan, and S-T Yau. Calabi-Yau four-folds for M- and F-theory compactifications. *Nuclear Physics B*, 518(3):515–574, 1998.

[85] Denis Klevers, David R Morrison, Nikhil Raghuram, and Washington Taylor. Exotic matter on singular divisors in F-theory. *Journal of High Energy Physics*, 2017(11):124, 2017.

[86] Denis Klevers and Washington Taylor. Three-index symmetric matter representations of SU(2) in F-theory from non-Tate form Weierstrass models. *Journal of High Energy Physics*, 2016(6):171, 2016.

[87] Kunihiko Kodaira. On compact analytic surfaces: II. *Annals of Mathematics*, pages 563–626, 1963.

[88] János Kollár. *Rational curves on algebraic varieties*, volume 32. Springer Science & Business Media, 2013.

[89] Maximilian Kreuzer and Harald Skarke. Calabi-Yau 4-folds and toric fibrations. *Journal of Geometry and Physics*, 26(3-4):272–290, 1998.

[90] Maximilian Kreuzer and Harald Skarke. Complete classification of reflexive polyhedra in four dimensions. *arXiv preprint hep-th/0002240*, 2000.

[91] Vijay Kumar, David R Morrison, and Washington Taylor. Global aspects of the space of 6D $\mathcal{N} = 1$ supergravities. *Journal of High Energy Physics*, 2010(11):118, 2010.

[92] Vijay Kumar, David R Morrison, and Washington Taylor. Mapping 6D $\mathcal{N} = 1$ supergravities to F-theory. *Journal of High Energy Physics*, 2010(2):99, 2010.

[93] Vijay Kumar and Washington Taylor. String universality in six dimensions. *Advances in Theoretical and Mathematical Physics*, 15(2):325–353, 2011.

[94] Craig Lawrie and Sakura Schäfer-Nameki. The tate form on steroids: resolution and higher codimension fibers. *Journal of High Energy Physics*, 2013(4):61, 2013.

[95] Naichung Conan Leung and Cumrun Vafa. Branes and toric geometry. *arXiv preprint hep-th/9711013*, 1997.

[96] Eduard Looijenga. Rational surfaces with an anti-canonical cycle. *Annals of Mathematics*, 114(2):267–322, 1981.

[97] Gabriella Martini and Washington Taylor. 6D F-theory models and elliptically fibered Calabi-Yau threefolds over semi-toric base surfaces. *Journal of High Energy Physics*, 2015(6):61, 2015.

[98] Kenji Matsuki. *Introduction to the Mori program*. Springer Science & Business Media, 2013.

[99] James E Mazo and Andrew M Odlyzko. Lattice points in high-dimensional spheres. *Monatshefte für Mathematik*, 110(1):47–61, 1990.

[100] Kenji Mohri. F theory vacua in four dimensions and toric threefolds. *International Journal of Modern Physics A*, 14(06):845–874, 1999.

[101] David Morrison and Washington Taylor. Classifying bases for 6D F-theory models. *Open Physics*, 10(5):1072–1088, 2012.

[102] David R Morrison and Daniel S Park. F-theory and the Mordell-Weil group of elliptically-fibered Calabi-Yau threefolds. *Journal of High Energy Physics*, 2012(10):128, 2012.

[103] David R Morrison and Daniel S Park. Tall sections from non-minimal transformations. *Journal of High Energy Physics*, 2016(10):33, 2016.

[104] David R Morrison, Daniel S Park, and Washington Taylor. Non-Higgsable Abelian gauge symmetry and F-theory on fiber products of rational elliptic surfaces. *arXiv preprint arXiv:1610.06929*, 2016.

[105] David R Morrison and Washington Taylor. Toric bases for 6d F-theory models. *Fortschritte der Physik*, 60(11-12):1187–1216, 2012.

[106] David R Morrison and Washington Taylor. Sections, multisections, and U(1) fields in F-theory. *arXiv preprint arXiv:1404.1527*, 2014.

[107] David R Morrison and Washington Taylor. Non-Higgsable clusters for 4d F-theory models. *Journal of High Energy Physics*, 2015(5):80, 2015.

[108] David R Morrison and Cumrun Vafa. Compactifications of F-theory on Calabi-Yau threefolds (II). *Nuclear Physics B*, 476(3):437–469, 1996.

[109] David R Morrison and Cumrun Vafa. Compactifications of F-theory on Calabi-Yau threefolds.(I). *Nuclear Physics B*, 473(1-2):74–92, 1996.

[110] Masayoshi Nagata et al. On rational surfaces, II. *Memoirs of the College of Science, University of Kyoto. Series A: Mathematics*, 33(2):271–293, 1960.

[111] Hirosi Ooguri and Cumrun Vafa. Non-supersymmetric AdS and the swampland. *arXiv preprint arXiv:1610.01533*, 2016.

[112] Daniel S Park and Washington Taylor. Constraints on 6d supergravity theories with abelian gauge symmetry. *Journal of High Energy Physics*, 2012(1):141, 2012.

[113] M. E. Peskin and D. V. Schroeder. *An introduction to quantum field theory*. Westview press, 1995.

[114] Joseph Polchinski. *String theory: Volume 1,2*. Cambridge university press, 1998.

[115] Nikhil Raghuram. Abelian F-theory models with charge-3 and charge-4 matter. *arXiv preprint arXiv:1711.03210*, 2017.

[116] Tom Rudelius. Constraints on axion inflation from the weak gravity conjecture. *Journal of Cosmology and Astroparticle Physics*, 2015(09):020, 2015.

[117] Augusto Sagnotti. A note on the Green-Schwarz mechanism in open-string theories. *Physics Letters B*, 294(2):196–203, 1992.

[118] Yuji Tachikawa. Six-dimensional DN theory and four-dimensional SO-USp quivers. *Journal of High Energy Physics*, 2009(07):067, 2009.

[119] John Tate. Algorithm for determining the type of a singular fiber in an elliptic pencil. In *Modular functions of one variable IV*, pages 33–52. Springer, 1975.

[120] Washington Taylor. Tasi lectures on supergravity and string vacua in various dimensions. *arXiv preprint arXiv:1104.2051*, 2011.

[121] Washington Taylor. On the Hodge structure of elliptically fibered Calabi-Yau threefolds. *Journal of High Energy Physics*, 2012(8):32, 2012.

[122] Washington Taylor and Andrew P Turner. An infinite swampland of U(1) charge spectra in 6D supergravity theories. *arXiv preprint arXiv:1803.04447*, 2018.

[123] Washington Taylor and Yi-Nan Wang. The F-theory geometry with most flux vacua. *JHEP*, 12:164, 2015.

[124] Washington Taylor and Yi-Nan Wang. A Monte Carlo exploration of threefold base geometries for 4d F-theory vacua. *JHEP*, 01:137, 2016.

[125] Washington Taylor and Yi-Nan Wang. Non-toric bases for elliptic Calabi-Yau threefolds and 6D F-theory vacua. *Adv. Theor. Math. Phys.*, 21:1063–1114, 2017.

[126] Washington Taylor and Yi-Nan Wang. Scanning the skeleton of the 4D F-theory landscape. *JHEP*, 01:111, 2018.

[127] Cumrun Vafa. Evidence for F-theory. *Nuclear Physics B*, 469(3):403–415, 1996.

[128] Cumrun Vafa. The string landscape and the swampland. *arXiv preprint hep-th/0509212*, 2005.

[129] Yi-Nan Wang. Generalized Cartan Calculus in general dimension. *Journal of High Energy Physics*, 2015(7):114, 2015.

[130] Yi-Nan Wang. Tuned and Non-Higgsable U(1)s in F-theory. *JHEP*, 03:140, 2017.

[131] Taizan Watari. Statistics of F-theory flux vacua for particle physics. *Journal of High Energy Physics*, 2015(11):65, 2015.

[132] Rania Wazir. Arithmetic on elliptic threefolds. *Compositio Mathematica*, 140(3):567–580, 2004.

[133] Timo Weigand. Lectures on F-theory compactifications and model building. *Classical and Quantum Gravity*, 27(21):214004, 2010.

[134] Steven Weinberg. *The quantum theory of fields. Vol. 1,2,3.* Cambridge university press, 1995.

[135] Edward Witten. On flux quantization in M-theory and the effective action. *Journal of Geometry and Physics*, 22(1):1–13, 1997.

[136] Oscar Zariski. The theorem of Riemann-Roch for high multiples of an effective divisor on an algebraic surface. *Annals of Mathematics*, pages 560–615, 1962.